ILLINOIS

UNIVERSITY OF ILLINOIS AT URBANA-CHAMPAIGN

-

PRODUCTION NOTE

University of Illinois at
Urbana-Champaign Library
Large-scale Digitization Project, 2007.

UNIVERSITY OF ILLINOIS
BULLETIN
Vol. 47 June, 1950 No. 77

ENGINEERING EXPERIMENT STATION
BULLETIN SERIES No. 387

THE EFFECT OF BRAKE SHOE ACTION ON THERMAL CRACKING AND ON FAILURE OF WROUGHT STEEL RAILWAY CAR WHEELS

BY

HARRY R. WETENKAMP
OMAR M. SIDEBOTTOM
HERMAN J. SCHRADER

PRICE: SIXTY CENTS

PUBLISHED BY THE UNIVERSITY OF ILLINOIS
URBANA

Published seven times each month by the University of Illinois. Entered as second-class matter December 11, 1912, at the post office at Urbana, Illinois, under the Act of August 24, 1912. Office of Publication, 358 Administration Building, Urbana, Illinois.

THE Engineering Experiment Station was established by act of the Board of Trustees of the University of Illinois on December 8, 1903. It is the purpose of the Station to conduct investigations and make studies of importance to the engineering, manufacturing, railway, mining, and other industrial interests of the State.

The management of the Engineering Experiment Station is vested in an Executive Staff composed of the Director and his Assistant, the Heads of the several Departments in the College of Engineering, the Professor in charge of Chemical Engineering, and the Director of Engineering Information and Publications. This Staff is responsible for establishing general policies governing the work of the Station, including the approval of material for publication. All members of the teaching staff of the College are encouraged to engage in scientific research, either directly or in cooperation with the Research Corps, composed of full-time research assistants, research graduate assistants, and special investigators.

To render the results of its scientific investigations available to the public, the Engineering Experiment Station publishes and distributes a series of bulletins. Occasionally it publishes circulars of timely interest presenting information of importance and a few reprints of articles appearing in the technical press written by members of the staff and others.

The volume and number at the top of the front cover page are merely arbitrary numbers and refer to the general publications of the University. *Above the title on the cover* is given the number of the Engineering Experiment Station bulletin, circular, or reprint which should be used in referring to these publications.

For copies of publications or for other information address

THE ENGINEERING EXPERIMENT STATION,
UNIVERSITY OF ILLINOIS,
URBANA, ILLINOIS

UNIVERSITY OF ILLINOIS
ENGINEERING EXPERIMENT STATION
BULLETIN SERIES No. 387

THE EFFECT OF BRAKE SHOE ACTION ON THERMAL CRACKING AND ON FAILURE OF WROUGHT STEEL RAILWAY CAR WHEELS

A REPORT OF AN INVESTIGATION

CONDUCTED BY

THE ENGINEERING EXPERIMENT STATION
UNIVERSITY OF ILLINOIS

IN COOPERATION WITH

THE TECHNICAL BOARD OF THE WROUGHT STEEL WHEEL INDUSTRY

BY

HARRY R. WETENKAMP
Research Associate in Engineering Materials

OMAR M. SIDEBOTTOM
Assistant Professor of Theoretical and Applied Mechanics

HERMAN J. SCHRADER
Research Professor of Theoretical and Applied Mechanics

PUBLISHED BY THE UNIVERSITY OF ILLINOIS

PRICE: SIXTY CENTS

4800—6-50—43535

UNIVERSITY
OF ILLINOIS
PRESS

ABSTRACT

This bulletin is a report of the progress that has been made to date on the investigation of steel car wheels being conducted at the University of Illinois. On some phases the investigation has been concluded; others require additional work. Laboratory tests were made on 369 wrought steel railway car wheels. Two types of tests were performed: (1) the wheels were stopped from high speed by using high brake shoe pressure, and (2) the wheels were tested under long-continued applications of the brake shoes. The stop tests were intended to produce thermal cracks in the wheel treads. The long-continued brake shoe applications were intended to produce fractures through the rims and plates of the wheels. In both types of tests the conditions imposed on the wheels were more severe than the wheels should receive in normal railway operation.

The studies of the effect of carbon content of the wheel material, various methods of heat treatment, and changes in wheel design, together with a qualitative analysis of the stresses developed in the wheels are presented.

The results of the tests are summarized in Chapter IX. The conclusions apply only to the types of wheels tested. These do not necessarily represent all wheels made by the various manufacturers. The types of failures, however, are in close accord with experience in service.

This page is intentionally blank.

CONTENTS

FIGURES

TABLES

I. Introduction

1. *Purpose of Investigation*

In railway service, car wheels are in general required to fulfill two functions: (1) to act as a wheel which supports the weight of the car as it moves along the rails and (2) to act as a brake drum. In this latter capacity the wheels, along with the brake shoes, are required to dissipate as heat the energy released in stopping or in controlling the speed of a train. With the trend toward increasing train speeds and greater loads per wheel, the wheels are subjected to increased braking demands, since the energy that must be dissipated varies as the square of the velocity of the train and directly with the load per wheel. This situation has focused attention on the types of wheel failures that result from heating due to brake shoe applications.

In recognition of the need for joint action in studies conducted with a view to determining the circumstances that influence the service performance of wrought steel wheels, and looking toward improvement of the product, the Technical Board of the Wrought Steel Wheel Industry was organized in 1938. Shortly after the formation of the Board, a cooperative research program was entered into between the University of Illinois and the Board for the purpose of studying the properties of the existing wheels and determining how wheels could be made more resistant to thermal cracking and to failure through rim and plate resulting from heating due to brake shoe applications. It is generally accepted that thermal action resulting from brake shoe applications may produce (1) thermal cracks[1] and (2) brittle-type rim and plate fractures[2]. The thermal cracks and the rim and plate fractures are in general produced by two different types of service conditions.

Thermal cracks are the result of a severe heating of the tread of the wheel at such a rate that a steep temperature gradient is produced. The quenching action of the cold material remaining in the rim can develop a change in the structure and can produce stresses sufficient to cause the formation of a thermal crack. The steep temperature gradient is produced by severe brake shoe applications of short duration such as occur, for instance, during the stopping of a train from a high speed with high brake shoe pressures. Typical thermal cracks caused by these conditions are shown in Fig. 1. Thermal cracks in general develop transverse to the tread of the wheel and are of varying length and depth. Further brake appli-

[1] See AAR Wheel and Axle Manual, 1945, revised edn., p. 43, Fig. 40.
[2] *Ibid.*, p. 54, Fig. 53.

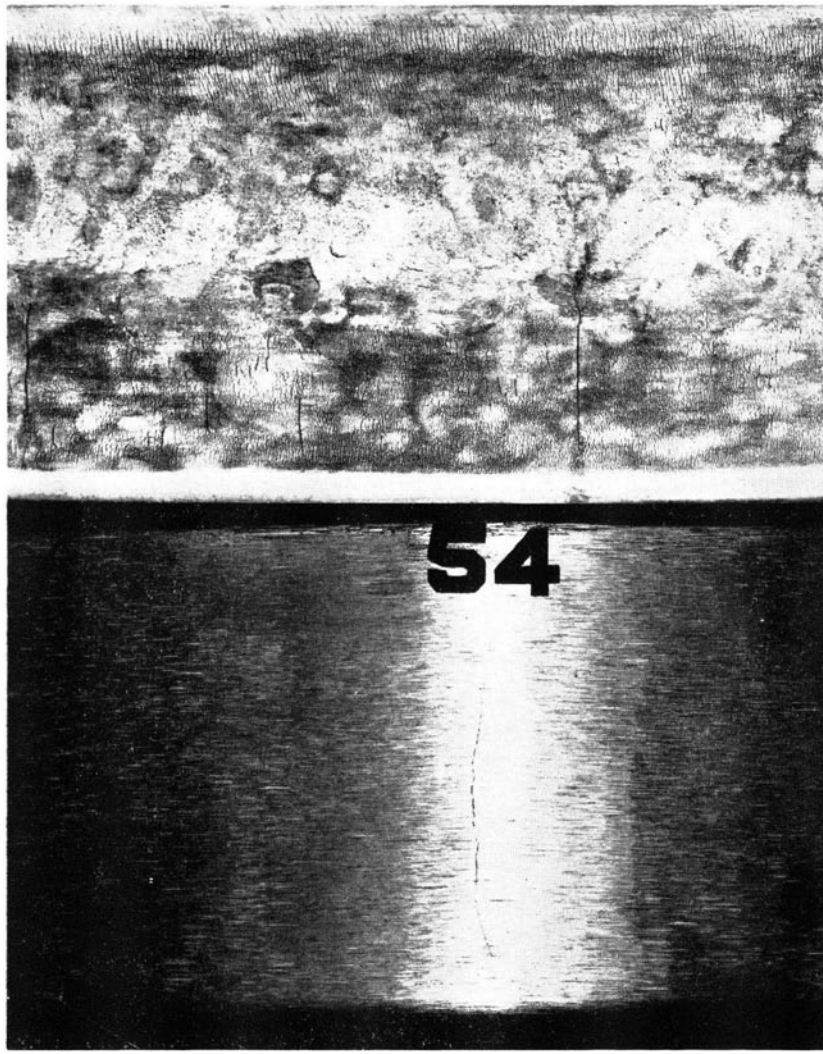

FIG. 1. TYPICAL THERMAL CRACKS IN WHEEL TREADS
Thermal cracks produced in service (top)
Thermal cracks produced in the laboratory (bottom)

cations after the formation of a thermal crack may cause it to grow in length and depth.

The brittle-type rim and plate fracture, which will be referred to as "wheel fracture," is produced by a braking condition that results in the general heating of the rim. This type of heating can be produced by light brake applications of appreciable duration such as might occur in controlling the speed of a train down long grades or when the brake shoes fail to release properly. The heating of the whole rim, and subsequent cooling, set up tensile stresses in a tangential direction in the rim. With repeated heating and cooling of the rim these tensile stresses may become large enough to rupture the rim and plate, especially if the stresses are intensified by a notch such as a thermal crack.

2. *Scope of Investigation*

With the wheel testing facilities at the University of Illinois the effect of brake shoe action on the wheels can be studied. Since the thermal cracking and failure mentioned above were believed to be caused by thermal action alone, it was not deemed necessary to alter the facilities to include the effect of rail loads. Two types of tests were developed for testing wheels, a "stop" test and a "drag" test.

The stop test, described in detail in Section 9, consists of applying brakes at a high pressure to a wheel which is rotating at a relatively high peripheral speed and stopping the wheel in somewhat the same manner as a train would be stopped by an emergency brake application. In the laboratory a flywheel which is keyed to the same shaft as the test wheel supplied a quantity of energy that is comparable to the energy that each wheel of a passenger train would have to dissipate in stopping the train. This severe short-time test has produced thermal cracks in test wheels in the laboratory. The thermal cracking problem is still under investigation, and a more extensive study is being made at the University of Illinois; hence the stop test data in this bulletin should be regarded as preliminary information.

The drag test, as the name implies, is one wherein the brake shoes are applied to the wheel while the wheel is rotated at constant speed for an appreciable period of time. The drag test is described in Section 8. This type of testing produces wheel fractures similar to those shown in Fig. 2. Considerable difficulty was experienced in developing a test procedure which would give relatively consistent results. The first drag test procedure was to subject the wheel to a series of

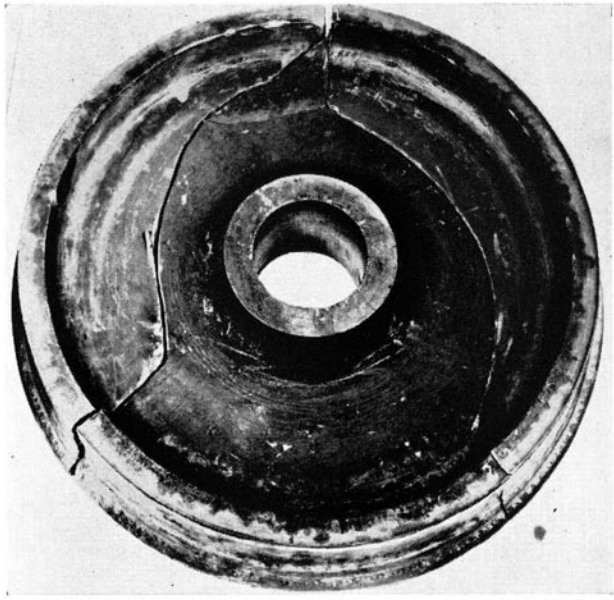

Wheel fracture produced in service

FIG. 2. TYPICAL WHEEL FRACTURES

Wheel fracture produced in the laboratory

drag tests; the wheel was then removed from the testing machine and a radial saw cut was made through the rim to induce a wheel fracture. The depth of the rim saw cut and the number of drags required to produce fracture were chosen as the criterion for comparing wheels.

This method gave erratic results and was abandoned in favor of a method referred to as a "Standard Drag Test" which involves sawing a simulated thermal crack in the rim of the wheel before subjecting the wheel to drag testing. While consideration was given to the plan of producing thermal cracks in the wheel rim by stop-testing the wheel until a thermal crack developed and then using the cracks thus developed for the wheel fracture study, it was felt that the simulated thermal cracks would give the more consistent results. The stop test program and the drag test program were therefore kept separate.

The stop testing and drag testing of wheels have been confined mainly to wheels of 36-in. diameter, though some data have been obtained and are reported on 33-in.-diam wheels. The 33-in.-diam wheels were made both by the conventional wrought steel manufacturing process, which is a combination of press forging and rolling, and by a drop-forging process.

Mechanical property data for the wheel material were obtained and are presented for wheels having two types of heat treatment, various carbon contents, and two methods of wheel manufacture. The data were from notched and unnotched static tension specimens, Brinell hardness determinations, and endurance limits for notched and unnotched rotating beam bending fatigue specimens. For a few types of wheels a photomicroscopic study was made of the structure of the material before and after drag testing.

A number of variables were investigated to determine their effect on the ability of the wheel to resist wheel fractures and thermal cracks. The variables considered are classified as follows: (1) heat treatment, (2) wheel design, (3) carbon content, and (4) method of wheel manufacture. Under heat treatment the investigation included two types of treatment recognized by the Association of American Railroads. These are (1) quenching the rim of a wheel by water followed by tempering of the entire wheel in a furnace, and (2) an all-over quench of the wheel by immersion in oil or water followed by tempering in a furnace. For these quenched wheels the effect of varying the draw temperature was investigated. Under "wheel design" the investigation included the effect of some changes in plate thickness, plate location, and rim thickness. The test results are presented under the four general classifications of the variables

listed above. Many of the tests conducted during the investigation were exploratory, and since the data obtained were not conclusive, the results are not presented in the main body of the bulletin but in Appendix B.

In Appendix A a qualitative stress analysis of the wheels is presented. Based on a concept of relaxation of stress which occurs at high temperatures when a member is subjected to constant strain, the stress analysis presents a qualitative picture of the reason for the effect of a given variable on the test results.

3. *Acknowledgments*

This investigation was undertaken as one of the researches of the Engineering Experiment Station of the University of Illinois, in cooperation with the Technical Board of the Wrought Steel Wheel Industry. The University and the Board shared the expense.

The Technical Board has been represented on the Advisory Committee in the planning and general arrangements for the tests by the following persons:

C. T. Ripley, Chief Engineer of the Technical Board of the Wrought Steel Wheel Industry until July 1946.

C. F. W. Rys, Secretary of the Technical Board of the Wrought Steel Wheel Industry until July 1941.

C. B. Bryant, Chief Engineer of the Technical Board of the Wrought Steel Wheel Industry since July 1946.

R. L. Kenyon, Associate Director, Research Laboratories, Armco Steel Corporation.

E. F. Kenny, Metallurgical Engineer, Bethlehem Steel Co., until October 1943.

L. H. Winkler, Metallurgical Engineer, Bethlehem Steel Co., since October 1943.

R. W. Steigerwalt, Metallurgical Engineer, Railway Materials and Forgings, Carnegie-Illinois Steel Corporation.

Lawford Fry, Railway Engineer, Edgewater Steel Co., until October 1943.

W. J. George, Assistant to President, Edgewater Steel Co., from October 1943 to April 1946.

D. W. Odiorne, Railway Engineer, Edgewater Steel Co., since April 1946.

J. D. Tyson, Chief Metallurgist, Standard Steel Works Division, until February 1943.

G. S. Baldwin, Chief Metallurgist, Standard Steel Works Division, from February 1943 to January 1949.

P. A. ARCHIBALD, Chief Metallurgist, Standard Steel Works Division, since January 1949.

H. B. WISHART, Chief Development Metallurgist, Carnegie-Illinois Steel Corporation, Gary Works, although not a member of the Technical Board, has served continuously as a liaison officer between the Board and the University and has rendered valuable service in expediting the investigation.

The work has been under the administrative direction of Deans M. L. ENGER (retired) and W. L. EVERITT, Director of the University of Illinois Engineering Experiment Station, and Professor F. B. SEELY, Head of the Department of Theoretical and Applied Mechanics.

Special acknowledgment is made of the assistance received from Professor R. E. CRAMER in making some of the metallurgical studies, Professor W. L. COLLINS in determining the mechanical properties of wheel materials, and Professor R. L. BROWN in making mechanical tests and developing methods of stress analysis.

II. Wheels Tested and Their Mechanical Properties

4. *Wheels Tested*

The wrought steel wheels used in this investigation were for the most part manufactured as standard 36C and standard 33C wheels (now designated as A36 and A33)[1]. After their manufacture, the treads of all the wheels were machined cylindrical. A cross-section of the wheel naming the important parts is shown in Fig. 3.

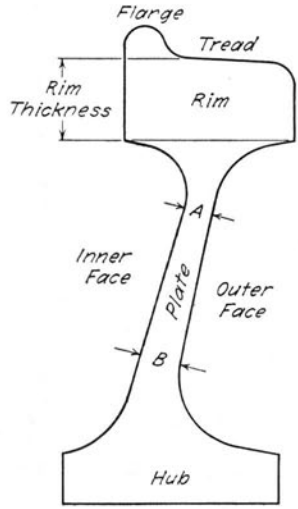

Fig. 3. Cross-Section of Wheel (Various Parts)

A number of variations in design were investigated. These special features were obtained by machining the standard wheels to give variations in rim thickness, plate thickness and plate locations. Each of the special features is described in the section where the information is pertinent. For comparative purposes a wheel designated as the "basic wheel" is herein defined as a wheel manufactured according to 36C design with a rim thickness of $2\frac{1}{2}$ in. and a plate thickness of approximately 1 in. and $1\frac{1}{4}$ in. as given by dimensions A and B respectively in Fig. 3.

The wheels are classified according to AAR specifications M-107-48[2] as to carbon content and heat treatment. The heat-treated wheels fall into three classes: Class A if the carbon is below 0.63 percent[3],

[1] See AAR Manual of Standard and Recommended Practice G-23-1949.
[2] See AAR Manual of Standard and Recommended Practice M-107-48.
[3] Effective March 7, 1949, a ruling of the AAR changed the maximum carbon content of Class A wheels from 0.63 percent to 0.57 percent.

Class B if the carbon is from 0.57 to 0.67 percent, Class C if the carbon is from 0.67 to 0.77 percent. The untreated wheels are classified as Class U and must fall within the carbon range of 0.65 to 0.77 percent carbon. There are two types of heat treatment recognized by the Association of American Railroads[2] — (1) entire wheel-quenching treatment and (2) rim-quenching treatment.

Of the wheels reported in this bulletin that were given the entire wheel-quenching treatment, the majority were quenched in a bath of oil; these are referred to as oil-quenched wheels. For wheels referred to as rim-quenched wheels the rims were water-quenched. All the heat-treated wheels were drawn at a suitable temperature to control hardness and residual stresses. In the tables presented in this bulletin the letters listed under heat treatment mean the following:

E — entire wheel quenched in oil (oil-quenched wheel)
W — entire wheel quenched in water (water-quenched wheel)
R — rim of wheel quenched in water (rim-quenched wheel)
U — wheel not subjected to a quench.

5. *Mechanical Properties*

Mechanical property tests were made on 36-in.-diam rim-quenched, oil-quenched, and entire water-quenched Class A wheels, rim-quenched and oil-quenched Class B wheels, and rim-quenched and oil-quenched Class C wheels. Mechanical property tests were also made on 33-in.-diam rolled and drop-forged untreated wheels. The data are presented in Tables 1, 1a and 2. In some cases the conditions of heat treatment are not present manufacturing practices.

Mechanical properties were determined as follows: (1) yield strength for 0.2 percent offset, ultimate strength, percent elongation, and percent reduction of area for unnotched tension specimens taken from the rim and plate of the wheel, (2) proportional limit and ultimate strength for notched tension specimens taken from the plate of the wheel, (3) rotating beam endurance limits for unnotched and notched specimens taken from the plate and rim of the wheel, and (4) Brinell hardness determinations across the cross-section of the wheel. The locations of the various specimens in the car wheel, along with dimensions of the various specimens, are shown in Fig. 4. Figure 5 shows the location at which BHN readings were taken. Attention is called to the fact that the unnotched static tension specimens taken from the rolled and the drop-forged 33-in.-diam untreated wheels were ¼ in. in diam, since the thin plate made it impossible to obtain a specimen ½ in. in diameter.

TABLE 1
MECHANICAL PROPERTIES OF STEEL CAR WHEEL MATERIALS

Wheel Test No.	Class	Carbon, percent	Heat Treatment	Draw Temp, deg F	Static Tensile Test							Rotating Beam Fatigue Test	
					Unnotched Specimens					Notched Specimens		Unnotched	Notched
					Location* of Specimen	Yield Strength 0.2 percent offset, p.s.i.	Ultimate Strength, p.s.i.	Elongation in 2 in., percent	Reduction of Area, percent	Proportional Limit, p.s.i.	Ultimate Strength, p.s.i.	Endurance Limit, p.s.i.	Endurance Limit, p.s.i.
35 BAR1P	A	0.52	R	870	Rim T†	71 000	120 000	21	42	.....	.....	.....	.....
					Plate R‡	54 000	97 000	27	44	.....	.....	42 000	26 000
5 IAO1P	A	0.52	E	990	Rim T	73 000	126 000	16	35	72 000	142 000	56 000	.....
					Plate T	74 000	125 000	17	35	75 000	141 000	58 000	28 000
					Plate R	73 000	123 000	17	38	.....	.....	.....	.....
23 SAW1P	A	0.48	W	800	Rim T	80 000	123 000	16	38	.....	.....	.....	.....
					Plate T	86 000	136 000	15	37	90 000	158 000	60 000	.....
					Plate R	90 000	136 000	16	40	99 000	159 000	61 000	28 000
41 BBR1P	B	0.61	R	870	Rim T	85 000	145 000	16	40	.....	.....	.....	.....
					Plate R	50 000	117 000	17	31	.....	.....	50 000	26 000
11 IBO1P	B	0.61	E	990	Rim T	80 000	139 000	16	36	.....	.....	.....	.....
					Plate T	82 000	138 000	15	34	95 000	156 000	58 000	.....
					Plate R	81 000	137 000	16	38	85 000	156 000	55 000	27 000
47 BCR1P	C	0.70	R	870	Rim T	88 000	156 000	14	37	.....	.....	.....	.....
					Plate R	47 000	117 000	18	30	.....	.....	52 000	25 000
17 ICO1P	C	0.72	E	1 040	Rim T	88 000	147 000	15	36	.....	.....	.....	.....
					Plate T	89 000	149 000	13	31	97 000	163 000	68 000	.....
					Plate R	89 000	149 000	16	40	96 000	169 000	66 000	30 000

* For location of test specimens see Fig. 4.
† T—Tangential.
‡ R—Radial.

TABLE 1A

MECHANICAL PROPERTIES OF STEEL CAR WHEEL MATERIALS

(Unnotched Specimens)

Wheel Test No.	Class	Carbon, percent	Heat Treatment	Location* of Specimen	Static Tensile Tests				Rotating Beam Fatigue Tests
					Yield Strength 0.2 percent offset, p.s.i.	Ultimate Strength, p.s.i.	Elongation in 2 in., percent	Reduction of Area, percent	Endurance Limit, p.s.i.
Rolled Wheel									
271 ICU4R	U	0.72	U	Rim A†	48 000	120 000	7.5	15	45 000
				Rim T‡	50 000	121 000	8.3	16	50 000
				Plate T	55 000	126 000	9.5	19	48 000
				Plate R¶	56 000	127 000	8.8	21	52 000
Drop-Forged Wheel									
255 LCU4R	U	0.72	U	Rim A	50 000	123 000	7.7	11	43 000
				Rim T	55 000	126 000	8.0	12	45 000
				Plate T	51 000	127 000	8.7	13	46 000
				Plate R	50 000	122 000	9.2	15	45 000

* For location of test specimens see Fig. 4.
† A—Axial.
‡ T—Tangential.
¶ R—Radial.

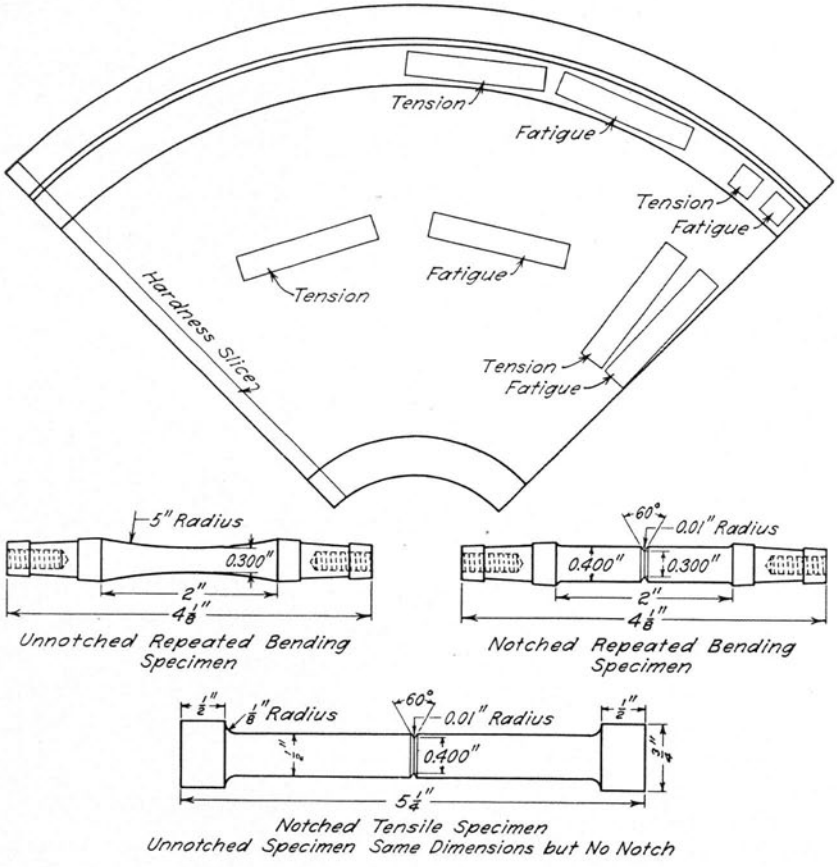

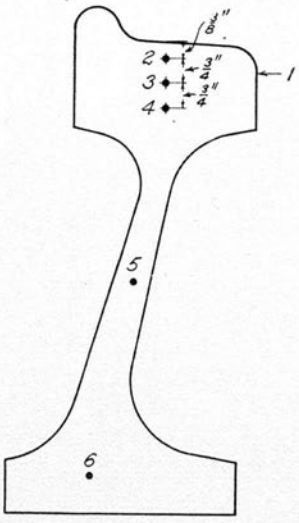

FIG. 4 (ABOVE). TEST SPECIMENS AND THEIR LOCATIONS

FIG. 5 (AT LEFT). WHEEL CROSS-SECTION, SHOWING BRINELL HARDNESS LOCATIONS

In general the yield strength, ultimate strength, and hardness increase with carbon content as indicated by the three Classes A, B, and C. For a particular class these properties of the material in the rim of the wheels are approximately the same for the rim-quenched and oil-quenched wheels having the same draw temperature. This condition would be expected, since the rim of the wheel is quenched in each type of heat treatment; however, a noticeable difference would be expected, and is shown, in the mechanical properties of the plate. For the oil-quenched wheels there is little difference in mechanical properties between the rim and plate, since the whole wheel was quenched; however, the strength properties of the plate of the rim-quenched wheels are considerably lower than for the rim, since the plate was not quenched. The strength properties for the rolled and drop-forged Class U wheels (see Table 1a) are considerably lower than for the heat-treated Class C wheels, although the carbon content of the two classes is nearly the same. The ductility of the material, as measured by the percent elongation and percent reduction in area, has an appreciably lower value for the untreated wheels than for the heat-treated wheels. Attention is directed to the fact that the tensile specimens taken from the untreated wheels were ¼ in. in diameter, whereas those from heat-treated wheels were of the standard ½-in. diameter. The specimen of smaller diameter with the same gage length showed a lower percent elongation than the same steel would exhibit in the standard specimen. The mechanical property data for the rolled and the drop-forged wheels shown in Table 1a do not indicate any significant difference between the two methods of manufacture.

Table 2 gives the Brinell hardness data of wheels drawn at different temperatures. These tests were made at the various locations on the cross-section of a wheel as shown in Fig. 5. The Brinell hardness data presented in Table 2 for the Number 1 position are the values obtained by the manufacturer. The remaining Brinell hardness data in Table 2 were obtained at the University on the cross-sections of the wheels used for residual stress determinations. The data presented in Table 2 show the same trends as were found for the ultimate strength of the unnotched static tension specimens.

6. *Metallographic Study*

Microstructural changes in a wheel occur as a result of brake applications. In an effort to ascertain the extent and possible effects of such changes, a metallographic study of drag-tested wheels was made. As a basis of comparison, photomicrographs were taken of the initial structure of an untreated wheel, and of oil-quenched and

TABLE 2
BRINELL HARDNESS READINGS OF STEEL CAR WHEELS

Wheel Test Number	Heat Number	Class	Carbon, percent	Heat Treatment	Draw Temp, deg F	Location of Hardness Readings*					
						1 B.H.N.	2 B.H.N.	3 B.H.N.	4 B.H.N.	5 B.H.N.	6 B.H.N
35 BAR1R	46L223	A	0.52	R	870		269	241	235	192	207
5 IAO1R	31077	A	0.52	E	990		269	248	235	255	235
23 SAW1R	E6270	A	0.48	W	800		262	241	241	269	255
41 BBR1R	46L256	B	0.61	R	870		311	293	277	223	241
11 IBO1R	37021	B	0.61	E	990		285	277	277	277	269
47 BCR1R	47L193	C	0.71	R	870		341	321	302	235	255
17 ICO1R	87120	C	0.72	E	1 040		302	293	285	293	269
66 ICR1R	46568	C	0.73	R	970		341	341	331	262	235
61 ICO1R	46568	C	0.73	E	970		331	321	302	331	302
76 ICR1R	46568	C	0.73	R	1 140		285	277	277	241	262
71 ICO1R	46568	C	0.73	E	1 140		285	277	262	277	269
81 ICU1R	46568	U	0.73	U	....		262	255	262	262	262
86 IFO1R	43607	C	0.73	E	970		331	311	302	311	293
247 BCR1R	59R316	C	0.71	R	870		341	321	302	241	235
267 BCR9R	59R316	C	0.71	R	870		341	321	311	248	241
307 ICR1R	921614	C	0.72	R	400	401	363	341	341	235	241
305 ICR1R	921614	C	0.72	R	700	375	363	341	321	248	241
306 ICR1R	921614	C	0.72	R	800	375	363	331	321	248	248
343 ICR1R	921614	C	0.72	R	860	352	352	341	321	255	248
304 ICR1R	921614	C	0.72	R	900	331	341	331	321	248	248
303 ICR1R	921614	C	0.72	R	1 000	321	311	302	302	241	248
296 ICR1R	921614	C	0.72	R	1 200	262	241	248	248	248	248
311 ICO1R	921614	C	0.72	E	400	388	341	321	302	311	311
310 ICO1R	921614	C	0.72	E	700	388	341	321	302	311	311
309 ICO1R	921614	C	0.72	E	800	375	352	321	302	311	311
308 ICO1R	921614	C	0.72	E	900	352	341	321	302	321	311
302 ICO1R	921614	C	0.72	E	1 000	321	311	302	285	302	293
301 ICO1R	921614	C	0.72	E	1 200	262	241	248	248	229	223
312 ICU1R	921614	U	0.72	U	.....	262	248	248	241	255	248
33-in.-diam Rolled Steel Wheel											
271 ICU4R	831021	U	0.72	U	....	...	241	248	...	255	248
33-in.-diam Drop-Forged Wheel											
255 LCU4R	831021	U	0.72	U	....	...	241	241	...	241	241

* For location of hardness readings see Fig. 5.

rim-quenched wheels drawn at temperatures of 1200 deg F, 800 deg F, and 400 deg F. Photomicrographs of the initial structure of rolled wheels and drop-forged wheels are also discussed.

To establish a uniform basis for a comparative metallographic study of wrought steel car wheels, a series of wheels made from one heat of steel (No. 921614) was examined. The chemical composition of the steel was as follows:

%C	%Mn	%P	%S	%Si
0.72	0.77	0.022	0.035	0.20

The rim structures at approximately ⅛ in. below the center of the tread of the wheels as received from the manufacturer are shown in the micrographs in Fig. 6. These micrographs are for wheels hav-

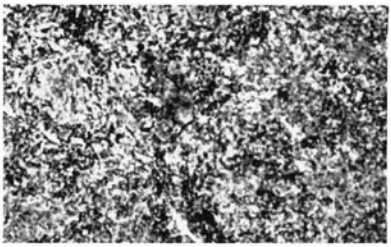

RIM-QUENCHED; DRAW TEMP. 1200° F

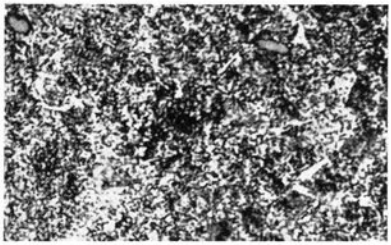

OIL-QUENCHED; DRAW TEMP. 1200° F

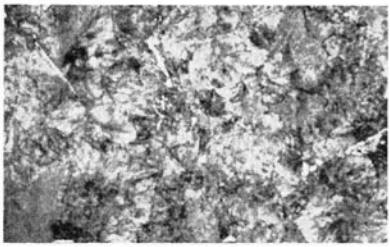

RIM-QUENCHED; DRAW TEMP. 800° F

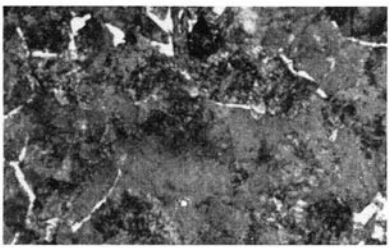

OIL-QUENCHED; DRAW TEMP. 800° F

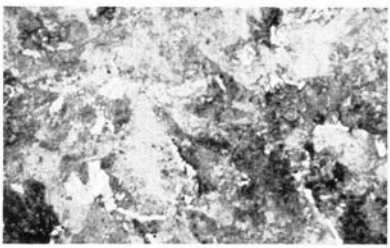

RIM-QUENCHED; DRAW TEMP. 400° F

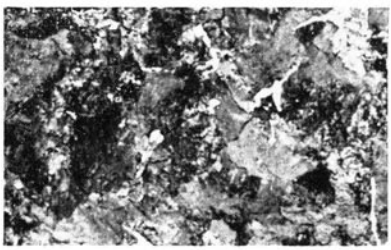

OIL-QUENCHED; DRAW TEMP. 400° F

Untreated

FIG. 6. MICROGRAPHS: STRUCTURE OF UNTREATED WHEEL COMPARED WITH RIM-QUENCHED AND OIL-QUENCHED WHEELS DRAWN AT INDICATED TEMPERATURES

The areas shown were on a radial plane approximately 1/8 in. below the tread surface. Magnification 600X.

RIM, DROP-FORGED WHEEL

RIM, ROLLED STEEL WHEEL

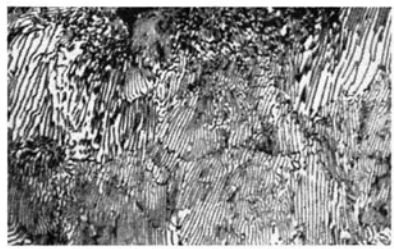

PLATE, DROP-FORGED WHEEL

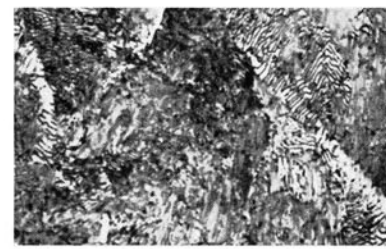

PLATE, ROLLED STEEL WHEEL

FIG. 7. MICROGRAPHS: STRUCTURE OF DROP-FORGED AND ROLLED STEEL WHEELS

The area shown for the rim structure was on a radial plane approximately ⅛ in. below the tread surface, and the area shown for the plate structure was on a radial plane at approximately the center of the plate. Both wheels received the same heat treatment after the hot-forming operation. Magnification 600X.

ing the three draw temperatures mentioned above. Although micrographs were obtained for wheels having the other draw temperatures, only the three representative micrographs are shown. No important metallurgical changes were noted until the 1200 deg F draw temperature was reached. Photomicrographs of the wheels drawn at 1200 deg F indicate spheroidization of cementite in the pearlite.

The photomicrographs of the structure at the center of the tread and the center of the plate of the drop-forged and rolled steel untested wheels are shown in Fig. 7. Additional sections of the wheel were examined and the structure was found to be similar to that shown. The drop-forged and rolled steel wheels were produced from the same heat of steel and received the same heat treatment after the forming process, the only difference being in the method used in the hot-forming operation. There is no significant difference in microstructure between the drop-forged and the rolled steel wheels.

When a steel car wheel is subjected to a standard drag test the

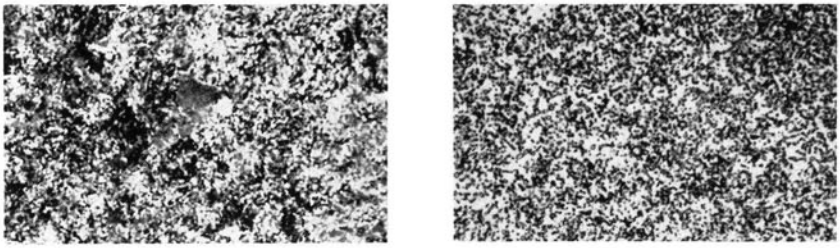

STRUCTURE 0.050″ BELOW TREAD STRUCTURE 0.175″ BELOW TREAD

FIG. 8. MICROGRAPHS: STRUCTURE BELOW TREAD AFTER WHEEL WAS SUBJECTED TO 75 DRAG TESTS
Rim-quenched wheel drawn at 800 deg F. Magnification 600X

tread of the wheel is heated to an austenitizing temperature. Figure 8 shows the microstructure below the surface of the tread of a rim-quenched wheel, drawn at 800 deg F, after it was subjected to 75 standard drag tests. The structure at the surface of the tread and to a depth of approximately 0.15 in. is primarily fine pearlite and free ferrite, with some carbides noted. The grain size of this area appears to be finer than that of the original structure; it indicates a transformation as a result of heating into the lower part of the austenitic range. From a depth of 0.15 in. to 0.30 in. below the center of the tread is a zone of spheroidization. The size and distribution of the spheroids are probably a function of the number and severity of brake applications. Traces of spheroidization were noted at varying depths below this region. The actual depth of the heat-affected zone is also related to the number and severity of the brake applications and the location on the wheel from which the specimen was removed.

As previously mentioned, the region between 0.15 in. and 0.30 in. below the surface of the tread was spheroidized; however, it should be borne in mind that the foregoing results were obtained by standard drag tests and that the depth is not necessarily the same at which spheroidization might occur in wheels subjected to railroad service. In service the depth of the heat-affected zone depends on the type of brake application and such other factors as load, rail, and weather conditions. However, the tread of the wheel can definitely be heated to an austenitizing temperature by brake shoe action. Once this temperature has been exceeded the hardness of the tread will, for practical purposes, depend on the type of quench the material receives, a higher hardness being obtained with faster cooling rates.

III. Test Procedure

7. *Testing Equipment*

The general design of the wheel testing machine is shown in Figs. 9 and 10. In Fig. 10 is shown a test wheel keyed to the main shaft; the main shaft also carries a heavy flywheel as shown in Fig. 9. A 300-hp steam engine supplies power to the main shaft through a flat belt and a positive clutch. By means of the clutch the main

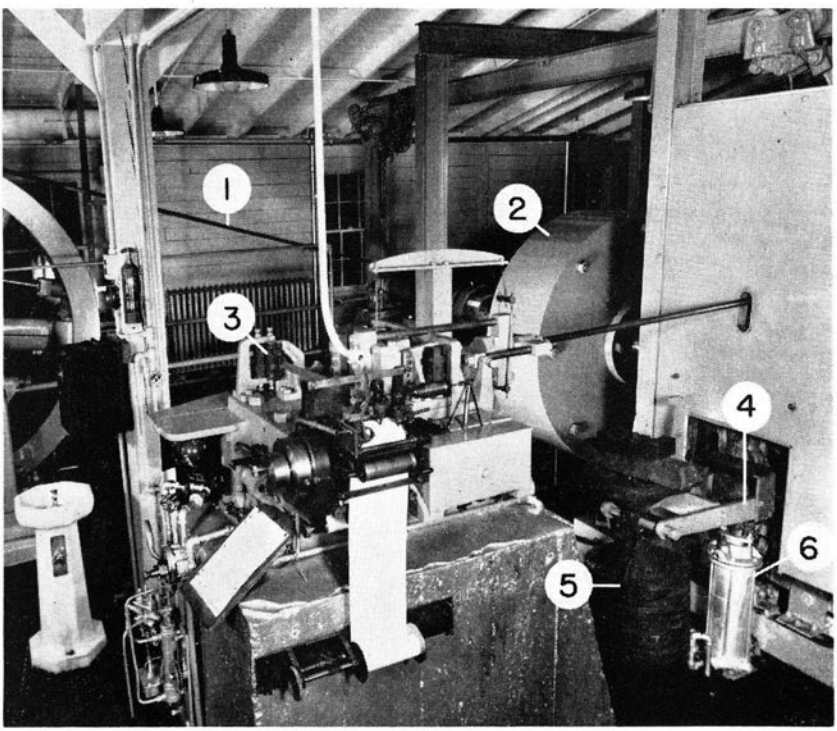

Fig. 9. Interior View of Wheel Testing Laboratory

(1) Transmission belt; (2) flywheel; (3) recording dynamometer; (4) loading lever; (5) dead weights; and (6) air cylinder.

shaft can be disconnected from the steam engine at any desired speed. The revolving mass of the main shaft, the flywheel, and a 36-in.-diam car wheel is equivalent to the energy of 20,000 lb moving at the peripheral speed of the 36-in.-diam car wheel. This represents the energy to be dissipated by each wheel of a passenger car carrying 20,000 lb per wheel when it is stopped from a given speed by the brake shoes.

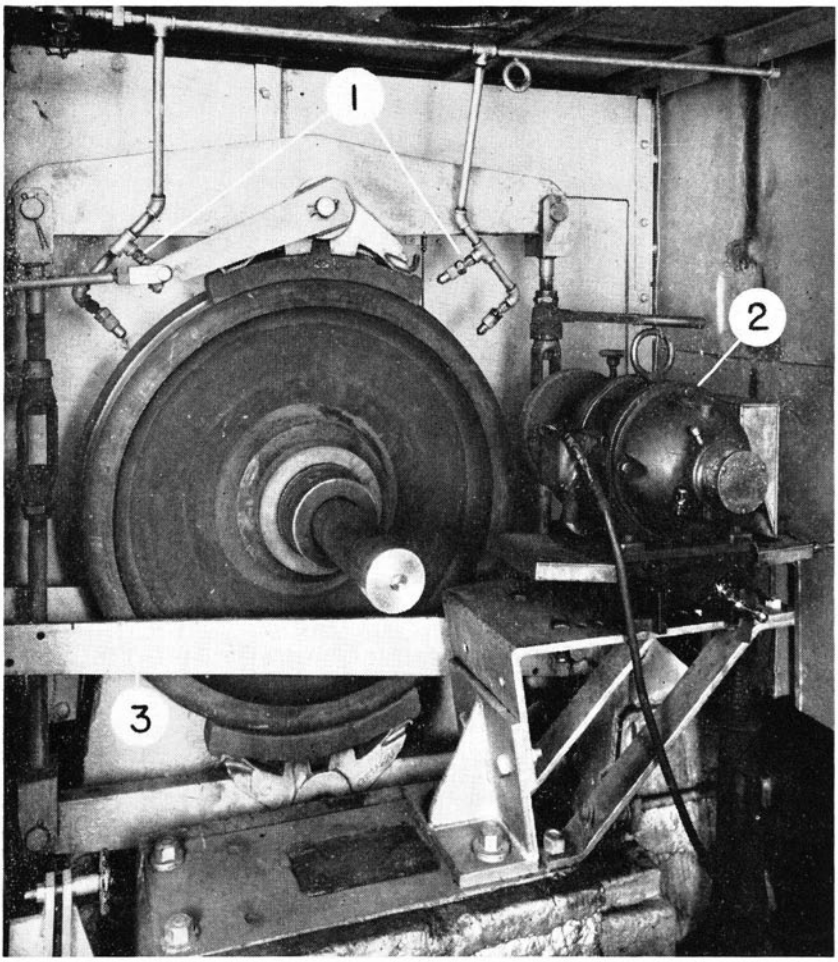

FIG. 10. CAR WHEEL IN TESTING MACHINE
(1) Cooling nozzles; (2) grinder; and (3) loading lever

Two standard brake shoes are applied to the wheel by a clasp brake arrangement as shown in Fig. 10. The brake shoes are forced against the wheel by dead weights through a lever mechanism. The brake shoe pressure can be varied from zero to 20,000 lb. The total frictional force developed between the upper brake shoe and the wheel is measured by the dynamometer shown in Fig. 9. A tachometer measures the number of revolutions per minute of the car wheel, and a revolution counter measures the total number of revolutions of the car wheel during a test.

8. *The Drag Test*

In order to establish a drag test procedure for testing wheels, four variables have to be considered: peripheral speed of the wheel, duration of test, brake shoe pressure (pounds), and the feasibility of using a simulated thermal crack.

At the beginning of the investigation the speed selected was 50 mph, a brake shoe pressure of approximately 3000 lb was used, and a duration of test of 30 min was selected. Under these conditions it was found that the shoes became so soft because of the excessive heat that they would last only 15–25 min. To attain a 30-min duration of test, the brake shoe pressure was reduced to 2600 lb. Even at this reduced pressure the shoes would not always last a full 30 min. To increase the life of the shoes so that a 30-min drag test could be run, an intermittent brake shoe application was introduced. The brake shoes were applied for 50 sec and released for 10 sec out of each minute. By applying the brake shoes intermittently, they would last 15 drag tests with a shoe pressure of 3000 lb and would last 8 drag tests with the shoe pressure increased to 4000 lb. Except for a few wheels used in the development of the drag test procedure, all wheel tests reported in this bulletin were run with intermittent brake shoe application.

At the beginning of the investigation the drag tests were performed without a simulated thermal crack. The wheels were first subjected to a number of drag tests and were then removed from the testing machine, and a radial saw cut was made to determine whether fracture would occur. If the wheel fractured during the saw cut, the fracture generally occurred just before or just as the saw cut passed through the rim. The relative merits of a wheel were determined by the number of drag tests that had been run on the wheel and whether or not fracture occurred on the saw cut. The results of testing wheels without a simulated thermal crack are shown in Table 3. A considerable number of variables were considered in these wheel tests: carbon content, heat treatment, shoe pressure, type of drag tests, and number of drags. The main purpose of these tests was to develop a test procedure. Although the data in Table 3 do show trends, the spread in the test data for different types of wheels is too great to permit definite conclusions.

To develop a more definite test the feasibility of a simulated thermal crack was considered. The notch used to simulate a thermal crack was a radial saw cut extending into the rim of the wheel. This saw cut was then filled with a snug-fitting shim of the same material as the wheel material. The shim was used to make the artificial

TABLE 3

DRAG TEST RESULTS OF WHEELS INITIALLY FREE OF SIMULATED THERMAL CRACK

36-in. basic design wheels. All tests at 50 mph.

Wheel Test No.	Carbon, percent	Heat Treatment	Shoe Pressure, lb	Time of Drag, min	Type of Drag	Number of Drags	Fracture on Saw Cut	Depth of Rim Saw Cut, percent
1 IAO1D	0.52	E	3 000	20	Continuous	10	No	100
8 IBO1D	0.61	E	3 000	20	Continuous	14	No	100
14 ICO1D	0.72	E	3 000	20	Continuous	12	Yes	90
19 SAW1D	0.48	W	3 000	20	Continuous	10	No	100
31 BAR1D	0.52	R	2 600	30	Continuous	12	No	100
32 BAR1D	0.52	R	2 600	30	Continuous	20	No	100
37 BBR1D	0.61	R	2 600	30	Continuous	8	No	100
38 BBR1D	0.61	R	2 600	30	Continuous	22	No	100
43 BCR1D	0.71	R	2 600	30	Continuous	8	Yes	100
44 BCR1D	0.71	R	2 600	30	Continuous	8	Yes	100
48 BCR1D	0.71	R	2 600	30	Continuous	14	Yes	100
2 IAO1D	0.52	E	2 600	30	Continuous	12	Yes	100
56 IEO1D	0.59	E	2 600	30	Continuous	10	Yes	100
57 IEO1D	0.59	E	2 600	30	Continuous	10	Yes	100
7 IBO1D	0.61	E	2 600	30	Continuous	6	Yes	95
13 ICO1D	0.72	E	2 600	30	Continuous	18	Yes	100
50 IDO1D	0.75	E	2 600	30	Continuous	10	Yes	100
51 IDO1D	0.75	E	2 600	30	Continuous	10	Yes	100
20 SAW1D	0.48	W	2 600	30	Continuous	8	No	100
131 IBR1D	0.61	R	3 000	30	Intermittent	10	No	100
67 ICR1D	0.73	R	3 000	30	Intermittent	12	Yes	100
68 ICR1D	0.73	R	3 000	30	Intermittent	6	Yes	100
77 ICR1D	0.73	R	3 000	30	Intermittent	12	Yes	90
78 ICR1D	0.73	R	3 000	30	Intermittent	6	Yes	90
80 ICR1D	0.73	R	3 000	30	Intermittent	3	Yes	100
104 IBO1D	0.61	E	3 000	30	Intermittent	10	Yes	100
112 IBO1D	0.61	E	3 000	30	Intermittent	10	No	100
115 IBO1D	0.61	E	3 000	30	Intermittent	10	No	100
124 IBO1D	0.61	E	3 000	30	Intermittent	10	Yes	100
62 ICO1D	0.73	E	3 000	30	Intermittent	12	Yes	70
63 ICO1D	0.73	E	3 000	30	Intermittent	6	Yes	80
65 ICO1D	0.73	E	3 000	30	Intermittent	1	Yes	95
72 ICO1D	0.73	E	3 000	30	Intermittent	6	Yes	100
73 ICO1D	0.73	E	3 000	30	Intermittent	3	Yes	100
75 ICO1D	0.73	E	3 000	30	Intermittent	1	Yes	100
87 IFO1D	0.73	E	3 000	30	Intermittent	6	Yes	100
88 IFO1D	0.73	E	3 000	30	Intermittent	3	Yes	100
54 IDO1D	0.75	E	3 000	30	Intermittent	14	Yes	100
82 ICU1D	0.73	U	3 000	30	Intermittent	12	Yes	100
83 ICU1D	0.73	U	3 000	30	Intermittent	6	Yes	100

thermal crack more nearly resemble the thermal crack that occurs in service. If a shim was not used, it was found, the saw cut would close during the drag test as the rim was heated. It was thought that by preventing this closing of the saw cut, the stresses developed at the bottom of the saw cut by drag testing would more nearly approach the stresses occurring at the bottom of a thermal crack.

Exploratory tests proved that a wheel could be fractured on the testing machine if a simulated thermal crack was introduced in the rim of the wheel. Two tests were made with a saw cut extending 100 percent through the rim. Each of these wheels fractured after the first drag; thus a 100 percent saw cut proved to be too severe.

TABLE 4

EFFECT OF SPEED ON NUMBER OF DRAG TESTS REQUIRED TO PRODUCE FRACTURE

36-in. Class B basic design wheels from heat 34519, tested with 50% saw cut and shim and 3000-lb intermittent brake shoe application

Wheel Test Number	Heat Treatment	Speed, mph	Number of Drags for Fracture
129 IBR1D	R	50	15
132 IBR1D	R	50	9
106 IBO1D	E	50	4
118 IBO1D	E	50	5
130 IBR1D	R	45	30
133 IBR1D	R	45	23
134 IBR1D	R	45	22
140 IBR1D	R	45	39
141 IBR1D	R	45	40
151 IBR1D	R	45	50
114 IBO1D	E	45	9
120 IBO1D	E	45	8
135 IBO1D	E	45	9
136 IBO1D	E	45	3
137 IBO1D	E	45	8
139 IBO1D	E	45	15
149 IBO1D	E	45	17
150 IBO1D	E	45	8
110 IBO1D	E	40	12
119 IBO1D	E	40	9
122 IBO1D	E	40	13
113 IBO1D	E	35	17
121 IBO1D	E	35	34
125 IBO1D	E	35	10
128 IBO1D	E	35	13

The saw cut depth was then decreased to 50 percent of the rim thickness. The drag test results for the 50 percent saw cut depth and at various speeds are shown in Table 4. The data therein indicate the possibility of using the number of drags required to produce fracture as a measure of the ability of a wheel to resist fracture.

To amplify the differences between the types of wheels, it was decided to use a test procedure such that the wheels most resistant to fracture would fail at a large number of drags. The severity of the test was varied by changing the peripheral speed of the wheel while keeping the shoe pressure at 3000 lb, the duration of test at 30 min, and the saw cut depth at 50 percent. The plot of the test results showing the effect of speed on the number of drag tests to produce fracture is given in Fig. 11. From these results it appears that the speed of 50 mph resulted in a drag test which was too severe. The low speeds were objectionable because the brake shoes were found to cut into the wheel tread; this was especially true of the tests run at 35 mph. In order to use as high a speed as possible so as to eliminate possible cutting of the wheel tread by the brake shoe and at the same time have a drag test that would give comparative results, 45 mph was chosen as the standard test speed.

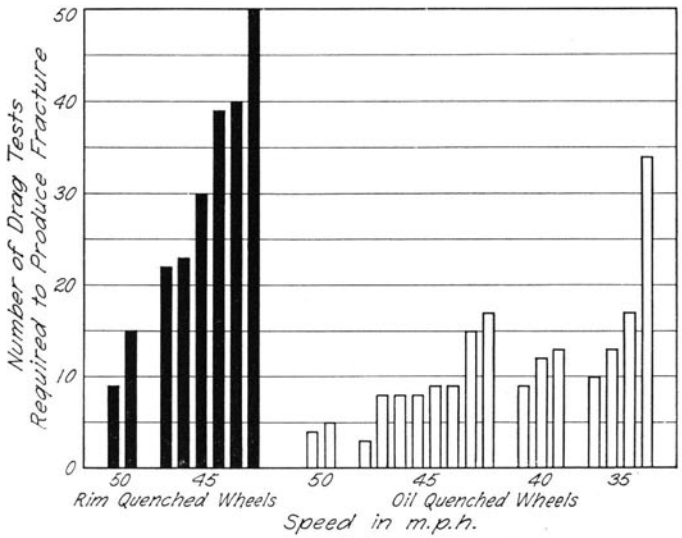

FIG. 11. EFFECT OF SPEED ON NUMBER OF DRAG TESTS REQUIRED TO PRODUCE FRACTURE
Class B, 36-in.-diam wheels

From the above-mentioned results the standard drag test procedure was developed. The procedure consisted, first, in preparing a wheel with a saw cut and snug-fitting shim extending 50 percent of the depth of the rim; the wheel was then placed on the testing machine, where it was subjected to drag tests. Each drag test consisted of rotating the wheel at a peripheral speed of 45 mph while two brake shoes were held against the wheel, each under a pressure of 3000 lb, for 50 sec and released 10 sec out of every minute for a total duration of 30 min. After the drag test the wheel was allowed to cool in air for 15 min, and the rim and plate were then sprayed with water to cool to room temperature. Whenever a new pair of brake shoes were required the car wheel was ground until the tread was cylindrical and all brake shoe material removed. Most of the drag test data presented in this bulletin were obtained under the standard drag test procedure. If the wheel did not fracture after 50 standard drag tests, testing was discontinued for the most part, because of the time involved. In order to fracture some types of wheels with fewer drag tests a more severe type of drag test was devised. The changes in the standard drag test procedure required to obtain the more severe drag test were an increase in saw cut depth to 75 percent and an increase of the shoe pressure to 4000 lb.

An enormous amount of energy is expended while dragging a car wheel that has two brake shoes sliding against its tread. Under a standard drag test it required approximately 100 hp to keep the wheel rotating at 45 mph. From the measurement of the tangential pull developed between the wheel and the upper brake shoe the coefficient of friction was determined by dividing the tangential pull by the shoe pressure (pounds). The values of the coefficient of friction are listed in Appendix B.

9. *The Stop Test*

A stop test is designed to simulate the treatment that a passenger car wheel might receive when a train is stopped from a high speed by an emergency brake application. In service a wheel will receive many types of brake shoe applications at various speeds and pressures. In the laboratory, however, it is advantageous to standardize and thereby to eliminate as many variables as possible. As previously mentioned, the wheel testing machine at the University of Illinois has a revolving mass, keyed to the same shaft as the test wheel, whose kinetic energy is equivalent to the energy of 20,000 lb moving at the same linear velocity as the periphery of a 36-in.-diam test car wheel; this may be considered as a 20,000-lb equivalent rail wheel load. The standard stop test on a 36-in.-diam car wheel was a stop made from an initial surface speed of 115 mph with clasp brakes (see Fig. 10) and a pressure of 20,000 lb on each shoe (200 percent braking ratio). After each stop the wheel was allowed to cool in air for 8 min, and then was cooled to room temperature by running water on the tread while the wheel revolved slowly. If thermal cracking occurred, the cracks usually developed about 2 min after the water was applied to the tread. All wheels that were stop-tested were ground cylindrical before each test so that no brake shoe material remained on the tread of the wheels. As little wheel material as possible was removed during each grinding. A 33-in.-diam wheel received approximately the same treatment as the 36-in.-diam wheel except that the initial tread speed was reduced to 105 mph, since the total energy to be dissipated was kept the same for both the 36-in. and the 33-in.-diam wheels. The kinetic energy of the flywheel is dependent only upon the number of revolutions per minute of the main shaft; therefore, the equivalent rail wheel load was automatically increased to 24,000 lb for the 33-in. wheel, since the kinetic energy of 24,000 lb moving at 105 mph is the same as 20,000 lb moving at 115 mph. In each case, the total kinetic energy of the revolving mass was approximately 9,000,000 ft-lb.

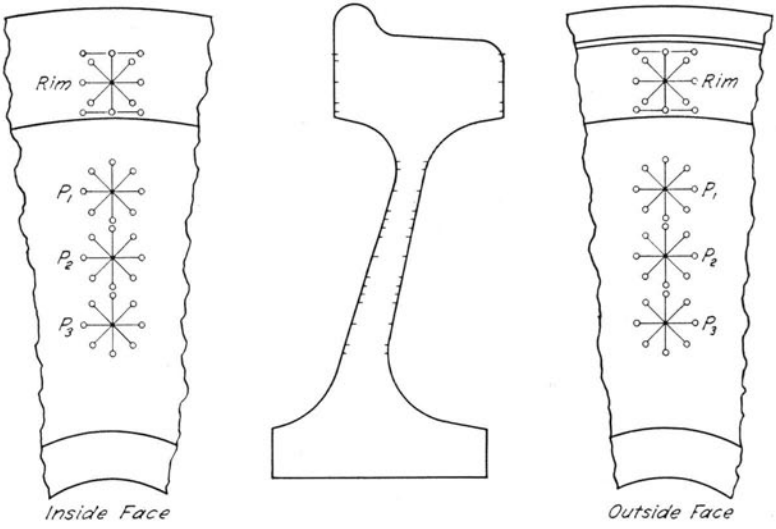

FIG. 12. LOCATION OF GAGE LINES FOR DETERMINING STRAINS

The number of revolutions that the wheel of given diameter makes before it is stopped depends upon the coefficient of friction developed between the wheel and the brake shoes. The average value of the coefficient of friction for each stop-tested wheel is given in Appendix B. It was obtained by dividing the total energy dissipated, by the product of the shoe pressure (pounds) and the peripheral distance traveled.

10. *Strain Determination and Rim Movement*

The drag testing of wheels developed tensile stresses in the tangential direction in the rims of wheels which increased with the number of tests and which in most cases eventually reached sufficient magnitude to produce wheel failures through the saw cuts. This change of stress was the result of plastic deformation which occurred during the test. In order to obtain strain data for a stress analysis, strains were measured at the various locations on the wheel as shown in Fig. 12. Using a Number 54 drill, strain gage holes for a 2-in. gage length were drilled in the wheel in the form of strain rosettes on the inner and outer face of the wheel on the rim, on the plate near the rim (P_1), on the center of the plate (P_2), and on the plate near the hub (P_3). In most cases these strain rosettes were drilled on two different radial lines at 90 deg to each other. For each strain rosette, strains were measured in four directions

at 45 deg. Only three readings were needed to determine the principal strains. The fourth reading was used as a check. Several methods are used for determining principal stresses from the strain data obtained from the rosettes. The method employed in this investigation was greatly simplified by the use of a specially constructed slide rule[1] which enables a rapid determination of the angle at which maximum principal stress occurs and the magnitudes of the principal stresses.

The strains were measured with an Olsen-de-Shazer strain gage having a 2-in. gage length. The sensitivity of the gage was such that 30 divisions on the dial represented 0.001 in. per in. strain. In taking strain readings, a number of readings were obtained for each pair of strain gage holes until the successive readings would agree within one division.

A photograph of two Olsen-de-Shazer gages is shown in Fig. 13. The legs on one of the gages were 1⅝ in. long and were used in taking strain readings at the bottom of ⅜-in.-diam holes drilled to depths of as much as 1½ in. below the surface of the rim of the wheel to determine the residual stresses at these depths. The gage, shown at the bottom of Fig. 13, measured the axial movement of the rim with respect to the hub of the wheel. The Ames dial measured the rim movement directly in increments of 0.001 in. for each dial division. All measurements on the wheels were made at room temperature.

In the determination of residual stresses on the surface of the wheel initial strain readings were taken for each of the rosettes before the wheel was sawed. Each rosette was sawed out of the wheel by cutting out a 2½-in.-by-2½-in.-by-¼-in. block. The differences in the initial and final strain reading were used in calculating the principal residual stresses at the various locations shown in Fig. 12.

In order to determine the residual stresses at various depths below the surface of the rim of the wheel, ⅜-in.-diam holes were drilled to the desired depths. A Number 54 drill was then used to drill strain gage holes at the bottoms of the large holes. Initial strain readings were taken before the wheel was sawed. Each gage line was sawed out of the wheel in the form of a block which was approximately ⅜ in. square and 2½ in. long, and final strain readings were then taken. Residual strains were measured in the circumferential direction, and in some tests in the axial direction. Since all three principal strains were not measured, the resulting residual stress determinations may be somewhat in error; however, the data are believed to be valuable for comparative purposes.

[1] See "Stresses in Car Wheels" by Reid L. Kenyon and Harry Tobin, *Railway Mechanical Engineer*, December 1941-January 1942.

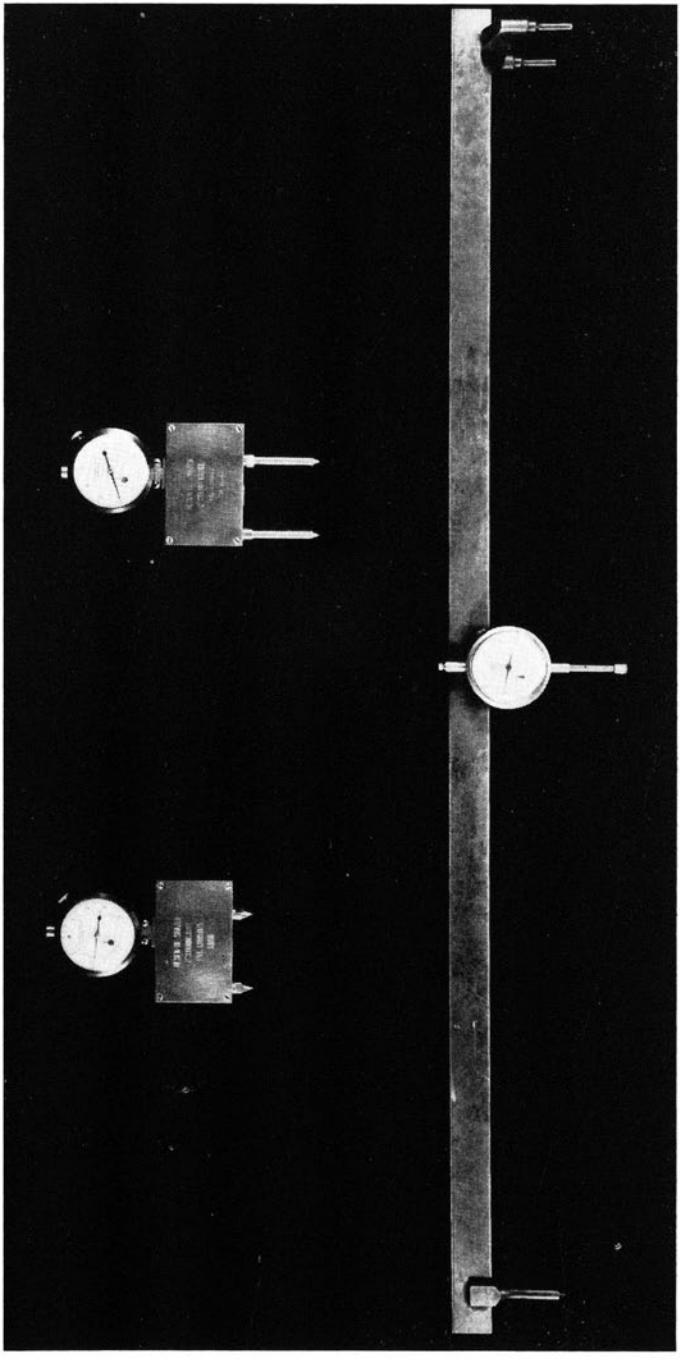

FIG. 13. OLSEN-DE-SHAZER 2-IN. STRAIN GAGES AND RIM MOVEMENT GAGE

IV. Effect of Heat Treatment on Test Results

11. *Drag Test Results of Rim-Quenched, Oil-Quenched and Untreated Wheels*

The results of drag testing are affected both by the type of heat treatment and by the draw temperature for a given type of heat treatment. The tests reported in this bulletin indicate that the rim-quenched wheels are superior to the oil-quenched wheels in their ability to resist the wheel fractures resulting from drag testing. The differences in the drag test results between the rim-quenched and oil-quenched wheels are attributed to the different types of residual stress distributions which result from the different heat treatments. The strain data which are required to analyze this problem are presented in Chapter VIII and Appendix A.

The drag test data showing the effect of heat treatment are presented in Tables 4 and 5 and plotted in Figs. 11 and 14. The data presented in Table 4 and plotted in Fig. 11 are drag test results for rim-quenched and oil-quenched wheels of the Class B Chemistry. At a speed of 45 mph the average number of drags required to produce fracture in the rim-quenched wheels was 34; for the oil-quenched wheels an average of approximately 10 drag tests was required to produce fracture. Thus the rim-quenched Class B wheels were about three times more resistant to wheel fracture than the oil-quenched Class B wheels. This same trend is also shown at a speed of 50 mph.

The data presented in Table 5 and plotted in Fig. 14 are drag test results for rim-quenched, oil-quenched, and untreated wheels of the Class C chemistry. The data plotted on Fig. 14a are for wheels having a rim thickness of 2 in.; those plotted on Fig. 14b are for wheels having a rim thickness of 2½ in. In each case the data are segregated into groups of rim-quenched and oil-quenched wheels for each of the various draw temperatures, while the untreated wheels are shown as a separate group for comparative purposes. It will be noticed that, regardless of the rim thickness or the draw temperature, the rim-quenched wheels are far more resistant to wheel fractures than the oil-quenched wheels. If the residual stress distribution is the important variable, the least difference between the two heat treatments would be expected, and was obtained, for the highest draw temperature of 1200 deg F. Presumably this arises from the fact that the residual stresses had become so small that the differences in stress distribution did not have an appreciable effect on drag test results. Although the wheels with the 1200 deg F draw temperature showed good resistance to wheel fracture, this high draw temperature is objectionable because of the low hardness.

TABLE 5

EFFECT OF DRAW TEMPERATURE ON NUMBER OF DRAG TESTS REQUIRED TO PRODUCE FRACTURE

36-in. Class C wheels having a plate thickness of 1 in. by 1¼ in., tested with standard test conditions

Wheel Test Number	Heat Number	Draw Temp, deg F	Heat Treatment	Nominal Rim Thickness, inches	Number of Drags	Fracture
234 ICR5D	40307	600	R	2	37	Yes
245 ICR5D	40307	600	R	2	34	Yes
237 ICO5D	40307	600	E	2	11	Yes
240 ICR5D	40307	800	R	2	50	No
243 ICR5D	40307	800	R	2	50	No
239 ICO5D	40307	800	E	2	18	Yes
244 ICO5D	40307	800	E	2	31	Yes
178 ICR5D	40307	960	R	2	31	Yes
183 ICR5D	40307	960	R	2	25	Yes
197 ICO5D	40307	960	E	2	18	Yes
204 ICO5D	40307	960	E	2	17	Yes
316 ICR1D	921614	400	R	2½	24	Yes
329 ICR1D	921614	400	R	2½	14	Yes
352 ICR1D	921614	400	R	2½	19	Yes
298 ICO1D	921614	400	E	2½	6	Yes
358 ICO1D	921614	400	E	2½	4	Yes
315 ICR1D	921614	700	R	2½	48	Yes
351 ICR1D	921614	700	R	2½	23	Yes
364 ICR1D	921614	700	R	2½	24	Yes
368 ICR1D	921614	700	R	2½	60	Yes
297 ICO1D	921614	700	E	2½	5	Yes
357 ICO1D	921614	700	E	2½	4	Yes
314 ICR1D	921614	800	R	2½	48	Yes
350 ICR1D	921614	800	R	2½	19	Yes
365 ICR1D	921614	800	R	2½	75	No
369 ICR1D	921614	800	R	2½	63	Yes
295 ICO1D	921614	800	E	2½	8	Yes
322 ICO1D	921614	800	E	2½	16	Yes
356 ICO1D	921614	800	E	2½	14	Yes
333 ICR1D	921614	860	R	2½	24	Yes
335 ICR1D	921614	860	R	2½	50	No
337 ICR1D	921614	860	R	2½	50	No
338 ICR1D	921614	860	R	2½	37	Yes
339 ICR1D	921614	860	R	2½	50	No
340 ICR1D	921614	860	R	2½	47	Yes
313 ICR1D	921614	900	R	2½	50	No
349 ICR1D	921614	900	R	2½	22	Yes
366 ICR1D	921614	900	R	2½	27	Yes
294 ICO1D	921614	900	E	2½	12	Yes
321 ICO1D	921614	900	E	2½	13	Yes
355 ICO1D	921614	900	E	2½	35	Yes
300 ICR1D	921614	1 000	R	2½	38	Yes
348 ICR1D	921614	1 000	R	2½	28	Yes
367 ICR1D	921614	1 000	R	2½	13	Yes
293 ICO1D	921614	1 000	E	2½	6	Yes
320 ICO1D	921614	1 000	E	2½	12	Yes
354 ICO1D	921614	1 000	E	2½	9	Yes
299 ICR1D	921614	1 200	R	2½	50	No
330 ICR1D	921614	1 200	R	2½	20	Yes
347 ICR1D	921614	1 200	R	2½	33	Yes
292 ICO1D	921614	1 200	E	2½	23	Yes
319 ICO1D	921614	1 200	E	2½	47	Yes
353 ICO1D	921614	1 200	E	2½	12	Yes
317 ICU1D	921614	.....	U	2½	8	Yes
318 ICU1D	921614	.....	U	2½	13	Yes
359 ICU1D	921614	.....	U	2½	4	Yes

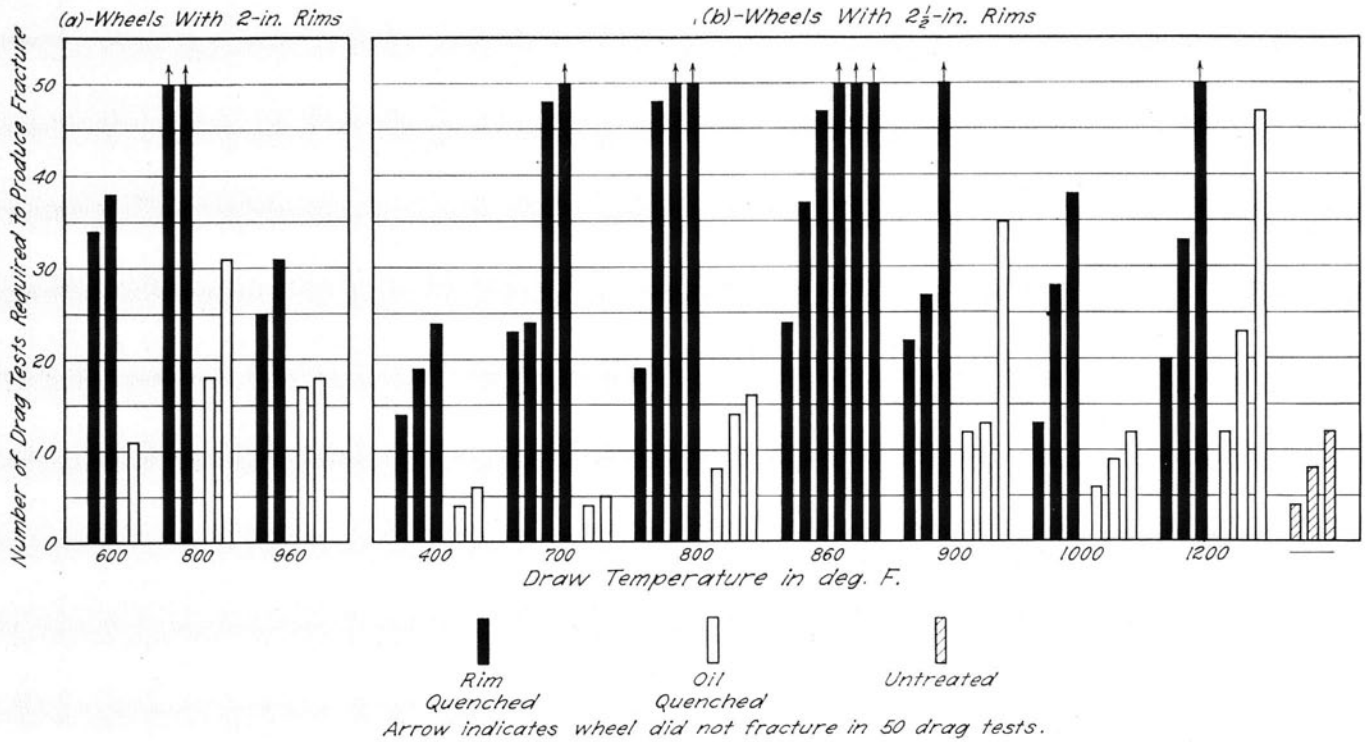

FIG. 14. EFFECT OF DRAW TEMPERATURE ON NUMBER OF DRAG TESTS REQUIRED TO PRODUCE FRACTURE
Class C, 36-in.-diam wheels

12. *Effect of Draw Temperature on Drag Test Results*

A number of wheels have been tested to determine the effect of draw temperature on the number of drag tests required to produce fracture in rim-quenched and oil-quenched wheels as produced by one manufacturer. The drag test data for the wheels used in the draw temperature investigation are presented in Table 5 and plotted in Fig. 14. These wheels were all Class C wheels. The group of wheels having 2-in. rim thicknesses were all from the same heat of steel; the drag test data for these wheels are plotted in Fig. 14a. The wheels having 2½-in. rim thicknesses were from another heat of steel; the drag test data for these wheels are plotted in Fig. 14b. The large amount of scatter of the test data makes it difficult to draw definite conclusions. Except, perhaps, for the lowest draw temperature the trend of the data indicate that the draw temperature has little effect on the number of drag tests required to produce fracture.

The effect of draw temperature upon the severity of fracture on the rim-quenched and oil-quenched wheels appears to be an important consideration. In Fig. 15 are shown fractures of wheels given the two types of heat treatment and drawn at temperatures of 1200 deg F, 1000 deg F, 900 deg F, 800 deg F, 700 deg F, and 400 deg F. The severity of fracture of the rim-quenched wheels decreases with a decrease of draw temperature; the opposite is true for the oil-quenched wheels.

FIG. 15. EFFECT OF DRAW TEMPERATURE ON SEVERITY OF

WHEEL FRACTURE OF RIM-QUENCHED AND OIL-QUENCHED WHEELS

V. Effect of Changes in Wheel Design on Test Results

13. *Effect of Plate Thickness on Drag Test Results*

Three different changes in wheel design have been investigated to determine the effect of a given change on the resistance of the wheel to fracture. The variables considered are plate thickness, plate location, and rim thickness. Of these, only a decrease in plate thickness has been found to increase appreciably the number of drag tests required to produce wheel fracture. Since a thin plate wheel was

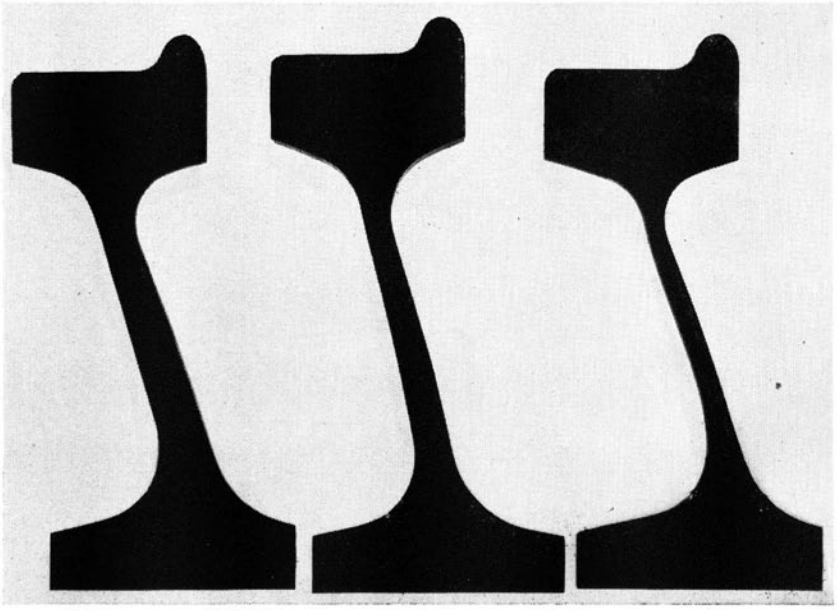

Fig. 16. Cross-Sections of Thick, Intermediate, and Thin Plate Wheels

found to offer great resistance to wheel fracture, static tests and fatigue tests were conducted to determine whether the thin plate would be strong enough to carry service loads.

The wheels which were used to determine the effect of plate thickness on the number of drag tests required to produce fracture were all made from the same heat of steel having Class C and Class U chemistry. These wheels were rim-quenched, oil-quenched and untreated 36-in.-diam wheels having a 2-in. rim thickness, and untreated 33-in.-diam wheels having a 1½-in. rim thickness.

TABLE 6

EFFECT OF PLATE THICKNESS ON NUMBER OF DRAG TESTS REQUIRED TO PRODUCE FRACTURE IN RIM-QUENCHED, OIL-QUENCHED, AND UNTREATED WHEELS

36-in. Class C wheels from heat 40307, having a rim thickness of 2 in.

Wheel Test Number	Nominal Plate Thickness* A, inches	B, inches	Brake Shoe Pressure, lb	Depth Saw Cut, percent	Number of Drags	Fracture
Standard Drag Test, Rim-Quenched Wheels						
178 ICR5D	1	1 1/4	3 000	50	31	Yes
183 ICR5D	1	1 1/4	3 000	50	25	Yes
199 ICR8D	3/4	7/8	3 000	50	50	No
200 ICR8D	3/4	7/8	3 000	50	50	No
180 ICR7D	1/2	5/8	3 000	50	50	No
184 ICR7D	1/2	5/8	3 000	50	50	No
203 ICR7D	1/2	5/8	3 000	50	50	No
205 ICR7D	1/2	5/8	3 000	50	50	No
207 ICR7D	1/2	5/8	3 000	50	50	No
Severe Drag Test, Rim-Quenched Wheels						
238 ICR5D	1	1 1/4	4 000	75	6	Yes
229 ICR8D	3/4	7/8	4 000	75	14	Yes
241 ICR8D	3/4	7/8	4 000	75	8	Yes
231 ICR7D	1/2	5/8	4 000	75	30	Yes
242 ICR7D	1/2	5/8	4 000	75	19	Yes
Standard Drag Test, Oil-Quenched Wheels						
197 ICO5D	1	1 1/4	3 000	50	18	Yes
204 ICO5D	1	1 1/4	3 000	50	17	Yes
209 ICO8D	3/4	7/8	3 000	50	50	No
214 ICO8D	3/4	7/8	3 000	50	50	No
198 ICO7D	1/2	5/8	3 000	50	50	No
206 ICO7D	1/2	5/8	3 000	50	50	No
Standard Drag Test, Untreated Wheels						
208 ICU5D	1	1 1/4	3 000	50	11	Yes
212 ICU5D	1	1 1/4	3 000	50	17	Yes
211 ICU8D	3/4	7/8	3 000	50	50	No
213 ICU8D	3/4	7/8	3 000	50	22	Yes
210 ICU7D	1/2	5/8	3 000	50	50	No
215 ICU7D	1/2	5/8	3 000	50	50	No

* See Fig. 3.

Three plate thicknesses were considered for the 36-in.-diam wheels: the thick plate of 1 in. by 1¼ in., the intermediate plate thickness of ¾ in. by ⅞ in., and the thin plate of ½ in. by ⅝ in. A photograph of these three wheel cross-sections is shown in Fig. 16. For the 33-in.-diam wheels only two plate thicknesses were considered, a thick plate of ¾ in. by 1 in. and a thin plate of ½ in. by ⅝ in. Most of the intermediate and thin plate wheels were contour-machined from wheels that were originally thick plate wheels. Two thin plate wheels which were rolled to the required plate thickness gave the same results as the wheels which were contour-machined.

The drag test data for the 36-in.-diam wheels are presented in Table 6 and plotted in Fig. 17. The standard drag test procedure was sufficiently severe to produce fracture in the thick plate wheels,

but only one intermediate plate and none of the thin plate wheels could be made to fracture when subjected to the standard drag test. Thus the test data obtained under the standard drag test procedure indicated that a decrease in plate thickness resulted in a much superior wheel for resisting wheel fracture, but the test results gave no relative magnitudes for comparing the merits of the three plate thicknesses. In order to have a comparison between the wheels of various plate thicknesses, a series of rim-quenched wheels were tested

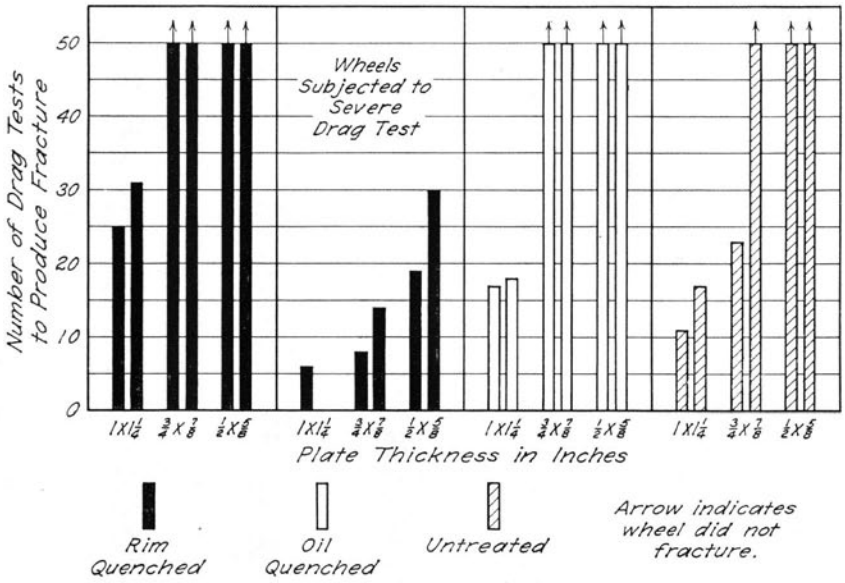

FIG. 17. EFFECT OF PLATE THICKNESS ON NUMBER OF DRAG TESTS REQUIRED TO PRODUCE FRACTURE

Rim-quenched, oil-quenched, and untreated Class C 36-in.-diam wheels

under a more severe drag test which was obtained by increasing the shoe pressure from 3000 lb to 4000 lb and increasing the simulated thermal crack depth from 50 percent to 75 percent of the rim thickness. The drag test results obtained under the severe drag test are also shown in Fig. 17. It will be noted that the intermediate plate wheels required approximately twice the number of drags that were required to produce fracture in the thick plate wheels.

The superiority of the thin plate wheel over the thick plate wheel for resisting wheel fractures was also shown conclusively for the 33-in.-diam untreated wheels when tested by the standard drag test. (See Table 7.) An average of 9 drag tests was required to produce

wheel fracture in thick plate wheels; however, fracture was not produced in any of the thin plate wheels. One thick plate wheel and 3 thin plate wheels were subjected to standard drag tests, except that the tests were run at a constant speed of 35 mph. The thick plate wheel fractured after 10 drag tests, whereas all three of the thin plate wheels withstood 30 drag tests without failure.

Of all the variables considered the plate thickness was found to have the greatest effect on the resistance of 33-in. and 36-in.-diam wheels to wheel fracture. A reduction in plate thickness of the thick

TABLE 7

EFFECT OF PLATE THICKNESS ON NUMBER OF DRAG TESTS REQUIRED TO PRODUCE FRACTURE IN 33-IN. UNTREATED WHEELS

Class U wheels from heat 40307, having a rim thickness of 1½ in.

Wheel Test No.	Nominal Plate Thickness* A, inches	B, inches	Speed, mph	Number of Drag Tests	Fracture
		Standard Test Conditions			
155 ICU3D	¾	1	45	5	Yes
157 ICU3D	¾	1	45	9	Yes
159 ICU3D	¾	1	45	8	Yes
161 ICU3D	¾	1	45	13	Yes
156 ICU4D	½	⅝	45	30	No
158 ICU4D	½	⅝	45	30	No
160 ICU4D	½	⅝	45	50	No
162 ICU4D	½	⅝	45	30	No
		Standard Test Conditions, Except Speed			
174 ICU3D	¾	1	35	10	Yes
173 ICU4D	½	⅝	35	30	No
175 ICU4D	½	⅝	35	30	No
176 ICU4D	½	⅝	35	30	No

* See Fig. 3.

plate (basic)[1] wheel by only ¼ in. was found to increase greatly the number of drag tests required to produce wheel fracture. The wheels with the reduced plate thickness were the only ones that required an increase in the severity of the drag test conditions in order to produce wheel fracture.

14. *Static and Fatigue Tests on Full-Size Thick and Thin Plate Wheels*

Since the thin plate wheels were found to be far superior to the thick plate wheels in their resistance to wheel fracture, additional tests were made to ascertain whether the thin plate would safely withstand loads which may be expected under railroad service conditions[2]. The loads chosen to simulate service conditions were a

[1] See p. 16, Section 4, of the present Bulletin.
[2] See AREA Proceedings, Vol. 49, 1948, pp. 735-746.

20,000-lb vertical rail load and an 8000-lb flange thrust load. The effect of a 20,000-lb flange thrust load was also considered.

Two thin and two thick plates of 36-in.-diam Class C rim-quenched wheels having 2-in. rims were used for the static load tests. Each pair of wheels was pressed on standard axles under standard shop practice. Each wheel and axle assembly was then subjected to static loads, using the equipment described in Bulletin 312 of the Engineering Experiment Station of the University of Illinois.

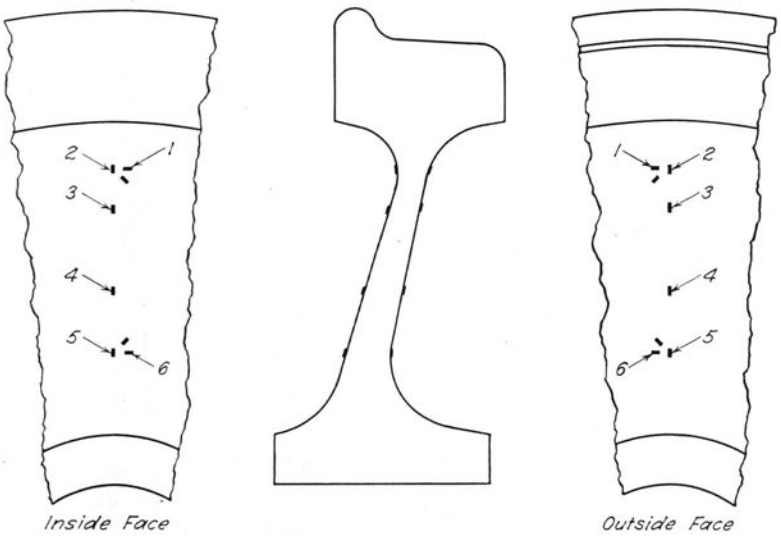

FIG. 18. LOCATION OF GAGE LINES ON WHEELS USED IN STATIC TESTS

Before placing the wheels in the testing machine, ¼-in. SR-4 electrical strain gages were cemented to the inside and outside faces of the plate of each wheel as shown in Fig. 18. At the minimum thickness of the plate near the rim and at the base of the fillet near the hub, strain gage rosettes were used to determine principal strains. After the strain gages were applied, the wheels and axle assembly was placed in the 3,000,000-lb capacity testing machine. Figure 19 shows the equipment for applying either a vertical load alone or a vertical load with a flange thrust load.

Three types of loads were applied: (1) a 20,000-lb vertical load, (2) a 20,000-lb vertical load with an 8000-lb flange thrust load, and

(3) a 20,000-lb vertical load with a 20,000-lb flange thrust load. The stress data obtained under these loads for the thin and thick plate wheels are shown in Table 8. For the thin plate wheels, stresses were determined on a radial gage line below the load point and on a radial gage line 180 deg from the load point; however, only the gage

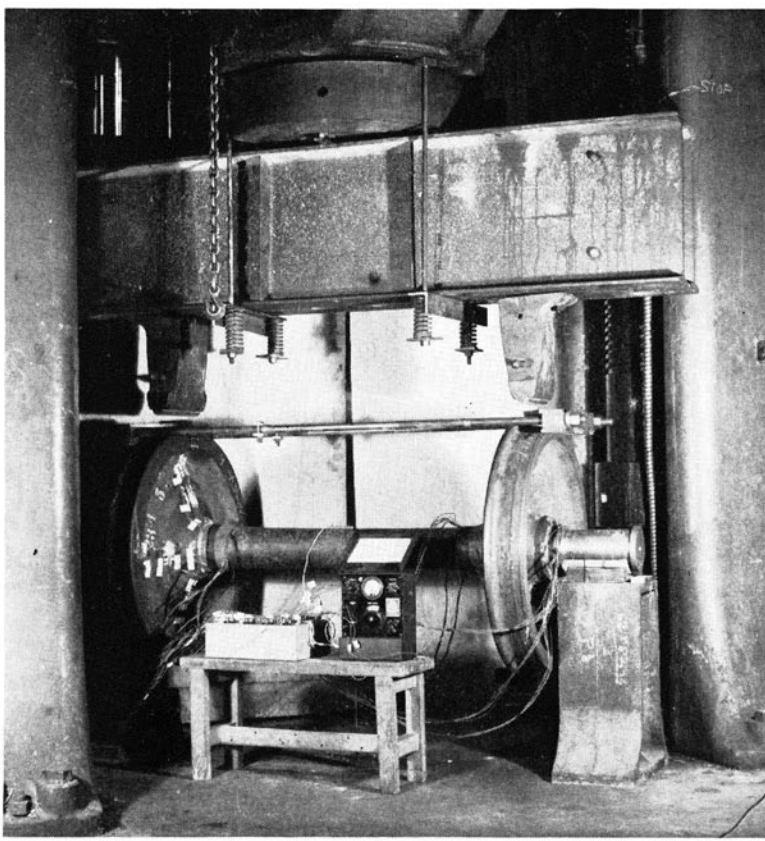

FIG. 19. WHEELS AND AXLE ASSEMBLY IN 3,000,000-LB CAPACITY TESTING MACHINE

line below the load point was considered for the thick plate wheels. The first two loading conditions are assumed to be comparable to service loads. For the 20,000-lb vertical load acting alone or for the 20,000-lb vertical load with the 8000-lb flange thrust load, the maximum stress for either the thin plate or the thick plate wheel was only 8000 p.s.i. This figure seems moderate when one considers

TABLE 8

STRESSES IN WHEELS DUE TO VERTICAL AND FLANGE THRUST LOADS

As determined by ¼-in. electric strain gages on 36-in.-diam Class C wheels with 2-in. rims
Stress × 1,000 p.s.i. + indicates tension; − indicates compression

Wheel Load, lb	Stress in Outer Face of Plate						Stresses in Inner Face of Plate					
	Tangential Near Rim	Radial Near Rim	Radial	Radial	Radial Near Hub	Tangential Near Hub	Tangential Near Rim	Radial Near Rim	Radial	Radial	Radial Near Hub	Tangential Near Hub
	(1)*	(2)	(3)	(4)	(5)	(6)	(1)	(2)	(3)	(4)	(5)	(6)
Thin Plate Wheels (½ × ⅝) **Stresses on radial gage line between load point and axle**												
20,000 Vertical	+2	0	0	−3	−6	0	−1	−7	−4	0	+5	+5
20,000 Vertical and 8,000 Thrust	+2	−4	−2	0	−2	0	−1	−7	−7	−3	−6	−2
20,000 Vertical and 20,000 Thrust	+1	−12	−8	−6	+4	+1	+1	−7	−10	−14	−24	−12
(Fatigue Machine) 20,000 Thrust	−2	−12	−8	−3	+9	+1	+3	+3	−3	−12	−26	−18
Stresses on radial gage line 180 deg from load point												
20,000 Vertical	0	−2	...	...	+3	0	+1	+2	...	...	−4	−1
20,000 Vertical and 8,000 Thrust	0	−1	...	...	−1	0	0	0	...	...	+2	0
20,000 Vertical and 20,000 Thrust	+1	−7	...	...	−8	+1	−3	−5	...	...	+14	+10
(Fatigue Machine) 20,000 Thrust	+1	−8	+5	0	−8	−1	−3	−5	−2	+4	+12	+8
Thick Plate Wheels (1 × 1¼) **Stresses on radial gage line between load point and axle**												
20,000 Vertical	+1	+1	0	−2	−4	0	−1	−6	−4	0	+2	+2
20,000 Vertical and 8,000 Thrust	+2	0	0	0	−1	0	−2	−8	−5	−4	−3	−1
20,000 Vertical and 20,000 Thrust	+3	0	0	+1	+5	+2	−3	−12	−6	−9	−13	−7
(Fatigue Machine) 20,000 Thrust	+3	−2	−1	+2	+9	+2	+1	−2	−4	−7	−12	−7

* Number refers to location of gage—see Fig. 18.

that for the rim-quenched wheel which has a low endurance limit for the plate material, the endurance limit for completely reversed stress on a notched specimen of this material is 25,000 p.s.i. (see Table 1).

Since the stresses for the assumed service loads are rather small, stresses were determined for a 20,000-lb vertical load with a 20,000-lb flange thrust load. The maximum range of stress found in the thin plate wheels by this loading was from 14,000 p.s.i. tension to 24,000 p.s.i. compression. From the full series of tests conducted, it was

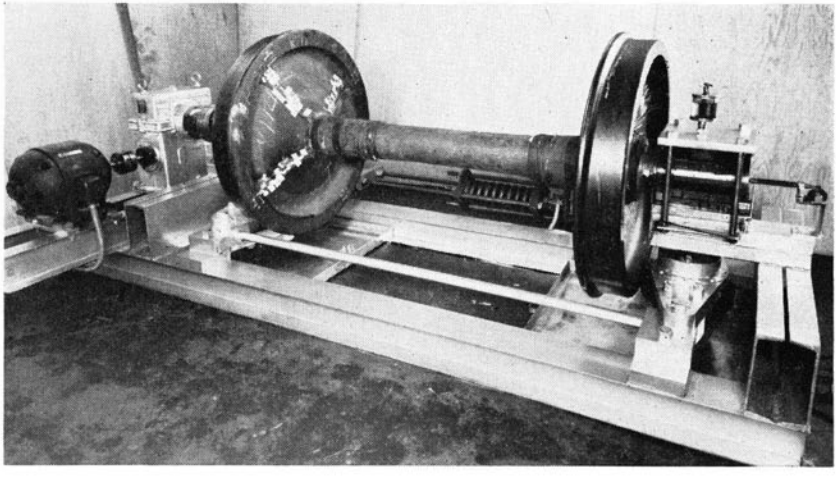

FIG. 20. WHEELS AND AXLE ASSEMBLY IN FATIGUE MACHINE

concluded that the stress produced in the plate of a wheel is more strongly affected by the flange thrust load than by the vertical load.

To obtain added information in regard to the advisability of recommending the thin plate wheels for railway service, a fatigue testing machine was built which would subject the plate of the wheels to stresses as great as, or greater than, would be expected under service conditions. A photograph of the fatigue machine is shown in Fig. 20. Since the static load test results indicated that the flange thrust load was the critical load, the fatigue machine was built to apply only a thrust load. A 20,000-lb thrust load was applied to the outer face of the rim of each wheel by rollers mounted in two levers. The load was applied through the levers by means of a calibrated spring. Under this load the wheel and axle assembly was

rotated by a 7.5-hp electric motor through a gear reducer at a speed of approximately 52 rpm.

After the wheel and axle assembly was placed in the testing machine the stresses in the wheels were determined under the 20,000-lb thrust load imposed by the fatigue machine. The maximum stresses measured were found to be on the inner face of the plate near the hub. This does not mean that all progressive failures in service necessarily occur at this point. The maximum stress cycle ranged from 12,000 p.s.i. tension to 26,000 p.s.i. compression in the thin plate wheels, as shown in Table 8. The range of stress at the same location for the assumed service loads was from 5000 p.s.i. tension to 4000 p.s.i. compression for the 20,000-lb vertical load, and 6000 p.s.i. compression to 2000 p.s.i. tension for the 20,000-lb vertical load with an 8000-lb thrust load. Thus, on the inner face of the plate near the hub the range of stress developed by thrust load in the fatigue machine was four times that produced by the assumed service loads of a 20,000-lb vertical load and an 8000-lb flange load. The thin plate wheels were subjected to 17,000,000 cycles of stress (30,000 miles) without producing fracture, and the thick plate wheels were subjected to 18,000,000 cycles of stress (32,000 miles) without producing fracture.

15. *Effect of Plate Location on Drag Test Results*

A photoelastic investigation of models having a cross-section similar in shape to that of the cross-section of a car wheel has been made at the University of Illinois to study the effect of plate location on the stress pattern set up in the plate[1]. As a result of this investigation, a group of wheels having three plate locations was drag tested, to determine the effect of plate location on the number of drags required to produce fracture. The standard plate location is usually central with respect to the width of the rim and hub. The other two plate locations were ½ in. toward the inner face of the wheel and ½ in. toward the outer face of the wheel. The three designs are illustrated in Fig. 21.

The wheels used for the plate location investigation were rim-quenched Class C wheels made from one heat of steel. The wheels were rolled in accordance with standard mill practice, with slight deviations in forging dies which were necessary in order to produce the wheels with the required plate locations. The wheels were all contour-machined.

[1] See Univ. of Ill. Eng. Exp. Sta. Bul. 312, pp. 52-62.

The effect of the three plate locations was studied for wheels with two different plate thicknesses: a thick plate with a thickness of 1 in. by 1¼ in., and an intermediate plate with a thickness of ¾ in. by 1 in. The test results for the thick plate wheels are given in the upper part of Table 9; those for the intermediate plate thickness, in the lower part of Table 9. The thick plate wheels were tested under the standard drag test procedure. The results indicate

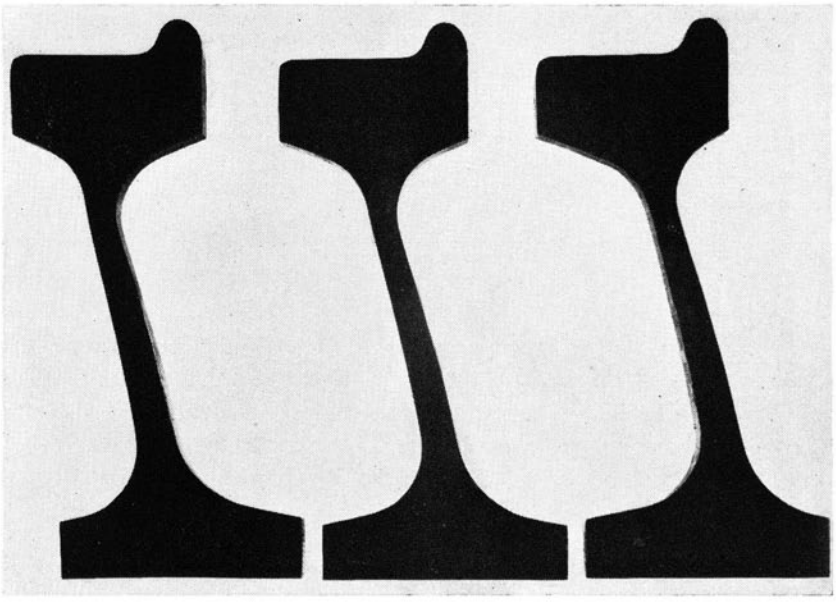

FIG. 21. CROSS-SECTIONS OF WHEELS WITH THREE PLATE LOCATIONS
Intermediate plate thickness

little effect of plate location on the resistance of the wheel to plate fracture. Since fracture could not be produced in the first two intermediate plate thickness wheels tested by the standard drag procedure, the remaining wheels were given the severe drag test (see Section 8). For the changes of plate location which were investigated the results indicate no effect of the plate location on the ability of the wheel to resist wheel fracture.

Attention is called to the wheel with test number 282, which required 46 drag tests to produce fracture — five times the number of drag tests required to produce fracture in the other three wheels of

that group. It is believed that the reason for the large number of drags is the reduced plate thickness of the wheel, which was caused by an error in machining. The plate thickness of this wheel near the rim was 0.1 in. less, and the thickness of the plate near the hub was 0.2 in. less, than the corresponding thickness of the other wheels. The test result for this wheel again illustrates the decided influence of plate thickness on resistance to wheel fracture.

TABLE 9

EFFECT OF PLATE LOCATION ON NUMBER OF DRAG TESTS REQUIRED TO PRODUCE FRACTURE IN RIM-QUENCHED WHEELS

36-in. Class C wheels from heat 59R316, having a rim thickness of 2½ in., tested with intermittent brake application

Wheel Test Number	Nominal Plate Thickness* A, inches	Nominal Plate Thickness* B, inches	Brake Shoe Pressure, lb	Depth Saw Cut, percent	Number of Drags	Fracture
		Plate Location Central				
249 BCR1D	1	1¼	3 000	50	15	Yes
252 BCR1D	1	1¼	3 000	50	18	Yes
					Av 16.5	
		Plate Location ½ in. Toward Inner Face				
250 BCR1D	1	1¼	3 000	50	14	Yes
253 BCR1D	1	1¼	3 000	50	30	Yes
					Av 22	
		Plate Location ½ in. Toward Outer Face				
251 BCR1D	1	1¼	3 000	50	25	Yes
254 BCR1D	1	1¼	3 000	50	15	Yes
					Av 20	
		Plate Location Central				
278 BCR9D	¾	1	3 000	50	50†	No
280 BCR9D	¾	1	4 000	75	10	Yes
283 BCR9D	¾	1	4 000	75	2	Yes
286 BCR9D	¾	1	4 000	75	9	Yes
289 BCR9D	¾	1	4 000	75	11	Yes
					Av 8	
		Plate Location ½ in. Toward Inner Face				
279 BCR9D	¾	1	3 000	50	50†	No
281 BCR9D	¾	1	4 000	75	6	Yes
284 BCR9D	¾	1	4 000	75	12	Yes
287 BCR9D	¾	1	4 000	75	6	Yes
290 BCR9D	¾	1	4 000	75	7	Yes
					Av 8	
		Plate Location ½ in. Toward Outer Face				
282 BCR9D	.72	.88	4 000	75	46†	Yes
285 BCR9D	¾	1	4 000	75	9	Yes
288 BCR9D	¾	1	4 000	75	6	Yes
291 BCR9D	¾	1	4 000	75	11	Yes
					Av 9	

* See Fig. 3.
† Not used in determining average.

16. *Effect of Rim Thickness on Drag Test Results*

Two rim thicknesses were considered in the investigation of 36-in.-diam wheels — the basic rim thickness of 2½ in. and a thin rim of 2 in. The results of the tests are given in Table 10. These wheels were drag-tested by means of the standard drag test procedure.

TABLE 10

EFFECT OF WHEEL RIM THICKNESS ON NUMBER OF DRAG TESTS REQUIRED TO PRODUCE FRACTURE IN RIM-QUENCHED AND OIL-QUENCHED WHEELS

36-in. Class C wheels having a plate thickness of 1 in. by 1¼ in., tested with standard test conditions

Wheel Test Number	Heat Number	Heat Treatment	Nominal Rim Thickness, inches	Number of Drags for Fracture
177 ICR1D	40307	R	2½	31
181 ICR1D	40307	R	2½	25
178 ICR5D	40307	R	2	31
183 ICR5D	40307	R	2	25
293 ICO1D	921614	E	2½	6
320 ICO1D	921614	E	2½	12
354 ICO1D	921614	E	2½	9
197 ICO5D	40307	E	2	18
204 ICO5D	40307	E	2	17

The relative depth of the simulated thermal crack was kept constant at 50 percent of the rim thickness for both the 2½-in. and the 2-in. rim thicknesses, so that the depth of notch did not remain the same. The rim-quenched wheels listed in the upper half of Table 10 were all from the same heat of steel. The oil-quenched wheels listed in the lower half of Table 10 were from two different heats of steel.

The foregoing data on the effect of rim thickness on the number of drag tests required to produce fracture are not conclusive, because the range of rim thickness investigation was not broad enough.

17. *Effect of Changes in Wheel Design on Stop Test Results*

The data that are available to determine the effect of changes in wheel design on the stop test results are presented in Table 11. The variables considered are heat treatment, wheel diameter, plate thickness, and rim thickness. The data are not sufficient to permit the drawing of definite conclusions.

TABLE 11

EFFECT OF CHANGES IN WHEEL DESIGN ON NUMBER OF STOP TESTS REQUIRED TO PRODUCE THERMAL CRACKS

Class C and Class U wheels from heat 40307 tested with standard stop test conditions

Wheel Test Number	Heat Treatment	Diameter, inches	Nominal Plate Thickness* A, inches	Nominal Plate Thickness* B, inches	Nominal Rim Thickness, inches	Number of Stops	Number of Thermal Cracks
189 ICR1S	R	36	1	1¼	2½	7	1
190 ICR6S	R	36	½	⅝	2½	7	1
191 ICR5S	R	36	1	1¼	2	35	1
192 ICR7S	R	36	½	⅝	2	50	0
165 ICU3S	U	33	¾	1	1½	30	0
167 ICU3S	U	33	¾	1	1½	30	0
166 ICU4S	U	33	½	⅝	1½	30	0
168 ICU4S	U	33	½	⅝	1½	30	0

* See Fig. 3.

VI. Effect of Carbon Content on Test Results

18. *The Effect of Carbon Content on Drag Test Results*

The drag test results of Class B and Class C rim-quenched and oil-quenched wheels are given in Table 12. These wheels were all tested under standard drag test procedure. The Class B wheels had a carbon content of 0.61 percent; the Class C wheels had a carbon content of from 0.71 percent to 0.73 percent. The rim-quenched Class B wheels withstood on an average 34 drag tests before wheel fracture, and the rim-quenched Class C wheels required an average of 23 drag tests to produce fracture. For the oil-quenched wheels the Class B wheels required an average of 11 drag tests, and the Class C wheels required an average of 9 drag tests, to produce wheel fracture. When it is considered that the Class B wheels had a plate thickness slightly greater than the Class C wheels, the Class B wheels appear to be the more resistant to wheel fracture. Thus the test results indicate that an increase in carbon content results in a slight decrease in the resistance of a wheel to wheel fracture.

Table 12

Effect of Carbon on Number of Drag Tests Required to Produce Fracture in Rim-Quenched and Oil-Quenched Wheels

36-in.-diam wheels having a rim thickness of 2½ in., tested with standard test conditions

Wheel Test Number	Heat Number	Carbon, percent	Heat Treatment	Plate Thickness* A, inches	Plate Thickness* B, inches	Number of Drags for Fracture
130 IBR1D	34519	0.61	R	1.20	1.41	30
133 IBR1D	34519	0.61	R	1.23	1.45	23
134 IBR1D	34519	0.61	R	1.11	1.41	22
140 IBR1D	34519	0.61	R	1.11	1.44	39
141 IBR1D	34519	0.61	R	1.12	1.36	40
151 IBR1D	34519	0.61	R	1.17	1.41	50
				Av 1.16	1.41	34
177 ICR1D	40307	0.73	R	1.05	1.25	31
181 ICR1D	40307	0.73	R	1.00	1.40	25
249 BCR1D	59R316	0.71	R	1.22	1.50	15
250 BCR1D	59R316	0.71	R	1.20	1.50	14
251 BCR1D	59R316	0.71	R	1.11	1.31	25
252 BCR1D	59R316	0.71	R	1.20	1.50	18
253 BCR1D	59R316	0.71	R	1.17	1.50	30
254 BCR1D	59R316	0.71	R	1.17	1.50	15
300 ICR1D	921614	0.72	R	0.94	1.31	38
348 ICR1D	921614	0.72	R	1.00	1.38	28
367 ICR1D	921614	0.72	R	1.00	1.50	13
				Av 1.10	1.42	23
114 IBO1D	34519	0.61	E	1.19	1.69	9
120 IBO1D	34519	0.61	E	1.22	1.42	8
135 IBO1D	34519	0.61	E	1.11	1.31	9
137 IBO1D	34519	0.61	E	1.11	1.36	8
139 IBO1D	34519	0.61	E	1.14	1.41	15
149 IBO1D	34519	0.61	E	1.13	1.44	17
150 IBO1D	34519	0.61	E	1.19	1.45	8
				Av 1.16	1.44	11
293 ICO1D	921614	0.72	E	1.00	1.38	6
320 ICO1D	921614	0.72	E	1.00	1.38	12
354 ICO1D	921614	0.72	E	0.94	1.50	9
				Av 0.98	1.42	9

* See Fig. 3.

19. *The Effect of Carbon Content on Stop Test Results*

The stop test data showing the effect of carbon are listed in Table 13 in the order of increasing carbon content. These wheels were all 36-in.-diam thick plate wheels with a rim thickness of 2½ in.

The test data indicate that an increase in carbon content increases the susceptibility of the wheel to thermal cracking. Of the six Class A wheels, four ran 50 stops without producing a thermal crack and the other two ran an average of 33 stops before producing a thermal crack. Of the 11 Class B wheels, four thermal-cracked, and in three of these only one stop each was required to produce a thermal crack. For the 11 Class C wheels tested, thermal cracks were produced in every wheel, with an average of less than three stops required to produce the thermal cracks.

The data include wheels subjected to various heat treatments within the classes A, B, and C, but the results do not indicate any appreciable influence of this variable on the resistance of wheels to thermal cracking.

TABLE 13

EFFECT OF CARBON ON NUMBER OF STOP TESTS REQUIRED TO PRODUCE A THERMAL CRACK

36-in.-diam basic design wheels tested with standard stop test conditions

Wheel Test Number	Heat Number	Heat Treatment	Carbon, percent	Number of Stops	Number of Thermal Cracks
21 SAW1S	E6270	W	0.48	50	0
22 SAW1S	E6270	W	0.48	50	0
33 BAR1S	46L223	R	0.52	50	0
34 BAR1S	46L223	R	0.52	30	1
3 IAO1S	31077	E	0.52	50	0
4 IAO1S	31077	E	0.52	36	1
9 IBO1S	37021	E	0.61	1	1
10 IBO1S	37021	E	0.61	1	1
39 BBR1S	46L256	R	0.61	50	0
40 BBR1S	46L256	R	0.61	50	0
142 IBO1S	34519	E	0.61	25	1
143 IBO1S	34519	E	0.61	50	0
144 IBO1S	34519	E	0.61	50	0
145 IBO1S	34519	E	0.61	50	0
146 IBO1S	34519	E	0.61	1	1
147 IBO1S	34519	E	0.61	50	0
148 IBO1S	34519	E	0.61	50	0
45 BCR1S	47L193	R	0.70	1	1
46 BCR1S	47L193	R	0.70	1	1
15 ICO1S	87120	E	0.72	1	1
16 ICO1S	87120	E	0.72	8	1
64 ICO1S	46568	E	0.73	1	2
69 ICR1S	46568	R	0.73	1	1
74 ICO1S	46568	E	0.73	1	4
79 ICR1S	46568	R	0.73	5	1
84 ICU1S	46568	U	0.73	1	1
85 ICU1S	46568	U	0.73	4	1
189 ICR1S	40307	R	0.73	7	1
89 IFO1S	43607	E	0.73	6	1

VII. Comparison of Wheels Manufactured by the Rolling and the Drop-Forging Processes

20. *Preliminary Statement*

To investigate the possibility of manufacturing wheels by a drop-forging process a number of 33-in.-diam wheels were made with plate thicknesses of ½ in. by ⅝ in. From the same heat of steel another group of 33-in. wheels were rolled in the conventional manner.

The two types of wheels were investigated in a number of ways: (1) by investigating the mechanical properties of the material, (2) by making a metallographic study of the structure of the material, (3) by subjecting wheels to drag tests, and (4) by subjecting wheels to stop tests.

The mechanical property data, which are presented in Table 1a, do not indicate any marked difference in the wheel material for the two types of manufacture. The photomicrographs shown in Fig. 7 do not denote any significant difference in microstructure.

21. *Drag Test Results of Rolled and Drop-Forged Wheels*

Standard drag tests were run on four wheels of each type of manufacture; the results are shown in Table 14. A total of 50 drag tests was run on each of the four rolled wheels without producing wheel fracture. Wheel fractures were produced in all of the drop-forged wheels after an average of 26 drags. These data indicate that the rolled steel wheels were more resistant to wheel fracture than the drop-forged wheels.

Table 14

Drag Test Results on Drop-Forged and Rolled 33-in.-diam Wheels

From Heat 831021

Wheel Test Number	Rim Thickness, inches	Number of Drags	Fracture
	Rolled Wheels		
274 ICU4D	1.50	50	No
275 ICU4D	1.50	50	No
276 ICU4D	1.50	50	No
277 ICU4D	1.50	50	No
	Drop-Forged Wheels		
257 LCU4D	1.37	23	Yes
259 LCU4D	1.31	20	Yes
260 LCU4D	1.31	35	Yes
261 LCU4D	1.34	24	Yes

22. *Stop Test Results of Rolled and Drop-Forged Wheels*

Stop tests were run on four wheels of each type of manufacture. The results are shown in Table 15. All the rolled wheels thermal-cracked; the number of stop tests required to produce a thermal crack in each of the four wheels was 4, 5, 31, and 50 respectively. Two of the four drop-forged wheels thermal-cracked; one ran 8 stop tests before thermal cracking, one ran 28 stop tests before thermal cracking, and the remaining two were removed from the testing machine after receiving 50 stop tests without thermal cracking. These data indicate that the drop-forged wheels were slightly more resistant to thermal cracking.

23. *General Summary of Drop-Forged and Rolled Wheels*

The economics to be considered, such as cost, ease of manufacture, etc., are not within the scope of this bulletin. Since the drop-forged wheels were not demonstrated by the tests to be superior to the wheels made by the conventional method, additional testing of drop-forged wheels was not undertaken.

TABLE 15

STOP TEST RESULTS ON DROP-FORGED AND ROLLED 33-IN.-DIAM WHEELS

From Heat 831021

Wheel Test Number	Initial Speed, mph	Rim Thickness, inches*	Number of Stops	Number of Thermal Cracks
		Rolled Wheels		
269 ICU4S	107	1.38	4	1
270 ICU4S	107	1.38	5	1
272 ICU4S	107	1.25	31	1
273 ICU4S	107	1.25	50	1
		Drop-Forged Wheels		
262 LCU4S	107	1.19	50	0
263 LCU4S	107	1.25	8	1
264 LCU4S	107	1.25	28	2
265 LCU4S	107	1.13	50	0

*Dimensions taken after tests.

VIII. Effect of Drag Testing on Residual Stress Distribution

24. *Residual Stress Distribution in the Wheels as Manufactured*

Residual stresses are defined as "locked up" stresses which are present in a wheel free of external load. These stresses may be present in an unused wheel and may be changed by service conditions. The "locked up" stresses, which are present in a wheel at any time during its life, will be referred to as residual stresses.

Initial residual stresses are not necessarily detrimental to a wheel, but may be helpful if of proper sign. During the investigation residual stress determinations and strain measurements during testing have been made on wheels of each type. The resulting volume of data is too great to be included in the bulletin in its entirety; therefore representative data are presented. Only the data from the wheels used for the draw temperature investigation are presented, since draw temperature and type of heat treatment had greater influence on the residual stresses than any of the other variables considered during the investigation.

The residual stress data for the rim-quenched and oil-quenched wheels used in the draw temperature investigation are presented in Table 16. As would be expected, the magnitude of the residual stresses increased with a decrease in draw temperature. The residual stresses for the outer and inner faces of the rim and the tread were found to be compression for both the oil-quenched and the rim-quenched wheels; however, these surface stresses are not fully representative of the average or subsurface stresses. The oil-quenched wheels were found to have tensile residual stresses in the center of the rim; for instance, the wheel having the 800 deg F draw temperature had stresses of 10,000 p.s.i. tension and 41,000 p.s.i. tension at ½ in. and 1 in. respectively below the surface of the tread. The residual stresses at ½ in. and 1 in. below the surface of the tread were 38,000 p.s.i. compression and 13,000 p.s.i. compression respectively for the rim-quenched wheel having 800 deg F draw temperature. The subsurface stresses presented were obtained by the method described in Section 10.

25. *Change in Residual Stress Distribution Due to Drag Testing*

In order that the residual stress distribution may be changed as a result of drag testing, plastic deformation must be produced by the drag testing. The mechanism of this plastic deformation will be considered first.

TABLE 16

RESIDUAL STRESSES IN WHEELS AS MANUFACTURED

Stress × 1000 p.s.i.

Wheel Test No.	Draw Temp, deg F	Outer Face								Inner Face								Distance Below Surface at Center of Tread					
		Rim		P_1		P_2		P_3		Rim		P_1		P_2		P_3		0″		½″		1″	
		R	T	R	T	R	T	R	T	R	T	R	T	R	T	R	T	A	T	A	T	A	T
Rim-Quenched Wheels																							
301 ICR1R	1 200°	−10	+1	−1	−5	−2	−8	+2	−2	+2	−2	+1	+1	+3	−1	+1	−4	0	−4				
303 ICR1R	1 000°	−10	−12	−6	+1	+2	+4	+4	+11	−9	−11	+3	+1	−5	−4	−9	−8	−10	−10				
304 ICR1R	900°	−13	−20	−6	+2	+11	+18	+18	+9	−10	−16	+8	+3	−9	−6	−11	−10	0	−6				
343 ICR1R	860°	−20	−25	−18	0	+8	+17	+24	+9	−5	−21	+15	+12	−14	−8	−11	−8	−14	−23				
306 ICR1R	800°	−25	−38	−18	+6	+14	+22	+30	+17	−29	−46	+23	+10	−10	−10	−26	−17	−26	−35	−10	−38	+3	−13
305 ICR1R	700°	−26	−44	−27	+7	+21	+27	+59	+27	−32	−58	+54	+18	−10	−14	−30	−21	−24	−44	−8	−57	+17	+4
307 ICR1R	400°	−48	−58	−71	0	+55	+45	+151*	+55	−51	−83	+87	+36	−47	−29	−71	−43	−73	−109				
Oil-Quenched Wheels																							
296 ICO1R	1 200°	−2	−6	−4	−7	−4	−8	+3	−1	+2	−1	+2	−6	+3	−13	−3	−6	....	....				
302 ICO1R	1 000°	−9	−12	−5	−18	−14	−16	−11	−15	−8	−9	−7	−12	−3	−10	−6	−9	−17	−13				
308 ICO1R	900°	−22	−24	−11	−20	−16	−21	−14	−20	−15	−17	−15	−19	−9	−16	−11	−16	−27	−24	−7	−2	+10	+17
309 ICO1R	800°	−37	−45	−13	−40	−35	−41	−34	−43	−42	−39	−40	−43	−22	−37	−18	−34	−57	−42	−9	+10	+23	+41
310 ICO1R	700°	−45	−53	−13	−55	−50	−66	−42	−61	−51	−45	−55	−71	−33	−61	−20	−49	−63	−46	−9	+15	+21	+45
311 ICO1R	400°	−73	−67	−29	−100	....	....	−62	−94	−57	−43	−69	−88	−46	−85	−32	−76	−84	−61	−10	+25	+26	+68
Untreated Wheels																							
312 ICU1R	Untreated	−7	−4	+1	−6	−5	−15	+2	−10	0	−2	−2	−8	+6	−5	−1	−6	+5	+3				

R-Radial; T-Tangential; A-Axial.

* Because of the relief of the biaxial state of stress upon sawing, yielding had probably taken place at this location.

As the wheel is subjected to a prolonged brake application in the drag test, the rim of the wheel is heated to a temperature in the neighborhood of 1000 deg F. During the same time the temperature of the hub increases less than 100 deg F. The rim tends to expand upon being heated, but the hub and plate, which are much cooler,

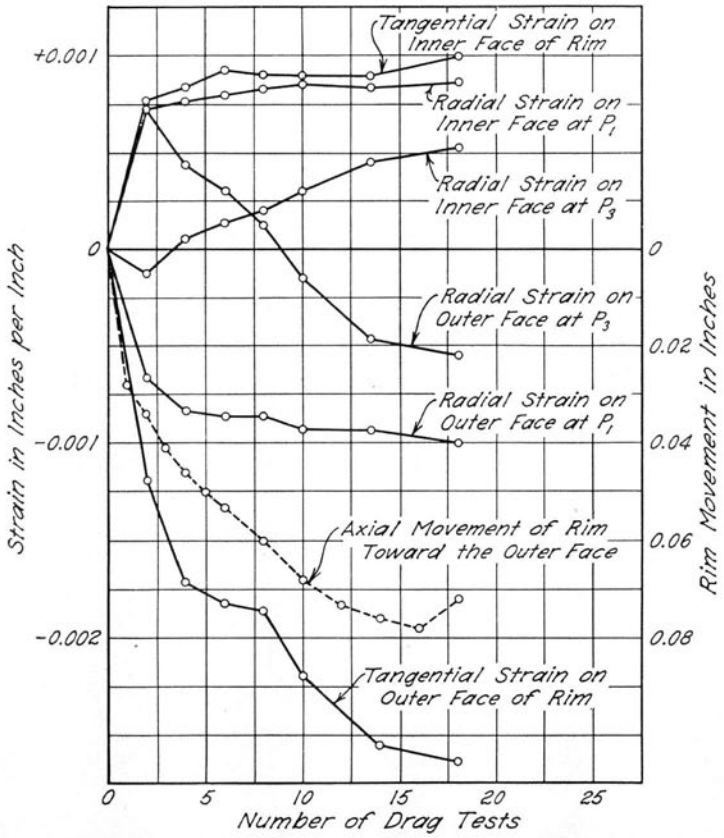

FIG. 22. EFFECT OF DRAG TESTING ON CHANGE IN STRAIN IN RIM-QUENCHED WHEEL
800-deg draw temperature; wheel test number 350

partly restrain the expansion. Thus the temperature gradient between the rim and the hub produces compressive stresses of appreciable magnitude in the tangential direction in the rim. Because of the reduction in yield strength at the high temperature, the material is not able to carry elastically the high compressive stresses; therefore plastic deformation occurs. Upon cooling to room temperature

the region of the rim, which has been plastically deformed (upset) in compression, tends to contract; but since it is restrained by the plate and hub, an increment of tangential tensile stress is developed which modifies the previous stress pattern.

Not all of the plastic deformation occurs on the first drag test; it may accumulate with each succeeding drag test as indicated in Figs. 22 and 23. The curves represented by solid lines illustrate the

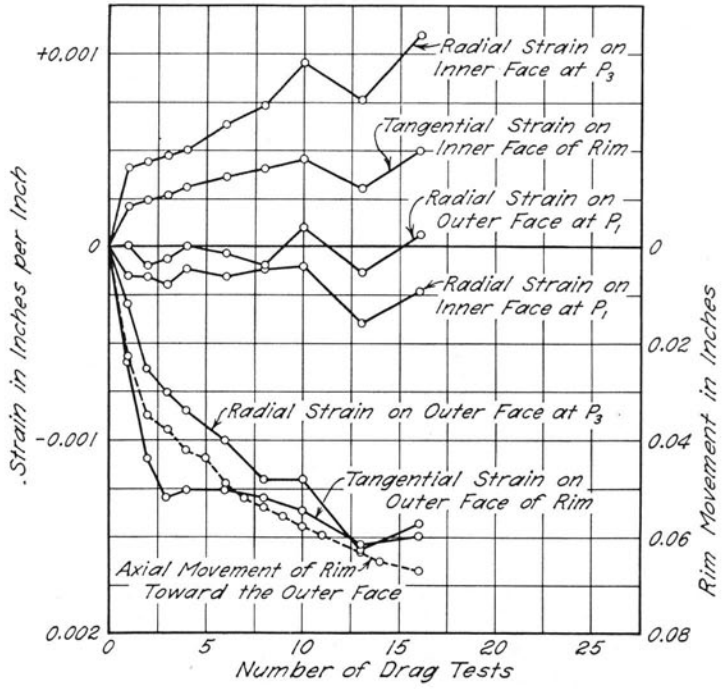

FIG. 23. EFFECT OF DRAG TESTING ON CHANGE IN STRAIN IN OIL-QUENCHED WHEEL

800-deg draw temperature; wheel test number 322

effect of the number of drags on the change in strain due to drag testing. Except for the curves for the radial strain at location P_3 (see Fig. 12) on the outer and inner faces of the rim-quenched wheel, the curves all exhibit a sharp rise for the first few drag tests and then a leveling off. The peculiar trend of the two curves is explained in Appendix A. As the circumference of the rim becomes shorter due to drag testing the angle of the plate from the vertical increases and the rim moves axially with respect to the hub, as represented by the dotted curves shown in Figs. 22 and 23.

The large amount of plastic deformation which is produced in wheels by drag testing causes a change in the residual stress pattern. In Table 17 are presented the residual stress data for the rim-quenched and the oil-quenched wheels which were used in the draw temperature investigation. The data are based on the last strain reading before fracture. The data for the oil-quenched wheels drawn at 700 deg F and 400 deg F were not presented, since the last strain reading was taken after the second drag test, and the wheels fractured after the fourth drag test. At this low number of drags the rate of plastic deformation occurring per drag test is still rather high (see Figs. 22 and 23).

The residual strains in the tangential direction on the outer and inner faces of the rim do not indicate high tensile stresses in the tangential direction in the rim. This point is cleared up if one considers the actual residual stress before and after testing as given in Fig. 24. These stress distributions are for rim-quenched wheels having 800 deg F draw temperature. The residual stress distribution given in Fig. 24a was obtained from a wheel that was not drag-tested, and the residual stresses indicate that most of the rim cross-section is in compression. The residual stress distribution given in Fig. 24b was obtained from a wheel that had been subjected to 75 drags without producing fracture. After completion of the 75 drag tests the wheel was removed from the machine and holes were drilled in the wheel to make residual stress determinations at the different depths. The gage holes were distributed around the wheel at eight stations so that no cross-section was reduced appreciably. The residual stresses indicate that the greater portion of the rim cross-section is in tension after drag testing. Thus drag testing has changed the stress distribution across the rim cross-section from one that is predominantly compression to one that is predominantly tension.

It will be noted that the residual stress distributions in the plates of the rim-quenched and oil-quenched wheels at fracture are nearly identical. Furthermore, these stress distributions are opposite to the initial residual stress distribution of the rim-quenched wheels and similar to those of the oil-quenched wheels.

The data presented indicated that drag testing of a wheel will change the residual stress pattern in a wheel and that the residual stresses produced can be great enough to cause wheel fracture if a notch such as a thermal crack or a saw cut is present.

TABLE 17

RESIDUAL STRESSES IN WHEELS AFTER DRAG TESTING

Stress × 1000 p.s.i.

Wheel Test No.	Draw Temp, deg F	No. Drags to Fracture	No. Drags Before Last Reading	Outer Face								Inner Face							
				Rim		P_1		P_2		P_3		Rim		P_1		P_2		P_3	
				R	T	R	T	R	T	R	T	R	T	R	T	R	T	R	T
Rim-Quenched Wheels																			
330 ICR1D	1 200	20	18	−12	−9	+9	−38	−34	−44	−70	−45	−3	+24	−42	−24	+12	−1	+40	+12
348 ICR1D	1 000	28	26	−5	−9	−6	−36	−39	−47	−68	−43	−2	+23	−38	−20	+11	−1	+31	−7
349 ICR1D	900	22	18	−8	−17	−4	−36	−33	−42	−71	−53	−13	+7	−31	−11	+11	−4	+44	+11
350 ICR1D	800	19	18	0	−14	+10	−45	−37	−49	−53	−37	−16	+2	−19	−18	+18	−3	+42	+13
351 ICR1D	700	23	22	−10	−12	−4	−52	−40	−51	−68	−45	−24	−10	−24	−20	+18	−7	+41	+10
329 ICR1D	400	14	12	0	−6	−5	−53	−38	−45	−52	−30	−16	−2	−28	−18	+13	−9	+41	+10
Oil-Quenched Wheels																			
319 ICO1D	1 200	47	44	−2	+3	+7	−34	−37	−50	−78	−48	+1	+28	−43	−32	+20	−6	+38	+5
320 ICO1D	1 000	12	11	0	−6	−11	−44	−45	−53	−68	−42	−10	−4	−39	−29	+16	−5	+25	+3
321 ICO1D	900	13	12	+2	−1	−1	−54	....	....	−72	−50	−8	+13	....	....	+22	−10	+36	−1
322 ICO1D	800	16	16	−4	−2	−21	−76	....	....	−85	−75	−25	+1	−41	−59	....	....	+26	−18
357 ICO1D	700	4	2																
358 ICO1D	400	4	2																

R — Radial; T — Tangential.

The residual stresses in a wheel as received from a manufacturer may be beneficial if of proper sign. Any heat treatment process that results in residual compression in the rim such as was found for the rim-quenching process will increase the resistance to wheel fracture, and residual tension stresses in the rim will lower the resistance to wheel fracture.

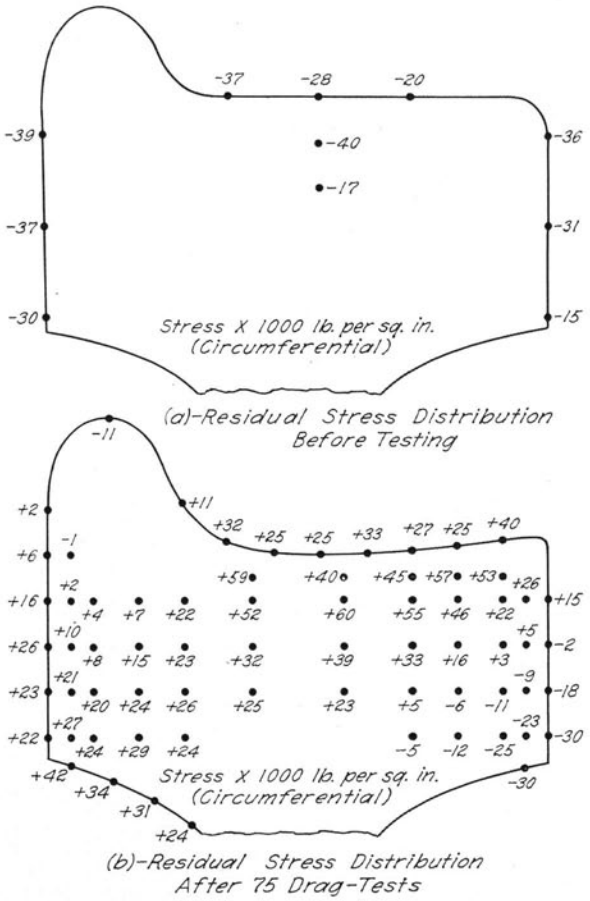

FIG. 24. EFFECT OF DRAG TESTING ON RESIDUAL STRESS DISTRIBUTION IN RIM OF RIM-QUENCHED WHEELS

800-deg draw temperature

IX. Summary and Conclusions

26. *Summary*

Though only a few designs and types of heat treatment of wheels have been covered in these investigations, in general the results are in close accord with service experience. The test results presented in this bulletin appear to justify the following conclusions and should serve as a guide in the future development of wrought steel railway car wheels.

27. *Conclusions Drawn from Drag Test Results*

(1) For the same design, carbon content, and draw temperature, the rim-quenched wheels in which residual compressive stresses predominate in the rim were found to be more resistant to wheel fracture than the oil-quenched wheels in which residual tensile stresses predominate in the rim. Furthermore, the fracture was usually less severe for the rim-quenched wheels than for the oil-quenched wheels.

(2) The draw temperature was found to have some effect on the resistance of wheels to wheel fracture. Except, perhaps, for the lowest draw temperature, which gave low resistance to wheel fracture, the trend of the data indicated that the draw temperature has little effect on the resistance of wheels to wheel fracture. The greatest effect of draw temperature was on the severity of fracture. With a decrease of draw temperature, the severity of fracture was found to increase for the oil-quenched wheels and to decrease for the rim-quenched wheels.

(3) A decrease of carbon content from 0.72 percent carbon to 0.61 percent carbon slightly increased the resistance to wheel fracture.

(4) In the range of rim thickness considered (2 in. and 2½ in.) the rim thickness did not have any appreciable effect on the resistance to wheel fracture.

(5) The shifting of the plate from the normal central position toward either the inner or the outer face of the wheel was found to have little effect on the resistance of the wheel to wheel fracture.

(6) Of all the variables investigated, plate thickness proved to have the greatest influence on resistance to wheel fracture. Even a decrease in plate thickness of ¼ in. was found to increase the resistance of a wheel to wheel fracture more than the maximum beneficial change of any other variable. Static load test and fatigue test results on the 36-in.-diam wheel with a ½-in. by ⅝-in. plate thickness indicate that the thin plate wheel may safely carry service loads.

28. *Conclusions Drawn from Stop Test Results*

The resistance of wheels to thermal cracking increases with a decrease in carbon content.

29. *Conclusion Drawn from Drag Testing and Stop Testing of Wheels Manufactured by the Drop-Forging and Rolling Processes*

The wheels manufactured by the rolling process were found to have slightly more resistance to wheel fracture and slightly less resistance to thermal cracking than those manufactured by the drop-forging process. Mechanical property tests and a metallurgical study did not indicate any significant difference between the wheels manufactured by the two processes.

APPENDIX A

Qualitative Stress Analysis of the Wheels Investigated

30. *Preliminary Statement*

A qualitative stress analysis based on the concept of relaxation of stress which occurs at high temperature when a member is subjected to constant strain is presented in this Appendix. The analysis seems to explain the variables that have been investigated, and it is thought that the theory presented will be helpful in determining how stresses are built up in a car wheel. Stop testing produces tensile stresses in the tread of the wheel which reach a sufficient magnitude to produce thermal cracks (see Fig. 1), and drag testing produces tensile stresses at the bottom of the saw cut of such magnitude as to produce wheel fracture (see Fig. 2). In each case the change in stress which occurs during testing is the result of plastic deformation. Before a satisfactory analysis of the strain data can be made or before a stress analysis can be made of either the wheel fracture problem or the thermal crack problem, the method by which the plastic deformation is produced in wheels by the drag test and the stop test must be determined and analyzed.

During the drag test the rim of the wheel is heated while the hub and plate remain relatively cool. The rim has a tendency to expand on heating, but the hub and plate, being much cooler, restrain the rim from expanding the full amount. This results in compressive stresses of appreciable magnitude being developed in the hot rim. At the high temperatures produced in the rim by the drag test, the material is not able to elastically carry these high compressive stresses, so that the rim upsets because of creep and relaxation[1]. On cooling, tensile stresses are produced in the rim because its contraction is restrained.

In principle, the phenomenon by which the tensile stresses are developed in the tread of the wheel by the stop test is the same as that by which the tensile stresses are developed in the rim of the wheel by the drag test. The extreme rate at which energy is applied to the tread of the wheel by the stop test heats the surface of the tread to an austenitizing temperature, and the short duration of the test does not allow a deep penetration of the heated zone. The steep temperature gradient produces large compressive stresses in

[1] Creep is defined as deformation continuing with time for a material subjected to a constant stress, and relaxation is defined as decrease of stress (as the result of inelastic deformation) continuing with time for a material subjected to a constant strain. Appreciable relaxation does not occur for steel except at elevated temperature.

the surface of the tread which are relieved by plastic deformation. As the tread cools after the stop test, tensile stresses are developed.

In the rim and tread of the wheel, where most of the inelastic deformation due to creep and relaxation at high temperature occurs, neither constant stress nor constant strain prevails; however, the inelastic deformation is predominantly a relaxation phenomenon (and

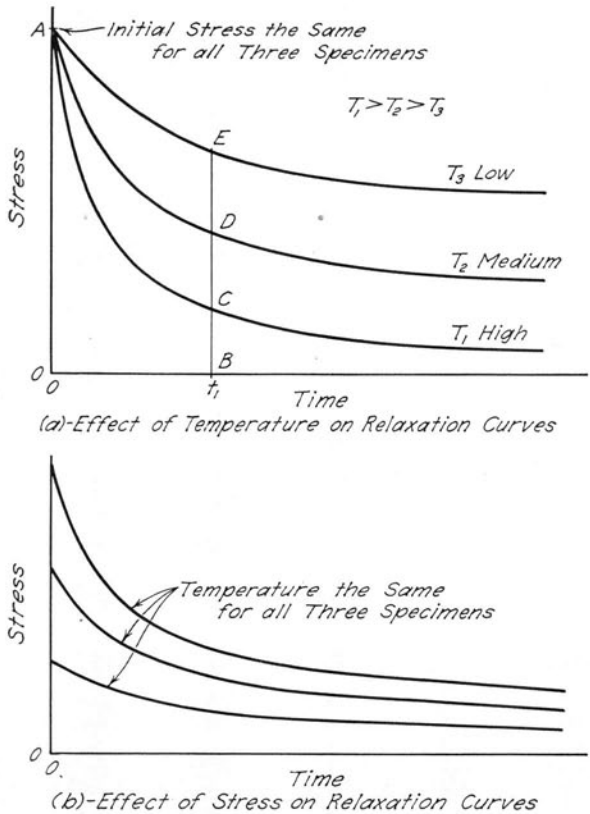

FIG. 25. TYPICAL RELAXATION CURVES FOR A STEEL
The specimens are subjected to constant strain

will be referred to as such hereinafter). Typical relaxation curves for steel are shown in Fig. 25. At present very little relaxation data is available. Some data have been reported by W. E. Trumpler, Jr.[1]

The curves in Fig. 25a show the effect of temperature on the relaxation curve. The three curves shown are relaxation curves for

[1] See "Relaxation of Metals at High Temperatures," *Journal of Applied Physics*, Vol. 12, March 1941, pp. 248-253.

specimens made from the same material, subjected to the same initial stress, but having different test temperature, T_1, T_2, and T_3, in which $T_1 > T_2 > T_3$. Each of the temperatures is high enough to produce creep or relaxation. At the beginning of the test each specimen is given the same initial elongation, which gives the same initial stress—represented by OA in Fig. 25a. If the strain is held constant, the stress in each specimen is relaxed with time, the total change of which depends on the temperature. At the end of a time interval given by t_1 the stress in the specimen with the highest temperature, T_1, has decreased from OA to BC; the stress in the specimen with the second highest temperature, T_2, has decreased from OA to BD; and the stress in the specimen with the lowest temperature, T_3, has decreased from OA to BE.

The relaxation curve is also affected by the initial stress imposed on the specimens, as indicated by the three curves shown in Fig. 25b. Each of the three specimens is tested at the same test temperature, but is subjected to a different initial elongation to give different initial stresses. The extent of the decrease in stress for a given time interval will be greatest for the largest initial stress.

The concept of the relaxation of stresses at high temperatures is most important in the analysis of the drag test and the stop test results. In the discussion which follows, an attempt is made to explain qualitatively the effect of heat treatment and plate thickness on the drag test results. In order to explain these effects, a thorough analysis of the strain data is presented, as is also a qualitative analysis of the stop test data.

31. *Buildup of Stress in the Wheel Due to Drag Testing*

When one considers the mechanism by which the stresses are built up in a wheel during a drag test, it becomes evident that a stress analysis will, at most, be qualitative. The stress change occurring in a wheel during a drag test is caused by plastic or inelastic deformation resulting from high stresses produced by a steep temperature gradient. The magnitude of the stress and the extent of the plastic deformation depend on the temperature, the temperature gradient, the stress gradient, and the duration of the test. Since fracture starts at the bottom of the saw cut, the problem is further complicated by the notch.

An analysis of the test data is possible without obtaining a mathematical relation between the stress at the bottom of the saw cut and the variables affecting its magnitude. If the mechanism by which the stresses are built up in the wheel can be determined, it is

necessary only to determine how a particular variable affects the stress buildup, in order to determine the effect of that variable on the drag test results.

Since wheels fracture as the result of tensile stresses developed in the rim of the wheel by the drag test, the mechanism by which these stresses are developed is considered first. To simplify the presentation, it will be assumed that there are no initial residual stresses in the wheel.

As was stated previously, the drag test results in the rim of the wheel being heated much more rapidly than the hub and plate. The resulting temperature gradient produces compressive stresses in the circumferential direction in the rim of the wheel that may reach an appreciable magnitude. At the high temperature to which the rim is heated the material is not able to elastically carry these high compressive stresses, so that they are relaxed with time.

Schematically, the effect of relaxation on the compressive stress developed in the rim of the wheel during the heating period of the drag test may be represented by the relaxation curve shown in Fig. 26. Let curve AB be the relaxation-time curve for the wheel steel for the given temperature, let OA represent the average compressive stress that would have been developed in the wheel if no relaxation had taken place, and let OC represent the interval of time during the drag test in which the temperature is high enough for appreciable relaxation to take place. At the end of the heating period of the first drag, the average compressive stress remaining is given by CD. If, on cooling, the rim diameter at room temperature returns to its value at the beginning of the first drag, the total change in stress in the rim will be equal to OA; it is shown by DF in Fig. 26. Thus, at the end of the first drag an average tensile stress of magnitude equal to CF is produced in the rim of the wheel, and this value is found to be equal to DE, which was the decrease of the compressive stress due to relaxation. Actually the rim of the wheel decreases in diameter during the test, so that the resulting tensile stress is smaller than that indicated above. However, the qualitative picture of the method by which the tensile stresses are built up in the rim of the wheel would not be changed by considering the effect of change in diameter of the wheel; hence the simplified picture will be considered.

The buildup of the average tensile stress in the rim with successive drags can also be explained by the relaxation curve shown in Fig. 26. In order to eliminate presenting a sequence of relaxation curves of short duration of time, the time required for cooling and reheating of the wheel has not been shown. Hence, the cooling cycle

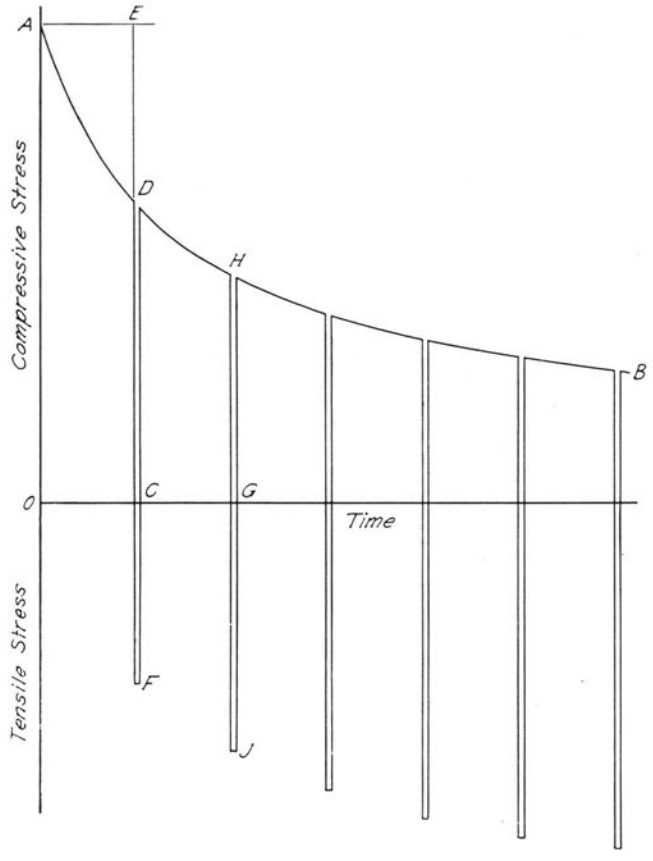

FIG. 26. RELAXATION-TIME CURVE FOR MATERIAL IN RIM OF WHEEL, SHOWING SCHEMATICALLY THE EFFECT OF RELAXATION ON THE AVERAGE STRESS DEVELOPED IN RIM DURING SUCCESSIVE DRAG TESTS

progressed along the line DCF, and the heating cycle for the second drag will progress along the line FCD. During the second drag the compressive stress will decrease because of relaxation along the curve from D to H. The amount of relaxation will not be as much during the second drag as for the first drag because the initial compressive stress at the beginning of the second drag was smaller than for the first drag (see Fig. 25b). On cooling after the second drag, the average tensile stress in the rim will have been increased to a value represented by GJ. With successive drags, the average tensile stress in the rim of the wheel will increase; however, the rate of increase with each drag decreases with the number of drags. This trend has definitely been observed in the strain measurements and in the rim

movement. As shown in Figs. 22 and 23, the strain curves as well as the rim movement curve exhibit a sharp rise for the first few drags and then level off as the number of drags increases. The analysis of these curves is given in Section 33.

The total increase in the average tensile stress in the rim of the wheel due to drag testing probably never reaches a magnitude equal to the fracture strength of the material. However, the stress at the bottom of the saw cut where fracture begins is necessarily many times larger than the average stress in the rim. The average stress across the section of the rim through the saw cut is approximately twice the average stress across the solid section of the rim, since the saw cut removes approximately 50 percent of the rim cross-section. Also, the stress concentration factor for the notch created by the saw cut must be considerably greater than unity.

The determination of the magnitude of the stress at the bottom of the saw cut is rather improbable. The only possibility of analyzing the result of the drag test is to make the obvious assumption that the stress at the bottom of the saw cut increases with the average stress in the rim. Thus the relation between the maximum tensile stress at the bottom of the saw cut and the number of drags will be assumed to have the same general relation as that between the average tensile stress in the rim and number of drags. Using this method of analysis, any variables that appreciably affect the relaxation phenomena will be expected to affect appreciably the number of drags required to produce fracture.

The relation between the number of drags and the maximum stress at the bottom of the saw cut for a wheel initially free from residual stresses is shown schematically in Fig. 27. This curve will be referred to as the stress-buildup curve. The general shape of the curve shown in Fig. 27 may be obtained from Fig. 26. As was found in the analysis of Fig. 26, the amount of relaxation is greatest during the first drag test; therefore the greatest increase in the tensile stress at the bottom of the saw cut will occur on the first drag test. Since the rate of relaxation decreases with the number of drags, the rate of increase in stress at the bottom of the saw cut will also decrease with the number of drags.

Fracture will occur in the wheel when the stress at the bottom of the saw cut attains a magnitude equal to the fracture stress, which is represented by OA in Fig. 27. In drawing the line AB, it is assumed that the fracture stress is not affected by the drag testing. No significant change in the structure of the material at the bottom of the saw cut was found in the metallographic study.

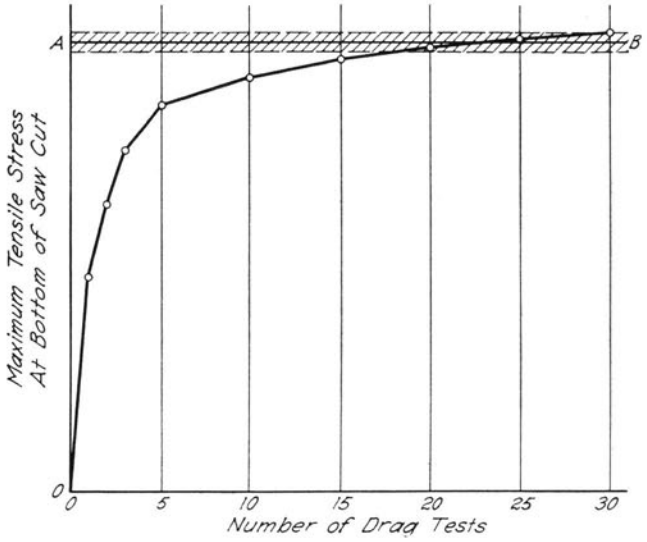

FIG. 27. RELATION BETWEEN MAXIMUM STRESS AT BOTTOM OF THE SAW-CUT AND NUMBER OF DRAG TESTS

Stress-buildup curve.

In Fig. 27 a shaded band is shown extending on each side of the line AB. This band may be considered the scatter band to account for the fact that the fracture stress is not a fixed value. Even though the scatter band may be relatively narrow, the number of drags required to produce fracture may be scattered over a wide range because of the characteristic shape of the stress-buildup curve. When one considers the possible variation in the test conditions, which will shift the stress-buildup curve up or down, in addition to the variation of the fracture stress, the scatter of the test data may be appreciable (see the scatter of the test results shown in the tables).

32. *Residual Stresses Introduced into the Wheel by the Heat Treatment Process*

An initial residual stress in the rim of a wheel has a decided influence on the number of drags required to produce fracture, since the initial stress determines the start of the stress-buildup curve shown in Fig. 27. If the wheel has an initial compressive stress in the rim, the start of the stress-buildup curve will be below the origin, and a greater number of drags will be required to attain the fracture stress. Conversely, initial tensile stress in the rim will decrease the number of drags required to produce fracture. The type and magnitude of the residual stresses are determined by the method of heat treatment, other factors being the same.

In the rim-quenching treatment only the rim of the wheel is quenched, so that the rim cools much more rapidly than the plate and the hub. The resulting temperature gradient is just opposite to that produced by the drag test, and the resulting residual stress distribution would be expected to be opposite to that produced by drag testing. The residual stresses presented in Tables 16 and 17 verify this assumption.

In the oil-quenching treatment the entire wheel is quenched in a bath of oil. Since the plate is the thinnest section, it cools much more rapidly than the rim and hub. The resulting temperature gradient between the rim and the plate is similar to that developed when drag testing, and the resultant residual stress upon cooling will tend toward an average tangential tension in the rim. Tangential stresses measured on the rim surfaces will be compression, due to the differential cooling from the surface to the center of the rim section. The temperature gradient between the hub and the plate will result in tension stresses being developed in the hub. These tension stresses in the hub will tend to reduce the magnitude of the tension stresses in the rim. The residual stress condition or pattern of the oil-quenched wheel is largely determined by the wheel design. In the A36 design wheel, which has a relatively long and thin plate and a relatively small hub mass compared to the rim mass, the tensile stresses produced in the hub probably have little influence on the rim stresses. In some wheel designs, in which the hub mass is large relative to the rim mass, it is possible that the tension stresses in the hub may change the stress pattern in the rim.

Residual stresses have been determined in A36 design oil-quenched Class C wheels; they are presented in Table 16. It will be noted that the rim surface stresses are compression in the tangential direction, while those at ½ in. and 1 in. below the center of the tread were found to be tension. The maximum measured tensile stresses were found at a depth of 1 in., which is near the bottom of the saw cut. The fact that the stresses in the rims of the oil-quenched wheels which were investigated were predominantly tension was verified when the wheels for residual stress determination having 400 deg F and 700 deg F draw temperatures were sawed. Both of these wheels fractured like a drag-tested wheel, when sawed through the rim.

33. *Analysis of the Strains Produced by Drag Testing*

The changes in strains produced by drag testing were determined at the locations shown in Fig. 12, with the 2-in. gage length Olsen-de-Shazer strain gage described in Chapter III, Section 10. Strains

were measured on the outer face and inner face of the wheel for a radial gage line at the saw cut and for a radial gage line located 90 deg from the saw cut. Since the strains in the plate were approximately the same for the two gage lines, only the strain data obtained at the gage line 90 deg from the saw cut are presented. At this gage line the strains measured in the rim are not affected by the saw cut. Attention should be called to the fact that in all cases the strain data were obtained while the wheels were at room temperature.

Only the strain data for the wheels used in the draw temperature investigation are considered, since the data for these wheels are the most nearly complete. To simplify the presentation, the strain data for the rim-quenched and oil-quenched wheels subjected to 800 deg F draw temperature are considered first. The strain data for these two wheels are shown in Table 18 and Figs. 22 and 23.

The data in Table 18 illustrate the method used to determine the plastic deformation which is produced in the wheel by drag testing. The data in Group 1 of Table 18 are the initial residual strains in the wheels as manufactured. The data in Group 2 are the total deformation, elastic and plastic, produced by drag testing companion wheels; they were obtained by taking the difference between the initial gage reading before starting the first drag test and the last gage reading before fracture. The algebraic addition of corresponding values of the data in Group 1 and Group 2 gives the data presented in Group 3, which would be the residual strain in the wheel at fracture if no plastic deformation had occurred[1]. The residual strains in the wheels after testing which are presented in Group 4 were obtained by sawing out the rosettes after fracture; they are based on the last strain reading before fracture. For most wheels, one or more drag tests were run after the last strain reading before fracture; the data are therefore somewhat in error. However, because of the leveling off of the strain-buildup curves (see Figs. 22 and 23) after several drag tests have been run, it is felt that the residual strain data in Table 18 are sufficiently accurate for comparative purposes. If corresponding values of Group 4 are subtracted algebraically from Group 3, the plastic deformation is obtained as shown in Group 5. The plus sign indicates that the plastic deformation was produced by tensile stresses; the negative sign, that the plastic deformation was produced by compressive stresses.

As indicated in Group 5 of Table 18, the plastic deformation

[1] The accuracy of the data in Group 3 is dependent upon the validity of the assumption that the residual stresses in companion wheels as manufactured are approximately the same. Since the stress data indicate that the differences in stress pattern between companion wheels may be small compared to differences between types of heat treatment or draw temperatures, the above assumption will be used to show the trends.

TABLE 18

STRAIN DATA FOR RIM-QUENCHED AND OIL-QUENCHED WHEELS HAVING 800-DEG F DRAW TEMPERATURE

Strain ÷ 10,000 in. per in.

Wheel Test Number	Heat Treatment	Number of Drags	Outer Face								Inner Face							
			Rim		P_1		P_2		P_3		Rim		P_1		P_2		P_3	
			R*	T	R	T	R	T	R	T	R	T	R	T	R	T	R	T
Group 1—Residual Strains in Wheels as Manufactured																		
306 ICR1R	R	None	−5	−10	−7	+4	+2	+6	+9	+3	−5	−12	+7	+1	−2	−2	−7	−3
309 ICO1R	E	None	−8	−11	−1	−12	−8	−11	−7	−11	−9	−9	−10	−11	−4	−11	−3	−10
Group 2—Change in Strain Due to Drag Testing																		
350 ICR1D	R	19	+27	−26	−10	−16	−10	−12	−5	−8	0	+10	+9	−7	+8	−2	+5	0
322 ICO1D	E	16	+24	−15	+1	−13	−6	−11	−14	−5	+1	+5	−2	−8	+6	−2	+11	−1
Group 3—Residual Strains at End of Testing if No Plastic Deformation Has Occurred																		
350 ICR1D	R	19	+22	−36	−17	−12	−8	−6	+4	−5	−5	−2	+16	−6	+6	−4	−2	−3
322 ICO1D	E	16	+16	−26	0	−25	−14	−22	−21	−16	−8	−4	−12	−19	+2	−13	+8	−11
Group 4—Residual Strains at End of Testing†																		
350 ICR1D	R	19	+2	−4	+8	−16	−8	−13	−14	−7	−6	+2	−3	−3	+6	−3	+13	0
322 ICO1D	E	16	−1	−1	0	−24	....	....	−21	−17	−9	+3	−7	−14	....	....	+10	−9
Group 5—Plastic Strain																		
350 ICR1D	R	19	+20	−32	−25	+4	0	+7	+18	+2	+1	−4	+19	−3	0	−1	−15	−3
322 ICO1D	E	16	+17	−25	0	−1	....	....	0	+1	+1	−7	−5	−5	....	....	−2	−2

* R — Radial; T — Tangential.

† The data are based on the last strain reading before fracture.

produced in the outer face of the rim of a wheel by drag testing is rather large. The plastic deformation in the tangential direction is negative, a fact which indicates that the plastic deformation occurred while the rim was subjected to compressive stress. This is in accord with the relaxation theory presented in Section 31. The plastic deformation in the tangential direction on the inner face of the rim is small compared to that on the outer face. This is due to the fact that the temperature of the inner face of the rim during a drag test is considerably lower than that of the outer face, because of the greater distance from the source of heat, so that the magnitude of the compressive stress developed on the inner face will be much less than that developed on the outer face; futhermore, the low temperature is not conducive to relaxation.

The plastic deformation in the radial direction in the rim is the result of relaxation of the high tensile stresses which are produced by the temperature gradient across the depth of the rim. This temperature gradient is the result of the fact that the energy is being impressed into the tread of the wheel, making it the hottest part of the rim; the temperature decreases with depth into the rim. Since higher temperature tends toward greater expansion, a radial tension stress is developed in the rim.

The changes in strain in the tangential direction on inner and outer faces of the rim due to drag testing are given in Group 2 of Table 18. The strain readings used in determining these values were recorded after various drags throughout the testing; they are plotted in Fig. 22 for the rim-quenched wheel and in Fig. 23 for the oil-quenched wheel. Besides the strain curves for the tangential direction in the rim, there are curves for strains in the radial direction at P_1 and P_3 in the plate (see Fig. 12) and a curve for the axial movement of the rim toward the outer face. Most of the curves have a sharp rise for the first few drags and then a leveling off, as was predicted by the relaxation theory presented in Section 31 and illustrated in Fig. 27. In Fig. 22 and again in Fig. 23 opposite trends are noted for the tangential strains in the rim on the outer and inner faces. The data presented in Group 5 of Table 18 show that the outer face of the rim undergoes plastic deformation during drag testing, whereas very little plastic deformation is produced on the inner face. A reduction in circumference of the outer face of the rim with little change on the inner face indicates that the rim is tipping during the drag testing. As the rim tips, the inner face increases in diameter. The result is small residual tension stresses in the tangential direction on this face, as given in Group 4 of Table 18. The data in Group

4 also indicate that the lower portion of the outer face of the rim is in compression after drag testing. This results from the tipping of the rim and from the fact that the extent of plastic deformation is smaller in this region than in the region near the tread because the temperature to which this region is heated by the drag test is less than that for the region near the tread.

Of particular interest are the strain data for the plate of the wheels, as shown in Group 5 of Table 18. The plastic strains in the

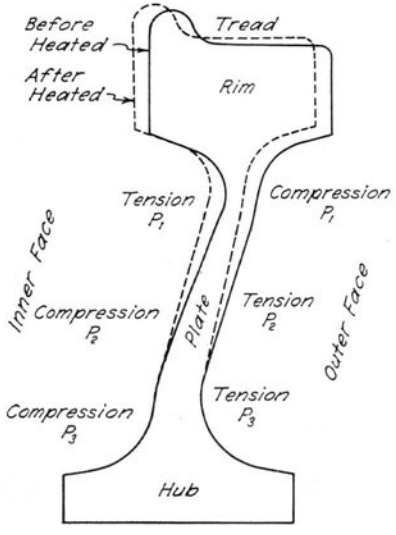

FIG. 28. CROSS-SECTION OF WHEEL SHOWING RIM MOVEMENT AND RESULTING BENDING STRESSES IN PLATE WHEN RIM OF WHEEL IS HEATED

plates of the rim-quenched wheels are large relative to the plastic strains in the plates of the oil-quenched wheels. Also, the residual strains in the plates of the rim-quenched wheels before drag testing have signs generally opposite to what they are after drag testing, whereas most of the residual strains do not change signs during the drag testing of the oil-quenched wheels.

In Fig. 28 is shown a cross-section of a wheel before starting the first drag test (solid lines) and while the rim of the wheel is heated during the drag test (dotted lines). As the rim of the wheel is heated, it expands and straightens the plate as shown (Fig. 28) by the cross-section with the dotted line. For the thick plate wheels the movement of the rim, from its initial position when cold to its position at the end of a drag test when hot, is approximately $\frac{1}{8}$ in. The straight-

ening of the plate introduces radial tension in the plate and produces bending stresses in the plate near the rim and near the hub. The type of stress due to bending at each location is given in Fig. 28. During the drag test the compressive stresses developed in the rim are relaxed, so that on cooling to room temperature after the first drag the the rim is shorter in circumference than before the test. The resulting tension in the rim produces a compressive force in the plate and bending stresses which are opposite to those shown in Fig. 28. Thus, when the wheel is cooled following the first drag the rim moves axially toward the outer face beyond its position before the test. The effect of a number of drags on the rim movement for the rim-quenched and oil-quenched wheels is shown by the dotted curves in Figs. 22 and 23.

For the rim-quenched wheel, it will be noted, the bending strains produced in the plate of the wheel when the rim is heated by drag testing (see Fig. 28) have the same sign as the initial residual strains given in Group 1 of Table 18. Since these strains add together, there is a possibility that during the drag test the stresses may be sufficient to produce yielding (plastic deformation which is independent of time). The plastic deformation data for the rim-quenched wheel indicate that appreciable yielding did take place. The plastic strains in the radial direction at P_3 are rather large for both the outer and the inner faces of the wheel. The temperature of the plate of the wheel near the hub (P_3) never reaches a sufficient magnitude to produce appreciable relaxation, so that the plastic strains at this location are due to yielding. Furthermore, all the yielding at P_3 must occur during the first drag, since the greatest movement of the rim in the axial direction toward the inner face occurs during the first drag test. This fact explains the reversal in trend of the strain-vs.-number-of-drags curves for P_3, as shown in Fig. 22. On cooling the wheel at the end of the first drag, the compressive strain produced in the radial direction at P_3 on the outer face is not sufficient to equal the plastic strain caused by yielding in tension when the rim was hot. With subsequent drags, however, the movement of the rim toward the outer face increases the compressive strains on the outer face at P_3, as shown in Fig. 22.

It will be noted in Group 5 of Table 18 that the plastic strains in the plate of a rim-quenched wheel have the same sign as the initial residual strains. This indicates that the plastic deformation at each location occurred during the heating part of the drag test.

For the oil-quenched wheels the residual strains in the plate before testing are in general opposite in sign to those for the rim-quenched wheels; consequently the plastic strains produced in the

plate of the oil-quenched wheels by drag testing are small, as indicated by the data in Group 5 of Table 18. Since the plastic strains in the radial direction at P_3 are negligible, the strain-vs.-number-of-drags curve for P_3 shown in Fig. 23 does not show a reversal of direction such as was found for the rim-quenched wheel in Fig. 22. Otherwise the trends of the curves for the oil-quenched wheel are similar to those for the rim-quenched wheel.

34. *Analysis of Effect of Heat Treatment on Drag Test Results*

The effect of the type of heat treatment on the drag test results can be explained by the stress-buildup curve shown in Fig. 27. Because of predominating residual compression in the rims of untested rim-quenched wheels and predominating residual tension in the rims of untested oil-quenched wheels, the start of the stress-buildup curve will be above the origin for the oil-quenched wheels and below the origin for the rim-quenched wheels, as shown in Fig. 29. Assuming that the fracture stress of the rim material is the same for the wheels with either type of heat treatment, because of similar mechanical properties, the number of drags required to produce fracture in the rim-quenched wheel would be expected to be appreciably greater than for the oil-quenched wheel. Attention should be called to the fact that the shape of the stress-buildup curve as well as the location of the start of curve is affected by the type of heat treatment. The initial residual stresses of the rim-quenched wheel add to those developed in the wheel when the rim is heated by the drag test (see the previous Section) so that rate of relaxation and the resulting buildup of the tensile stress in the rim-quenched wheel are greater than for the oil-quenched wheel. This offsets to some extent the initial advantageous residual stress distribution of the rim-quenched wheels. However, a number of drag tests are required on the rim-quenched wheels to change the residual stress distribution to one that is comparable with the initial residual stress distribution in the oil-quenched wheels. Consequently, the rim-quenched wheels are more resistant to wheel fracture than the oil-quenched wheels, as indicated by the drag test data presented in Tables 4 and 5 and plotted in Figs. 11 and 14.

The location of the start of the stress-buildup curves shown in Fig. 29 is affected by the draw temperature and other manufacturing factors. By sufficiently increasing the draw temperature, the residual stresses in the wheel after manufacture will approach zero, and the stress-buildup curves for rim-quenched and oil-quenched wheels will coincide. The test data presented in Table 5 and plotted in Fig. 14

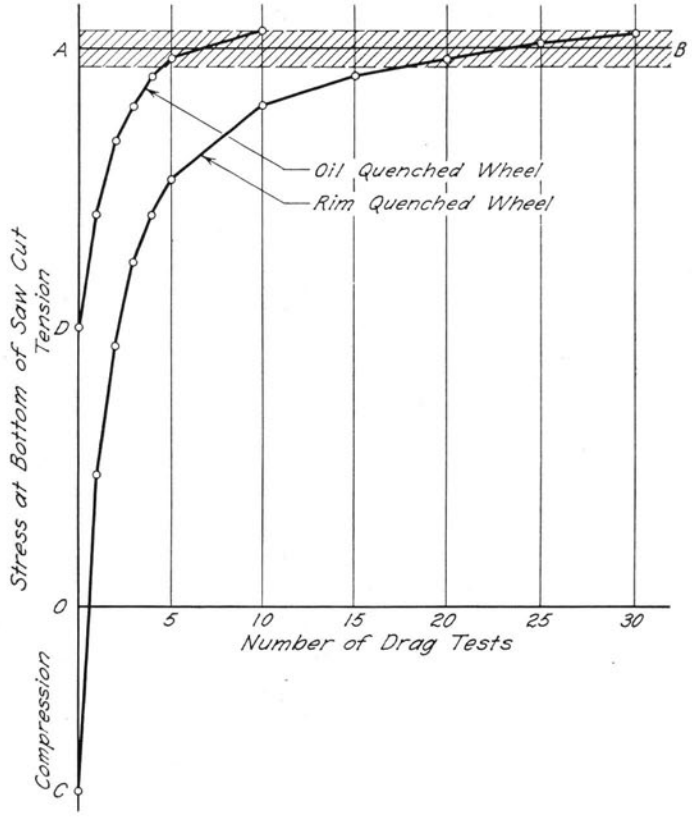

FIG. 29. EFFECT OF RESIDUAL STRESS ON STRESS-BUILDUP CURVE

indicate that the least difference between the two heat treatments occurs at the highest draw temperature of 1200 deg F. Since a decrease in draw temperature lowers the start of the stress-buildup curve for rim-quenched wheels and raises it for the oil-quenched wheels, a decrease in draw temperature might be expected to increase the number of drags required to produce wheel fracture for the rim-quenched wheels and decrease the number of drags for the oil-quenched wheels. The plot of the test data presented in Fig. 14 does not bear out this assumption.

There are at least two reasons why the drag test data for the wheels used in the draw temperature investigation do not follow the trend indicated by the stress-buildup curve shown in Fig. 29. In the first place, at any given draw temperature the higher residual stresses will decrease (through relaxation) more rapidly than the

lower residual stresses. Thus, there will be developed a changed relationship between the residual stresses at various locations. Such stress relationships may be an important variable in influencing the resistance of the wheels to wheel fracture. In the second place, the changes in mechanical properties resulting from the higher draw temperature may have an appreciable effect on the resistance of wheels to wheel fracture.

For the lower draw temperatures in which the metallurgical structure was not appreciably affected (see Chapter II, Section 6), the drag test data for the oil-quenched wheels agreed with the theory. The residual tangential stresses 1 in. below the tread (Table 16) indicate that the residual tensile stresses at this location increase with a decrease in draw temperature, thus shifting the start of the stress-buildup curve upward (see Fig. 29). The drag test data for the oil-quenched wheels drawn at low temperatures are in agreement with this theory, and the oil-quenched wheels were found to have low resistance to wheel fracture.

The drag test data for the rim-quenched wheels drawn at the lower temperatures do not show an increase in resistance to wheel fracture, as was indicated by the theory. The theory was based on the assumption that the residual stresses in the tangential direction in the center of the rim were compression, which increased appreciably with a decrease in draw temperature. Actually these residual stresses are small as compared to the surface stresses, and the data presented in Table 16 indicate that the residual compressive stresses at 1 in. below the tread may decrease rather than increase when the wheel is drawn at lower temperatures. Thus, below a given draw temperature the start of the stress-buildup curve may be raised rather than lowered; this fact will account for a decrease in resistance to wheel fracture for the low draw temperatures.

The strain data for the wheels used in the draw temperature investigation are presented in Tables 19 and 20. The data are arranged in the same form as those presented in Table 18. The strain data for the rim-quenched wheels presented in Table 19 indicate that at fracture the residual stress distribution has to a large extent reversed itself. The initial residual strains, the change in strain due to drag testing, and the plastic strains all increase with a decrease in draw temperature. The strain data for the oil-quenched wheels given in Table 20 indicate an increase in the residual strains, a decrease in change in strain due to drag testing, and a decrease in plastic strain, with a decrease in draw temperature. The residual strain distribution after testing is similar to what it was before testing.

35. *Analysis of Effect of Changes in Wheel Design on Drag Test Results*

For wheels of specific chemical analysis and heat treatment, the resistance to wheel fracture can be increased by a change in geometry, if the given change lowers the rate of stress-buildup. If the stress-buildup curve shown in Fig. 27 is representative of a basic wheel, then the stress-buildup curve of a wheel of improved design would fall below that curve. A change in geometry of the wheel can lower the rate of stress-buildup only if the change will decrease the amount of relaxation of the compressive stresses occurring in the rim of the wheel when the wheel is heated. From the relaxation curves shown in Fig. 25 it would appear that for a given wheel design the amount of relaxation can be decreased either by lowering the temperature or by decreasing the time, neither of which is feasible; or by lowering the compressive stress. Since the compressive stresses are developed in the outer portion of the wheel because the inner portion is too stiff to let the rim expand when it is heated, the logical solution to the problem would be to make the plate more flexible.

There are two changes in the geometry which should increase the flexibility of the plate — a decrease in plate thickness or an increase in the angle of the plate. The drag test data presented in Section 13 indicated that the number of drags required to produce fracture can be greatly increased by decreasing the plate thickness. If the plate thickness is decreased by one-half, the resistance of the plate to bending is reduced to approximately one-quarter and the resistance to a radial load is reduced to approximately one-half. The drag test data plotted in Fig. 16 indicate that the thin plate wheel has about four times as much resistance to wheel fracture as the thick plate wheel. As yet, no wheels have been tested to determine the effect of the angle of the plate on the ability of the wheel to resist wheel fracture. With the present truck design it is not feasible to change the angle of the plate to any large extent.

36. *Stress Analysis of Stop-Tested Wheels*

During the stop test, the high rate of energy input to the tread of the wheel heats the tread to an austenitizing temperature, but the short duration of test does not allow very deep penetration of the heated zone into the rim. The resulting temperature gradient produces large compressive stresses in the tread of the wheel. Both the high temperature and the high stress are conducive to extremely rapid relaxation, so that a large percentage of the compressive stress will be relieved by the end of the 25–50-sec duration of the stop test.

TABLE 19
STRAIN DATA FOR RIM-QUENCHED WHEELS
Strain ÷ 10,000 in. per in.

Wheel Test No.	Draw Temp, deg F	No. Drags to Fracture	No. Drags before Last Reading	Outer Face								Inner Face							
				Rim		P_1		P_2		P_3		Rim		P_1		P_2		P_3	
				R	T	R	T	R	T	R	T	R	T	R	T	R	T	R	T
Group 1—Residual Strains in Wheels as Manufactured																			
301 ICR1R	1 200			+5	0	−1	−2	−1	−3	0	−1	−2	−1	0	−1	+2	−2	−2	−1
303 ICR1R	1 000			−2	−3	−2	+1	+1	0	+3	+1	−2	−2	+1	0	−2	−1	−3	−2
304 ICR1R	900			−3	−4	−2	+2	+2	+6	+5	+1	−1	−5	+2	0	−2	−1	−3	−2
306 ICR1R	800			−5	−10	−7	+4	+2	+6	+9	+3	−5	−12	+7	+1	−2	−2	−7	−3
305 ICR1R	700			−5	−12	−10	+6	+4	+7	+18	+4	−6	−17	+17	+2	−3	−4	−8	−4
307 ICR1R	400			−9	−12	−23	+8	+12	+12	+48	+2	−9	−23	+27	+5	−13	−6	−19	−7
Group 2—Change in Strain Due to Drag Testing*																			
330 ICR1D	1 200	20	18	+11	−12	−3	−7	−5	−5	0	−3	+2	+3	0	−3	+5	0	−1	0
348 ICR1D	1 000	28	26	+12	−14	−4	−10	−7	−7	−3	−5	+2	+7	+1	−2	+6	0	+6	0
349 ICR1D	900	22	18	+21	−14	−6	−9	−7	−6	−1	−4	+1	+9	0	−7	+5	0	+4	−1
350 ICR1D	800	19	18	+27	−26	−10	−16	−10	−12	−5	−8	0	+10	+9	−7	+8	−2	+5	0
351 ICR1D	700	23	22	+30	−35	−13	−18	−10	−13	−7	−8	+1	+16	+7	−7	+10	−1	+8	+1
329 ICR1D	400	14	12	+37	−29	−5	−23	−13	−19	−17	−11	+6	+10	+2	−10	+12	−2	+13	+2
Group 3—Residual Strains at End of Testing if No Inelastic Deformation Has Occurred																			
330 ICR1D	1 200	20	18	+16	−12	−4	−9	−6	−8	0	−4	0	+2	0	−4	+7	−2	−3	−1
348 ICR1D	1 000	28	26	+10	−17	−6	−9	−6	−7	0	−4	0	+5	+2	−2	+4	−1	+3	−2
349 ICR1D	900	22	18	+18	−18	−8	−7	−5	0	+4	−3	0	+4	+2	−7	+3	−1	+1	−3
350 ICR1D	800	19	18	+22	−36	−17	−12	−8	−6	+4	−5	−5	−2	+16	−6	+6	−4	−2	−3
351 ICR1D	700	23	22	+25	−47	−23	−12	−6	−6	+11	−4	−5	−1	+24	−5	+7	−5	0	−3
329 ICR1D	400	14	12	+28	−41	−28	−15	−1	−7	+31	−9	−3	−13	+29	−5	−1	−8	−6	−5

R — Radial; T — Tangential.
* The data are based on the last strain reading before fracture.

TABLE 19 (CONCLUDED)
STRAIN DATA FOR RIM-QUENCHED WHEELS
Strain ÷ 10,000 in. per in.

Wheel Test No.	Draw Temp, deg F	No. Drags to Fracture	No. Drags before Last Reading	Outer Face								Inner Face							
				Rim		P_1		P_2		P_3		Rim		P_1		P_2		P_3	
				R	T	R	T	R	T	R	T	R	T	R	T	R	T	R	T
Group 4—Residual Strains at End of Testing*																			
330 ICR1D	1 200	20	18	−3	−2	+6	−14	−7	−11	−18	−7	−3	+6	−12	−4	+5	−1	+12	−1
348 ICR1D	1 000	28	26	−2	−3	+1	−12	−9	−12	−18	−8	−3	+9	−10	−3	+4	−1	+10	−7
349 ICR1D	900	22	18	−1	−5	+2	−12	−7	−11	−18	−11	−5	+3	−11	−2	+4	−2	+14	−1
350 ICR1D	800	19	18	+2	−4	+8	−16	−8	−13	−14	−7	−6	+2	−3	−3	+6	−3	+13	0
351 ICR1D	700	23	22	−2	−4	+3	−17	−9	−13	−18	−8	−7	−1	−7	−5	+7	−5	+13	0
329 ICR1D	400	14	12	0	−2	+3	−18	−8	−11	−14	−5	−5	+1	−8	−4	+5	−5	+13	−1
Group 5—Inelastic Deformation																			
330 ICR1D	1 200	20	18	+19	−10	−10	+5	+1	+3	+18	+3	+3	−4	+12	0	+2	−1	−15	0
348 ICR1D	1 000	28	26	+12	−14	−7	+3	+3	+5	+18	+4	+3	−4	+12	+1	0	0	−7	+5
349 ICR1D	900	22	18	+19	−13	−10	+5	+2	+11	+22	+8	+5	+1	+13	−5	−1	+1	−13	−2
350 ICR1D	800	19	18	+20	−32	−25	+4	0	+7	+18	+2	+1	−4	+19	−3	0	−1	−15	−3
351 ICR1D	700	23	22	+27	−43	−26	+5	+3	+7	+29	+4	+2	0	+31	0	0	0	−13	−3
329 ICR1D	400	14	12	+28	−39	−31	+3	+7	+4	+45	−4	+2	−14	+37	−1	−6	−3	−19	−4

* The data are based on the last strain reading before fracture.

TABLE 20
STRAIN DATA FOR OIL-QUENCHED WHEELS
Strain ÷ 10,000 in. per in.

Wheel Test No.	Draw Temp, deg F	No. Drags to Fracture	No. Drags before Last Reading	Outer Face								Inner Face							
				Rim		P_1		P_2		P_3		Rim		P_1		P_2		P_3	
				R	T	R	T	R	T	R	T	R	T	R	T	R	T	R	T
Group 1—Residual Strains in Wheels as Manufactured																			
296 ICO1R	1 200			−1	−1	−1	−1	−1	−3	+3	−2	0	−1	+1	−3	+1	−3	0	−2
302 ICO1R	1 000			−1	−3	−1	−5	−4	−5	−3	−5	−2	−2	−1	−3	0	−4	−1	−2
308 ICO1R	900			−5	−6	−2	−6	−3	−6	−3	−5	−4	−4	−4	−5	−2	−5	−2	−5
309 ICO1R	800			−8	−11	−1	−12	−8	−11	−7	−11	−9	−9	−10	−11	−4	−11	−3	−10
310 ICO1R	700			−10	−13	−1	−17	−11	−18	−8	−16	−12	−10	−11	−17	−5	−17	−2	−15
311 ICO1R	400			−14	−17	−1	−30	....	−23	−12	−26	−15	−9	−14	−23	−7	−20	−4	−23
Group 2—Change in Strain Due to Drag Testing*																			
319 ICO1D	1 200	47	44	+20	−20	0	−15	−9	−11	−14	−8	−2	+2	−5	−8	+7	0	+8	0
320 ICO1D	1 000	12	11	+17	−15	0	−11	−7	−8	−11	−6	0	+3	−3	−5	+5	−1	+6	0
321 ICO1D	900	13	12	+22	−13	+1	−13	−7	−9	−12	−5	+3	+5	−1	−5	+8	0	+9	+1
322 ICO1D	800	16	16	+24	−15	+1	−13	−6	−11	−14	−5	+1	+5	−2	−8	+6	−2	+11	−1
357 ICO1D	700	4	2	+11	−2	0	−7	−4	−5	−6	−3	+2	+4	0	−2	+4	−1	+4	0
358 ICO1D	400	4	2	+16	−9	−1	−6	−5	−6	−7	−3	+4	+4	+1	−3	+3	−1	+4	0
Group 3—Residual Strains at End of Testing if No Inelastic Deformation Occurred																			
319 ICO1D	1 200	47	44	+19	−21	−1	−16	−10	−14	−11	−10	−2	+2	−4	−11	+8	−3	+8	−2
320 ICO1D	1 000	12	11	+16	−18	−1	−16	−11	−13	−14	−11	−2	+1	−4	−8	+5	−5	+5	−2
321 ICO1D	900	13	12	+17	−19	−1	−19	−10	−15	−15	−10	−1	+1	−5	−10	+6	−5	+7	−4
322 ICO1D	800	16	16	+16	−26	0	−25	−14	−22	−21	−16	−8	−4	−12	−19	+2	−13	+8	−11
357 ICO1D	700	4	2	+1	−15	−1	−24	−15	−23	−14	−19	−10	−6	−11	−19	−1	−18	+2	−15
358 ICO1D	400	4	2	+2	−26	−2	−36	....	−29	−19	−29	−11	−5	−13	−26	−4	−21	0	−23

* The data are based on the last strain reading before fracture.

TABLE 20 (CONCLUDED)
STRAIN DATA FOR OIL-QUENCHED WHEELS
Strain ÷ 10,000 in. per in.

Wheel Test No.	Draw Temp, deg F	No. Drags to Fracture	No. Drags before Last Reading	Outer Face								Inner Face							
				Rim		P_1		P_2		P_3		Rim		P_1		P_2		P_3	
				R	T	R	T	R	T	R	T	R	T	R	T	R	T	R	T
Group 4—Residual Strains at End of Testing*																			
319 ICO1D	1 200	47	44	−1	+1	+6	−12	−8	−13	−21	−8	−3	+9	−11	−7	+7	−4	+12	−2
320 ICO1D	1 000	12	11	−1	−1	+1	−13	−10	−13	−19	−9	−3	+5	−10	−6	+6	−4	+8	−2
321 ICO1D	900	13	12	+1	0	+5	−18	....	....	−19	−10	−4	+5	....	....	+8	−5	+12	−4
322 ICO1D	800	16	16	−1	−1	0	−24	....	....	−21	−17	−12	+3	−7	−14	....	....	+10	−9
357 ICO1D	700	4	2	−10	−7	−2	−26	....	....	−19	−22	−13	−6	−12	−19	−6	−19	0	−14
358 ICO1D	400	4	2	−3	−9	−7	−33	....	....	−24	−32	−15	−5	−23	−28	−10	−31	−3	−26
Group 5—Inelastic Deformation																			
319 ICO1D	1 200	47	44	+20	−22	−7	−4	−2	−1	+10	−2	+1	−7	+7	−4	+1	+1	−4	0
320 ICO1D	1 000	12	11	+17	−17	−2	−3	−1	0	+5	−2	+1	−4	+6	−2	−1	−1	−3	0
321 ICO1D	900	13	12	+16	−19	−6	−1	....	....	+4	0	+3	−4	....	....	−2	0	−5	0
322 ICO1D	800	16	16	+17	−25	0	−1	....	....	0	+1	+4	−7	−5	−5	....	....	−2	−2
357 ICO1D	700	4	2	+11	−8	+1	+2	....	....	+5	+3	+3	0	+1	0	+5	+1	+2	−1
358 ICO1D	400	4	2	+5	−17	+5	−3	....	....	+5	+3	+4	0	+10	+2	+6	+10	+3	+3

* The data are based on the last strain reading before fracture.

After the wheel is cooled following a stop test, tensile stresses are developed in the region of the tread where the plastic deformation has taken place. Since the total volume of the material in the rim that is plastically deformed by the stop test is small, the changes in strain at the strain rosettes shown in Fig. 12 are small. Because no method has been developed to determine the stresses in the tread of the wheel and it was not thought that the small stresses in the outer and inner faces of the rim and plate were indicative of the high tread stresses, few strain data were taken during the stop testing, and none are presented in this bulletin.

APPENDIX B

General Data for All Wheels Tested

Tests of an exploratory nature were made on a number of wheels. Though not reported in the body of this bulletin, the results of these tests are included in Tables 21, 22, 23, 24, and 25 of this Appendix. These tables show the general data obtained from each wheel tested. In Tables 21, 22, and 23 the average coefficient of friction is given in the last column for both the drag-tested and the stop-tested wheels.

TABLE 21

SUMMARY OF DRAG TEST RESULTS OF 36-IN.-DIAM WHEELS TESTED WITHOUT SIMULATED THERMAL CRACK

Wheel Test No.	Heat No.	Class	Heat Treatment	Draw Temp, deg F	Plate Thickness* A, inches	Plate Thickness* B, inches	Rim Thickness, inches	Speed, mph	Brake Shoe Pressure, lb	No. of Drags	Fracture on Saw Cut	Type of Drag	Av Coef. of Friction
1 IAO1D	31077	A	E	990	1.00	1.09	2.31	50	3 000	10	No	20 min.†	0.121
2 IAO1D	31077	A	E	990	0.88	1.06	2.53	50	2 600	12	Yes	30 min.	0.128
7 IBO1D	37021	B	E	990	0.94	1.38	2.25	50	2 600	6	Yes	30 min.	0.122
8 IBO1D	37021	B	E	990	1.00	1.31	2.28	50	3 000	14	No	20 min.	0.121
13 ICO1D	87120	C	E	1 040	1.03	1.03	2.28	50	2 600	18	Yes	30 min.	0.114
14 ICO1D	87120	C	E	1 040	1.00	0.94	2.41	50	3 000	12	Yes	20 min.	0.110
19 SAW1D	E6270	A	W	800	0.97	1.13	2.53	50	3 000	10	No	20 min.	0.137
20 SAW1D	E6270	A	W	800	1.03	1.25	2.63	50	2 600	8	No	30 min.	0.132
31 BAR1D	46L223	A	R	870	1.06	1.31	2.56	50	2 600	12	No	30 min.	0.144
32 BAR1D	46L223	A	R	870	1.00	1.38	2.69	50	2 600	20	No	30 min.	0.128
37 BBR1D	46L256	B	R	870	1.06	1.34	2.59	50	2 600	8	No	30 min.	0.136
38 BBR1D	46L256	B	R	870	0.94	1.28	2.69	50	2 600	22	Yes	30 min.	0.126
43 BCR1D	47L193	C	R	870	0.94	1.28	2.75	50	2 600	8	Yes	30 min.	0.128
44 BCR1D	47L193	C	R	870	0.94	1.41	2.69	50	2 600	8	Yes	30 min.	0.123
48 BCR1D	47L193	C	R	870	0.97	1.41	2.69	50	2 600	14	Yes	30 min.	0.127
50 IDO1D	28087	C	E	970	1.06	1.19	2.72	50	2 600	10	Yes	30 min.	0.123
51 IDO1D	28087	C	E	970	0.94	1.06	2.63	50	2 600	10	Yes	30 min.	0.127
54 IDO1D	28087	C	E	970	1.03	1.13	2.53	50	3 000	14	Yes	Int.‡	0.121
56 IEO1D	28090	B	E	970	1.09	1.00	2.53	50	2 600	10	Yes	30 min.	0.131
57 IEO1D	28090	B	E	970	1.00	1.03	2.69	50	2 600	10	Yes	30 min.	0.132
62 ICO1D	46568	C	E	970	1.09	1.31	2.66	50	3 000	12	Yes	Int.	0.110
63 ICO1D	46568	C	E	970	1.13	1.38	2.69	50	3 000	6	Yes	Int.	0.116

* See Fig. 3.
† Continuous application.
‡ "Int." stands for "intermittent."

TABLE 21 (CONCLUDED)

SUMMARY OF DRAG TEST RESULTS OF 36-IN.-DIAM WHEELS TESTED WITHOUT SIMULATED THERMAL CRACK

Wheel Test No.	Heat No.	Class	Heat Treatment	Draw Temp, deg F	Plate Thickness* A, inches	Plate Thickness* B, inches	Rim Thickness, inches	Speed, mph	Brake Shoe Pressure, lb	No. of Drags	Fracture on Saw Cut	Type of Drag	Av Coef. of Friction
65 ICO1D	46568	C	E	970	1.13	1.41	2.69	50	3 000	1	Yes	Int.	0.115
67 ICR1D	46568	C	R	970	1.06	1.38	2.72	50	3 000	12	Yes	Int.	0.116
68 ICR1D	46568	C	R	970	1.19	1.25	2.75	50	3 000	6	Yes	Int.	0.109
72 ICO1D	46568	C	E	1 140	1.09	1.41	2.72	50	3 000	6	Yes	Int.	0.123
73 ICO1D	46568	C	E	1 140	1.13	1.31	2.72	50	3 000	3	Yes	Int.	0.100
75 ICO1D	46568	C	E	1 140	1.03	1.25	2.63	50	3 000	1	Yes	Int.	0.106
77 ICR1D	46568	C	R	1 140	1.06	1.34	2.63	50	3 000	12	Yes	Int.	0.121
78 ICR1D	46568	C	R	1 140	1.19	1.25	2.66	50	3 000	6	Yes	Int.	0.122
80 ICR1D	46568	C	R	1 140	0.97	1.22	2.78	50	3 000	3	Yes	Int.	0.118
82 ICU1D	46568	U	U	....	1.06	1.31	2.75	50	3 000	12	Yes	Int.	0.112
83 ICU1D	46568	U	U	....	1.13	1.31	2.59	50	3 000	6	Yes	Int.	0.109
87 IFO1D	43607	C	E	970	0.94	1.28	2.63	50	3 000	6	Yes	Int.	0.104
88 IFO1D	43607	C	E	970	1.03	1.31	2.75	50	3 000	3	Yes	Int.	0.114
104 IBO1D	34519	B	E	930	1.08	1.45	2.63	50	3 000	10	Yes	Int.	0.117
107 IBO1D	34519	B	E	930	1.03	1.44	2.59	40	3 000	10	No	Int.	0.139
108 IBO1D	34519	B	E	930	1.19	1.50	2.61	45	3 000	10	Yes	Int.	0.131
112 IBO1D	34519	B	E	930	1.20	1.55	2.61	50	3 000	10	No	Int.	0.127
115 IBO1D	34519	B	E	930	1.22	1.55	2.59	50	3 000	10	No	Int.	0.121
116 IBO1D	34519	B	E	930	1.16	1.42	2.59	40	3 000	10	No	Int.	0.132
117 IBO1D	34519	B	E	930	1.13	1.38	2.69	55	3 000	10	No	Int.	0.113
123 IBO1D	34519	B	E	930	1.19	1.55	2.56	55	3 000	10	Yes	Int.	0.110
124 IBO1D	34519	B	E	930	1.22	1.53	2.61	50	3 000	10	Yes	Int.	0.123
131 IBR1D	34519	B	R	930	1.16	1.45	2.67	50	3 000	10	No	Int.	0.128

* See Fig. 3.

TABLE 22

SUMMARY OF DRAG TEST RESULTS OF WHEELS HAVING A SIMULATED THERMAL CRACK

Brakes applied for 50 sec of each minute for the duration of the 30 minute test

Wheel Test No.	Heat No.	Class	Heat Treatment	Draw Temp, deg F.	Diameter, in.	Plate Thickness* A, in.	Plate Thickness* B, in.	Rim Thickness, inches	Speed, mph	Brake Shoe Pressure, lb	Depth Saw Cut, %	No. of Drags	Fracture	Av Coef. of Friction
70 ICR1D	46568	C	R	970	36	1.03	1.34	2.72	50	3 000	100†	1	Yes	0.110
105 IBO1D	34519	B	E	930	36	1.29	1.58	2.63	50	3 000	100	1	Yes	0.127
106 IBO1D	34519	B	E	930	36	1.19	1.42	2.58	50	3 000	50	4	Yes	0.115
109 IBO1D	34519	B	E	930	36	1.16	1.47	2.64	50	3 000	100†	1	Yes	0.120
110 IBO1D	34519	B	E	930	36	1.20	1.45	2.58	40	3 000	50	12	Yes	0.146
111 IBO1D	34519	B	E	930	36	1.17	1.61	2.59	40	3 000	100	1	Yes	0.134
113 IBO1D	34519	B	E	930	36	1.16	1.33	2.52	35	3 000	50	17	Yes	0.142
114 IBO1D	34519	B	E	930	36	1.19	1.69	2.59	45	3 000	50	9	Yes	0.136
118 IBO1D	34519	B	E	930	36	1.29	1.72	2.61	50	3 000	50	5	Yes	0.114
119 IBO1D	34519	B	E	930	36	1.19	1.53	2.56	40	3 000	50	9	Yes	0.132
120 IBO1D	34519	B	E	930	36	1.22	1.42	2.53	45	3 000	50	8	Yes	0.130
121 IBO1D	34519	B	E	930	36	1.23	1.42	2.20	35	3 000	50	34	Yes	0.129
122 IBO1D	34519	B	E	930	36	1.19	1.67	2.56	40	3 000	50	13	Yes	0.142
125 IBO1D	34519	B	E	930	36	1.22	1.53	2.47	35	3 000	50	10	Yes	0.139
126 IBO1D	34519	B	E	930	36	1.14	1.38	2.31	‡	3 000	50	5	No	0.129
127 IBO1D	34519	B	E	930	36	1.28	1.61	2.61	¶	3 000	50	9	Yes	0.131
128 IBO1D	34519	B	E	930	36	1.06	1.41	2.53	35	3 000	50	13	Yes	0.133
129 IBR1D	34519	B	R	930	36	1.17	1.39	2.47	50	3 000	50	15	Yes	0.120
130 IBR1D	34519	B	R	930	36	1.20	1.41	2.47	45	3 000	50	30	Yes	0.136
132 IBR1D	34519	B	R	930	36	1.17	1.53	2.56	50	3 000	50	9	Yes	0.118
133 IBR1D	34519	B	R	930	36	1.23	1.45	2.44	45	3 000	50	23	Yes	0.138
134 IBR1D	34519	B	R	930	36	1.11	1.41	2.53	45	3 000	50	22	Yes	0.131
135 IBO1D	34519	B	E	930	36	1.11	1.31	2.59	45	3 000	50	9	Yes	0.136
136 IBO1D	34519	B	E	930	36	1.13	1.44	2.52	45	3 000	50	3	Yes	0.120
137 IBO1D	34519	B	E	930	36	1.11	1.36	2.52	45	3 000	50	8	Yes	0.133
139 IBO1D	34519	B	E	930	36	1.14	1.41	2.48	45	3 000	50	15	Yes	0.137
140 IBR1D	34519	B	R	930	36	1.11	1.44	2.39	45	3 000	50	39	Yes	0.133
141 IBR1D	34519	B	R	930	36	1.12	1.36	2.39	45	3 000	50	40	Yes	0.134
149 IBO1D	34519	B	E	930	36	1.13	1.44	2.66	45	3 000	50	17	Yes	0.138
150 IBO1D	34519	B	E	930	36	1.19	1.45	2.59	45	3 000	50	8	Yes	0.140
151 IBR1D	34519	B	R	930	36	1.17	1.41	2.70	45	3 000	50	50	Yes	0.132

* See Fig. 3.
† Wheel tested without shim.
‡ One test each at 35, 40, 45, 50, and 55 mph.
¶ Two tests each at 35, 40, 45, 50, and one test at 55 mph.

TABLE 22 (CONTINUED)

SUMMARY OF DRAG TEST RESULTS OF WHEELS HAVING A SIMULATED THERMAL CRACK

Brakes applied for 50 sec of each minute for the duration of the 30 minute test

Wheel Test No.	Heat No.	Class	Heat Treatment	Draw Temp, deg F	Diameter, in.	Plate Thickness* A, in.	Plate Thickness* B, in.	Rim Thickness, inches	Speed, mph	Brake Shoe Pressure, lb.	Depth Saw Cut, %	No. of Drags	Fracture	Av Coef. of Friction
152 IBR1D	34519	B	R	930	36	1.17	1.34	2.62	45	3 000	50	30	No	0.132
155 ICU3D	40307	U	U		33	0.78	1.00	1.37‡	45	3 000	50	5	Yes	0.131
156 ICU4D	40307	U	U		33	0.44	0.60	1.44‡	45	3 000	50	30	No	0.123
157 ICU3D	40307	U	U		33	0.72	1.00	1.37‡	45	3 000	50	9	Yes	0.128
158 ICU4D	40307	U	U		33	0.53	0.62	1.34	45	3 000	50	30	No	0.133
159 ICU3D	40307	U	U		33	0.75	1.00	1.56	45	3 000	50	8	Yes	0.134
160 ICU4D	40307	U	U		33	0.47	0.62	1.19‡	45	3 000	50	50	No	0.135
161 ICU3D	40307	U	U		33	0.72	1.10	1.44	45	3 000	50	13	Yes	0.136
162 ICU4D	40307	U	U		33	0.56	0.75	1.28‡	45	3 000	50	30	No	0.124
169 ICU3D†	40307	U	U		33	0.75	0.99	1.36‡	45	3 500	50	50	No	0.127
170 ICU3D†	40307	U	U		33	0.75	1.06	1.47	55	3 500	50	33	Yes	0.098
171 ICU4D†	40307	U	U		33	0.66	0.72	1.41	55	3 500	50	50	No	0.100
172 ICU4D†	40307	U	U		33	0.62	0.67	1.44	45	3 500	50	50	No	0.108
173 ICU4D	40307	U	U		33	0.53	0.70	1.37‡	35	3 000	50	30	No	0.139
174 ICU3D	40307	U	U		33	0.75	1.03	1.53	35	3 000	50	10	Yes	0.137
175 ICU4D	40307	U	U		33	0.50	0.68	1.53	35	3 000	50	30	No	0.128
176 ICU4D	40307	U	U		33	0.50	0.65	1.52	35	3 000	50	30	No	0.134
177 ICR1D	40307	C	R	960	36	1.05	1.25	2.48	45	3 000	50	31	Yes	0.130
178 ICR5D	40307	C	R	960	36	1.12	1.40	2.02	45	3 000	50	31	Yes	0.133
179 ICR6D	40307	C	R	960	36	0.48	0.63	2.55	45	3 000	50	50	No	0.131
180 ICR7D	40307	C	R	960	36	0.52	0.63	1.98	45	3 000	50	50	No	0.132
181 ICR1D	40307	C	R	960	36	1.00	1.40	2.55	45	3 000	50	25	Yes	0.130
182 ICR6D	40307	C	R	960	36	0.55	0.72	2.55	45	3 000	50	50	No	0.136
183 ICR5D	40307	C	R	960	36	0.97	1.34	2.03	45	3 000	50	25	Yes	0.135
184 ICR7D	40307	C	R	960	36	0.53	0.69	2.00	45	3 000	50	50	No	0.136
197 ICO5D	40307	C	E	960	36	1.03	1.25	2.06	45	3 000	50	18	Yes	.....
198 ICO7D	40307	C	E	960	36	0.59	0.72	2.06	45	3 000	50	50	No	0.145
199 ICR8D	40307	C	R	960	36	0.77	0.94	2.09	45	3 000	50	50	No	0.147
200 ICR8D	40307	C	R	960	36	0.75	0.87	2.14	45	3 000	50	50	No	0.151
203 ICR7D	40307	C	R	960	36	0.53	0.69	2.03	45	3 000	50	50	No	0.149
204 ICO5D	40307	C	E	960	36	1.00	1.25	2.03	45	3 000	50	17	Yes	0.151

* See Fig. 3.

† These wheels were tested with 5-min continuous drag tests.

‡ Measurement taken after tests.

TABLE 22 (CONTINUED)

SUMMARY OF DRAG TEST RESULTS OF WHEELS HAVING A SIMULATED THERMAL CRACK

Brakes applied for 50 sec of each minute for the duration of the 30 minute test

Wheel Test No.	Heat No.	Class	Heat Treatment	Draw Temp, deg F	Diameter, in.	Plate Thickness* A, in.	Plate Thickness* B, in.	Rim Thickness, inches	Speed, mph	Brake Shoe Pressure, lb	Depth Saw Cut, %	No. of Drags	Fracture	Av Coef. of Friction
205 ICR7D	40307	C	R	960	36	0.50	0.75	2.05	45	3 000	50	50	No	0.148
206 ICO7D	40307	C	E	960	36	0.50	0.66	2.03	45	3 000	50	50	No	0.148
207 ICR7D	40307	C	R	960	36	0.50	0.81	2.00	45	3 000	50	50	No	0.148
208 ICU5D	40307	U	U		36	1.02	1.28	2.00	45	3 000	50	11	Yes	0.152
209 ICO8D	40307	C	E	960	36	0.75	0.87	2.08	45	3 000	50	50	No	0.145
210 ICU7D	40307	U	U		36	0.50	0.64	2.03	45	3 000	50	50	No	.....
211 ICU8D	40307	U	U		36	0.77	0.91	2.03	45	3 000	50	50	No	0.145
212 ICU5D	40307	U	U		36	1.00	1.25	1.97	45	3 000	50	17	Yes	0.140
213 ICU8D	40307	U	U		36	0.82	0.96	2.00	45	3 000	50	22	Yes	0.146
214 ICO8D	40307	C	E	960	36	0.77	0.87	2.06	45	3 000	50	50	No	0.148
215 ICU7D	40307	U	U		36	0.48	0.62	2.00	45	3 000	50	50	No	0.147
220 ICO8D	40307	C	E	960	36	¾	⅞	2.00	55	3 000	50	50	No	0.133
									45	3 500	50	3	No	0.144
									45	4 000	50	3	No	0.137
221 ICO8D	40307	C	E	960	36	¾	⅞	2.00	50	3 000	50	50	No	0.134
									45	3 000	75	3	No	.....
									45	4 000	75	6	Yes	.....
222 ICR8D	40307	C	R	960	36	¾	⅞	2.00	50	3 000	50	50	No	0.134
223 ICR8D	40307	C	R	960	36	¾	⅞	2.00	55	3 000	50	50	No	0.133
224 BBR1D	40307	B	R	870	36	1	1¼	2½	45	3 000	50	50	No	.....
									45	4 000	50	30	No	.....
225 IBO1D	34519	B	E	930	36	1	1¼	2½	45	4 000	50	7	Yes	0.137
226 IBO1D	34519	B	E	930	36	1	1¼	2½	45	3 000	75	15	Yes	0.162
227 IBO1D	34519	B	E	930	36	1	1¼	2½	45	4 000	50	7	Yes	0.142
228 IBO1D	34519	B	E	930	36	1	1¼	2½	45	4 000	75	6	Yes	0.132
229 ICR8D	40307	C	R	960	36	0.83	0.91	1.97	45	4 000	75	14	Yes	0.135
231 ICR7D	40307	C	R	960	36	0.53	0.69	1.99	45	4 000	75	30	Yes	0.128
234 ICR5D	40307	C	R	600	36	1.02	1.08	2.05	45	3 000	50	38	Yes	0.160
237 ICO5D	40307	C	E	600	36	1.03	1.33	2.00	45	3 000	50	11	Yes	.....
238 ICR5D	40307	C	R	960	36	1.09	1.28	1.98	45	4 000	75	6	Yes	0.133
239 ICO5D	40307	C	E	800	36	1.03	1.28	2.00	45	3 000	50	18	Yes	0.151

* See Fig. 3.

TABLE 22 (CONTINUED)

SUMMARY OF DRAG TEST RESULTS OF WHEELS HAVING A SIMULATED THERMAL CRACK

Brakes applied for 50 sec of each minute for the duration of the 30 minute test

Wheel Test No.	Heat No.	Class	Heat Treatment	Draw Temp, deg F	Diameter, in.	Plate Thickness* A, in.	Plate Thickness* B, in.	Rim Thickness, inches	Speed, mph	Brake Shoe Pressure, lb	Depth Saw Cut, %	No. of Drags	Fracture	Av Coef. of Friction
240 ICR5D	40307	C	R	800	36	1.03	1.31	2.00	45	3 000	50	50	No	0.150
241 ICR8D	40307	C	R	960	36	0.81	0.94	2.06	45	4 000	75	8	Yes	0.112
242 ICR7D	40307	C	R	960	36	0.55	0.64	2.00	45	4 000	75	19	Yes	0.111
243 ICR5D	40307	C	R	800	36	1.06	1.31	2.00	45	3 000	50	50	No	0.150
244 ICO5D	40307	C	E	800	36	1.03	1.28	2.02	45	3 000	50	31	Yes	0.157
245 ICR5D	40307	C	R	600	36	1.05	1.30	2.06	45	3 000	50	34	Yes	0.166
249 BCR1D	59R316	C	R	870	36	1.22	1.50	2.34	45	3 000	50	15	Yes	0.157
250 BCR1D	59R316	C	R	870	36	1.20	1.50	2.36	45	3 000	50	14	Yes	0.154
251 BCR1D	59R316	C	R	870	36	1.11	1.31	2.31	45	3 000	50	25	Yes	0.165
252 BCR1D	59R316	C	R	870	36	1.20	1.50	2.31	45	3 000	50	18	Yes	0.161
253 BCR1D	59R316	C	R	870	36	1.17	1.50	2.39	45	3 000	50	30	Yes	0.163
254 BCR1D	59R316	C	R	870	36	1.17	1.50	2.38	45	3 000	50	15	Yes	0.163
257 LCU4D	831021	U	U		33	0.69	0.81	1.37	45	3 000	50	23	Yes	0.132
259 LCU4D	831021	U	U		33	0.64	0.78	1.31	45	3 000	50	20	Yes	0.133
260 LCU4D	831021	U	U		33	0.66	0.75	1.31	45	3 000	50	35	Yes	0.134
261 LCU4D	831021	U	U		33	0.69	0.81	1.34	45	3 000	50	24	Yes	0.142
274 LCU4D	831021	U	U		33	0.66	0.88	1.50	45	3 000	50	50	No	0.119
275 LCU4D	831021	U	U		33	0.66	0.81	1.50	45	3 000	50	50	No	0.126
276 LCU4D	831021	U	U		33	0.63	0.94	1.50	45	3 000	50	50	No	0.114
277 LCU4D	831021	U	U		33	0.59	0.81	1.50	45	3 000	50	50	No	0.102
278 BCR9D	59R316	C	R	870	36	0.81	1.06	2.31	45	3 000	50	50	No	0.114
279 BCR9D	59R316	C	R	870	36	0.78	1.09	2.25	45	3 000	50	50	No	0.129
280 BCR9D	59R316	C	R	870	36	0.81	1.00	2.28	45	4 000	75	10	Yes	0.120
281 BCR9D	59R316	C	R	870	36	0.78	1.13	2.25	45	4 000	75	6	Yes	0.113
282 BCR9D	59R316	C	R	870	36	0.72	0.88	2.25	45	4 000	75	46	Yes	0.112
283 BCR9D	59R316	C	R	870	36	0.84	1.06	2.22	45	4 000	75	2	Yes	0.109
284 BCR9D	59R316	C	R	870	36	0.81	1.06	2.22	45	4 000	75	12	Yes	0.109
285 BCR9D	59R316	C	R	870	36	0.84	1.06	2.16	45	4 000	75	9	Yes	0.114
286 BCR9D	59R316	C	R	870	36	0.81	1.06	2.25	45	4 000	75	9	Yes	0.113
287 BCR9D	59R316	C	R	870	36	0.81	1.09	2.25	45	4 000	75	6	Yes	0.109
288 BCR9D	59R316	C	R	870	36	0.81	1.09	2.22	45	4 000	75	6	Yes	0.113

* See Fig. 3.

TABLE 22 (CONTINUED)

SUMMARY OF DRAG TEST RESULTS OF WHEELS HAVING A SIMULATED THERMAL CRACK

Brakes applied for 50 sec of each minute for the duration of the 30 minute test

Wheel Test No.	Heat No.	Class	Heat Treatment	Draw Temp, deg F	Diameter, in.	Plate Thickness* A, in.	Plate Thickness* B, in.	Rim Thickness, inches	Speed, mph	Brake Shoe Pressure, lb	Depth Saw Cut, %	No. of Drags	Fracture	Av Coef. of Friction
289 BCR9D	59R316	C	R	870	36	0.81	1.19	2.25	45	4 000	75	11	Yes	0.124
290 BCR9D	59R316	C	R	870	36	0.69	1.06	2.19	45	4 000	75	7	Yes	0.110
291 BCR9D	59R316	C	R	870	36	0.78	1.13	2.19	45	4 000	75	11	Yes	0.106
292 ICO1D	921614	C	E	1 200	36	1.00	1.31	2.69	45	3 000	50	23	Yes	0.141
293 ICO1D	921614	C	E	1 000	36	1.00	1.38	2.75	45	3 000	50	6	Yes	0.142
294 ICO1D	921614	C	E	900	36	1.00	1.38	2.75	45	3 000	50	12	Yes	0.147
295 ICO1D	921614	C	E	800	36	1.00	1.28	2.78	45	3 000	50	8	Yes	0.133
297 ICO1D	921614	C	E	700	36	0.97	1.31	2.63	45	3 000	50	5	Yes	0.118
298 ICO1D	921614	C	E	400	36	0.97	1.31	2.75	45	3 000	50	6	Yes	0.122
299 ICR1D	921614	C	R	1 200	36	1.06	1.31	2.69	45	3 000	50	50	No	0.142
300 ICR1D	921614	C	R	1 000	36	0.94	1.31	2.69	45	3 000	50	38	Yes	0.142
313 ICR1D	921614	C	R	900	36	0.94	1.38	2.72	45	3 000	50	50	No	0.135
314 ICR1D	921614	C	R	800	36	0.97	1.31	2.67	45	3 000	50	48	Yes	0.135
315 ICR1D	921614	C	R	700	36	0.94	1.28	2.75	45	3 000	50	48	Yes	0.136
316 ICR1D	921614	C	R	400	36	1.00	1.34	2.72	45	3 000	50	24	Yes	0.133
317 ICU1D	921614	U	U		36	0.97	1.38	2.81	45	3 000	50	8	Yes	0.131
318 ICU1D	921614	U	U		36	1.00	1.38	2.69	45	3 000	50	13	Yes	0.123
319 ICO1D	921614	C	E	1 200	36	1.00	1.25	2.69	45	3 000	50	47	Yes	0.136
320 ICO1D	921614	C	E	1 000	36	1.00	1.38	2.75	45	3 000	50	12	Yes	0.139
321 ICO1D	921614	C	E	900	36	0.91	1.31	2.75	45	3 000	50	13	Yes	0.137
322 ICO1D	921614	C	E	800	36	1.00	1.38	2.81	45	3 000	50	16	Yes	0.133
323 ICO1D	921614	C	E	700	36	1.00	1.38	2.75	45	3 000	50	4	Yes	0.127
324 ICO1D	921614	C	E	400	36	0.97	1.31	2.75	45	3 000	50	4	Yes	0.130
325 ICR1D	921614	C	R	1 000	36	1.00	1.31	2.63	45	3 000	50	8	Yes	0.141
326 ICR1D	921614	C	R	900	36	1.00	1.31	2.75	45	3 000	50	5	Yes	0.138
327 ICR1D	921614	C	R	800	36	0.97	1.31	2.81	45	3 000	50	8	Yes	0.151
328 ICR1D	921614	C	R	700	36	1.00	1.34	2.69	45	3 000	50	8	Yes	0.141
329 ICR1D	921614	C	R	400	36	0.97	1.31	2.75	45	3 000	50	14	Yes	0.151
330 ICR1D	921614	C	R	1 200	36	0.97	1.44	2.69	45	3 000	50	20	Yes	0.149
331 BCR9D	59R316	C	R	870	36	0.81	1.06	2.56	45	4 000	75	4	Yes	0.123
332 LCU4D	831021	U	U		33	0.69	0.88	1.38	45	3 000	50	50	Yes	0.154

* See Fig. 3.

TABLE 22 (CONCLUDED)

SUMMARY OF DRAG TEST RESULTS OF WHEELS HAVING A SIMULATED THERMAL CRACK

Brakes applied for 50 sec of each minute for the duration of the 30 minute test

Wheel Test No.	Heat No.	Class	Heat Treatment	Draw Temp, deg F	Diameter, in.	Plate Thickness* A, in.	Plate Thickness* B, in.	Rim Thickness, inches	Speed, mph	Brake Shoe Pressure, lb	Depth Saw Cut, %	No. of Drags	Fracture	Av Coef. of Friction
333 ICR1D	921614	C	R	860	36	0.94	1.59	2.69	45	3 000	50	24	Yes	0.156
334 ICR1D	921614	C	R	860	36	0.88	1.50	2.59	45	3 000	50	14	Yes	0.156
335 ICR1D	921614	C	R	860	36	0.94	1.50	2.69	45	3 000	50	50	No	0.153
336 ICR1D	921614	C	R	860	36	0.91	1.38	2.63	45	3 000	50	17	Yes	0.144
337 ICR1D	921614	C	R	860	36	0.94	1.50	2.69	45	3 000	50	50	No	0.143
338 ICR1D	921614	C	R	860	36	0.94	1.44	2.63	45	3 000	50	37	Yes	0.149
339 ICR1D	921614	C	R	860	36	0.97	1.31	2.69	45	3 000	50	50	No	0.151
340 ICR1D	921614	C	R	860	36	1.09	1.38	2.69	45	3 000	50	47	Yes	0.145
341 ICR1D	921614	C	R	860	36	0.97	1.44	2.69	45	3 000	50	13	Yes	0.157
342 ICR1D	921614	C	R	860	36	0.97	1.59	2.66	45	3 000	50	17	Yes	0.149
345 ICR1D	921614	C	R	860	36	1.00	1.44	2.69	45	3 000	50	10	Yes	0.148
346 ICR1D	921614	C	R	860	36	1.06	1.38	2.78	45	3 000	50	15	Yes	0.159
347 ICR1D	921614	C	R	860	36	1.00	1.56	2.44	45	3 000	50	33	Yes	0.153
348 ICR1D	921614	C	R	1 000	36	1.00	1.38	2.66	45	3 000	50	28	Yes	0.151
349 ICR1D	921614	C	R	900	36	1.00	1.38	2.75	45	3 000	50	22	Yes	0.154
350 ICR1D	921614	C	R	800	36	0.97	1.38	2.63	45	3 000	50	19	Yes	0.149
351 ICR1D	921614	C	R	700	36	0.97	1.31	2.69	45	3 000	50	23	Yes	0.144
352 ICR1D	921614	C	R	400	36	0.94	1.56	2.81	45	3 000	50	19	Yes	0.146
353 ICO1D	921614	C	E	1 200	36	0.94	1.38	2.69	45	3 000	50	12	Yes	0.148
354 ICO1D	921614	C	E	1 000	36	0.94	1.50	2.63	45	3 000	50	9	Yes	0.136
355 ICO1D	921614	C	E	900	36	0.94	1.50	2.69	45	3 000	50	35	Yes	0.145
356 ICO1D	921614	C	E	800	36	0.94	1.50	2.69	45	3 000	50	14	Yes	0.140
357 ICO1D	921614	C	E	700	36	1.00	1.31	2.69	45	3 000	50	4	Yes	0.141
358 ICO1D	921614	C	E	400	36	1.00	1.38	2.78	45	3 000	50	4	Yes	0.140
359 ICU1D	921614	U	U		36	0.94	1.50	2.63	45	3 000	50	4	Yes	0.131
364 ICR1D	921614	C	R	700	36	0.97	1.62	2.50	45	3 000	50	24	Yes	0.146
365 ICR1D	921614	C	R	800	36	0.97	1.50	2.56	45	3 000	50	75	No	0.152
366 ICR1D	921614	C	R	900	36	0.97	1.63	2.69	45	3 000	50	27	Yes	0.137
367 ICR1D	921614	C	R	1 000	36	1.00	1.50	2.63	45	3 000	50	13	Yes	0.145
368 ICR1D	921614	C	R	700	36	0.97	1.50	2.63	45	3 000	50	60	Yes	0.143
369 ICR1D	921614	C	R	800	36	0.94	1.50	2.56	45	3 000	50	63	Yes	0.140

* See Fig. 3.

Table 23
Summary of Stop-Tested Wheels

All wheels were stopped from 1073 rpm by shoe pressure of 20,000 lb on each of two shoes

Wheel Test No.	Heat No.	Class	Heat Treatment	Draw Temp, deg F	Diameter, in.	Plate Thickness* A, in.	Plate Thickness* B, in.	Rim Thickness,* in.	Speed, mph	Number of Stops	Number of Thermal Cracks	Av Coef. of Friction
3 IAO1S	31077	A	E	990	36	1	1¼	2½	115	50	0	0.072
4 IAO1S	31077	A	E	990	36	1	1¼	2½	115	36	1	0.070
9 IBO1S	37021	B	E	990	36	1	1¼	2½	115	1	1	0.066
10 IBO1S	37021	B	E	990	36	1	1¼	2½	115	1	1	0.092
15 ICO1S	87120	C	E	1 040	36	1	1¼	2½	115	1	1	0.087
16 ICO1S	87120	C	E	1 040	36	1	1¼	2½	115	8	1	0.074
21 SAW1S	E6270	A	W	800	36	1	1¼	2½	115	50	0	0.066
22 SAW1S	E6270	A	W	800	36	1	1¼	2½	115	50	0	0.062
33 BAR1S	46L223	A	R	870	36	1	1¼	2½	115	50	0	0.061
34 BAR1S	46L223	A	R	870	36	1	1¼	2½	115	30	1	0.061
39 BBR1S	46L256	B	R	870	36	1	1¼	2½	115	50	0	0.063
40 BBR1S	46L256	B	R	870	36	1	1¼	2½	115	50	0	0.060
45 BCR1S	47L193	C	R	870	36	1	1¼	2½	115	1	1	0.063
46 BCR1S	47L193	C	R	870	36	1	1¼	2½	115	1	1	0.071
52 IDO1S†	28087	C	E	970	36	1	1¼	2½	115	1	3	0.076
53 IDO1S†	28087	C	E	970	36	1	1¼	2½	115	1	4	0.081
58 IEO1S†	28090	B	E	970	36	1	1¼	2½	115	1	2	0.077
59 IEO1S†	28090	B	E	970	36	1	1¼	2½	115	1	3	0.082
64 ICO1S	46568	C	E	970	36	1	1¼	2½	115	1	2	0.073
69 ICR1S	46568	C	R	970	36	1	1¼	2½	115	1	1	0.077
74 ICO1S	46568	C	E	1 140	36	1	1¼	2½	115	1	4	0.076
79 ICR1S	46568	C	R	1 140	36	1	1¼	2½	115	5	1	0.074
84 ICU1S	46568	U	U		36	1	1¼	2½	115	1	1	0.071
85 ICU1S	46568	U	U		36	1	1¼	2½	115	4	1	0.076

* Dimensions given as fractions are nominal values. See Fig. 3.
† Special low-manganese wheels.

TABLE 23 (CONCLUDED)
SUMMARY OF STOP-TESTED WHEELS

All wheels were stopped from 1073 rpm by shoe pressure of 20,000 lb on each of two shoes

Wheel Test No.	Heat No.	Class	Heat Treatment	Draw Temp, deg F	Diameter, in.	Plate Thickness* A, in.	Plate Thickness* B, in.	Rim Thickness,* in.	Speed, mph	Number of Stops	Number of Thermal Cracks	Av Coef. of Friction
89 IFO1S	43607	C	E	970	36	1	1¼	2½	115	6	1	0.084
142 IBO1S	34519	B	E	930	36	1.09	1.47	2.56	115	25	1	0.067
143 IBR1S	34519	B	R	930	36	1.16	1.44	2.42	115	50	0	0.067
144 IBO1S	34519	B	E	930	36	1.10	1.45	2.69	115	50	0	0.066
145 IBR1S	34519	B	R	930	36	1.19	1.36	2.69	115	50	0	0.071
146 IBO1S	34519	B	E	930	36	1.13	1.38	2.63	115	1	1	0.072
147 IBR1S	34519	B	R	930	36	1.20	1.50	2.58	115	50	0	0.069
148 IBO1S	34519	B	E	930	36	1.17	1.53	2.62	115	50	0	0.069
165 ICU3S	40307	U	U		33	0.78	1.03	1.41	107	30	0	0.067
166 ICU4S	40307	U	U		33	0.58	.72	1.44	107	30	0	0.066
167 ICU3S	40307	U	U		33	0.75	1.01	1.45	107	30	0	0.067
168 ICU4S	40307	U	U		33	0.53	.69	1.39	107	30	0	0.069
189 ICR1S	40307	C	R	960	36	1	1¼	2½	115	7	1	0.062
190 ICR6S	40307	C	R	960	36	½	⅝	2½	115	7	1	0.065
191 ICR5S	40307	C	R	960	36	1	1¼	2	115	35	1	0.061
192 ICR7S	40307	C	R	960	36	½	⅝	2	115	50	0	0.065
262 LCU4S	831021	U	U		33	0.69	0.81	1.19†	107	50	0	0.058
263 LCU4S	831021	U	U		33	0.66	0.78	1.25†	107	8	1	0.060
264 LCU4S	831021	U	U		33	0.69	0.81	1.25†	107	28	2	0.059
265 LCU4S	831021	U	U		33	0.69	0.81	1.13†	107	50	0	0.058
269 ICU4S	831021	U	U		33	0.69	0.81	1.38†	107	4	1	0.060
270 ICU4S	831021	U	U		33	0.69	0.81	1.38†	107	5	1	0.061
272 ICU4S	831021	U	U		33	0.69	0.81	1.25†	107	31	1	0.058
273 ICU4S	831021	U	U		33	0.72	0.81	1.25†	107	50	1	0.059

* Dimensions given as fractions are nominal values. See Fig. 3.
† Measurement taken after tests.

TABLE 24

GENERAL DATA FOR WHEELS TESTED FOR RESIDUAL STRESSES

Wheel Test Number	Heat Number	Class	Heat Treatment	Draw Temp, deg F	Diam, in.	Nominal Plate Thickness* A, in.	Nominal Plate Thickness* B, in.	Nominal Rim Thickness, inches
5 IAO1R	31077	A	E	990	36	1	1 1/4	2 1/2
6 IAO1R	31077	A	E	990	36	1	1 1/4	2 1/2
11 IBO1R	37021	B	E	990	36	1	1 1/4	2 1/2
12 IBO1R	37021	B	E	990	36	1	1 1/4	2 1/2
17 ICO1R	87120	C	E	1 040	36	1	1 1/4	2 1/2
18 ICO1R	87120	C	E	1 040	36	1	1 1/4	2 1/2
23 SAW1R	E6270	A	W	800	36	1	1 1/4	2 1/2
24 SAW1R	E6270	A	W	800	36	1	1 1/4	2 1/2
35 BAR1R	46L223	A	R	870	36	1	1 1/4	2 1/2
41 BBR1R	46L256	B	R	870	36	1	1 1/4	2 1/2
47 BCR1R	47L193	C	R	870	36	1	1 1/4	2 1/2
49 IDO1R	28087	C	E	970	36	1	1 1/4	2 1/2
55 IEO1R	28090	B	E	970	36	1	1 1/4	2 1/2
61 ICO1R	46568	C	E	970	36	1	1 1/4	2 1/2
66 ICR1R	46568	C	R	970	36	1	1 1/4	2 1/2
71 ICO1R	46568	C	E	1 140	36	1	1 1/4	2 1/2
76 ICR1R	46568	C	R	1 140	36	1	1 1/4	2 1/2
81 ICU1R	46568	U	U		36	1	1 1/4	2 1/2
86 IFO1R	43607	C	E	970	36	1	1 1/4	2 1/2
101 ICU2R	40495	C	U		33	1/2	3/4	2
153 IBO1R	34519	B	E	930	36	1	1 1/4	2 1/2
154 IBR1R	34519	B	R	930	36	1	1 1/4	2 1/2
163 ICU3R	40307	U	U		33	3/4	1	1 1/2
164 ICU4R	40307	U	U		33	1/2	5/8	1 1/2
185 ICR6R	40307	C	R	960	36	1/2	5/8	2 1/2
186 ICR1R	40307	C	R	960	36	1	1 1/4	2 1/2
187 ICR5R	40307	C	R	960	36	1	1 1/4	2
188 ICR7R	40307	C	R	960	36	1/2	5/8	2
201 ICO5R	40307	C	E	960	36	1	1 1/4	2
202 ICO7R	40307	C	E	960	36	1/2	5/8	2
216 ICU5R	40307	U	U		36	1	1 1/4	2
217 ICU8R	40307	U	U		36	3/4	7/8	2
218 ICU7R	40307	U	U		36	1/2	5/8	2
219 ICO8R	40307	C	E	960	36	3/4	7/8	2
232 ICO5R	40307	C	E	600	36	1	1 1/4	2
233 ICR5R	40307	C	R	600	36	1	1 1/4	2
235 ICR5R	40307	C	R	800	36	1	1 1/4	2
236 ICO5R	40307	C	E	800	36	1	1 1/4	2
246 BCR1R	59R316	C	R	870	36	1	1 1/4	2 1/2
247 BCR1R	59R316	C	R	870	36	1	1 1/4	2 1/2
248 BCR1R	59R316	C	R	870	36	1	1 1/4	2 1/2
255 LCU4R	831021	U	U		33	1/2	5/8	1 1/2
266 BCR9R	59R316	C	R	870	36	3/4	7/8	2 1/2
267 BCR9R	59R316	C	R	870	36	3/4	7/8	2 1/2
268 BCR9R	59R316	C	R	870	36	3/4	7/8	2 1/2
271 ICU4R	831021	U	U		33	1/2	5/8	1 1/2
296 ICO1R	921614	C	E	1 200	36	1	1 1/4	2 1/2
301 ICR1R	921614	C	R	1 200	36	1	1 1/4	2 1/2
302 ICO1R	921614	C	E	1 000	36	1	1 1/4	2 1/2
303 ICR1R	921614	C	R	1 000	36	1	1 1/4	2 1/2
304 ICR1R	921614	C	R	900	36	1	1 1/4	2 1/2
305 ICR1R	921614	C	R	700	36	1	1 1/4	2 1/2
306 ICR1R	921614	C	R	800	36	1	1 1/4	2 1/2
307 ICR1R	921614	C	R	400	36	1	1 1/4	2 1/2
308 ICO1R	921614	C	E	900	36	1	1 1/4	2 1/2
309 ICO1R	921614	C	E	800	36	1	1 1/4	2 1/2
310 ICO1R	921614	C	E	700	36	1	1 1/4	2 1/2
311 ICO1R	921614	C	E	400	36	1	1 1/4	2 1/2
312 ICU1R	921614	U	U		36	1	1 1/4	2 1/2
343 ICR1R	921614	C	R	860	36	1	1 1/4	2 1/2
360 ICR1R	921614	C	R	700	36	1	1 1/4	2 1/2
361 ICR1R	921614	C	R	800	36	1	1 1/4	2 1/2
362 ICR1R	921614	C	R	900	36	1	1 1/4	2 1/2
363 ICR1R	921614	C	R	1 000	36	1	1 1/4	2 1/2

* See Fig. 3.

TABLE 25
LADLE HEAT ANALYSIS BY MANUFACTURE

Heat Number	C, percent	Mn, percent	P, percent	S, percent	Si, percent
28087	0.75	0.38	0.013	0.031	0.17
28090	0.59	0.44	0.017	0.030	0.19
31077	0.52	0.71	0.030	0.029	0.21
34519	0.61	0.74	0.015	0.038	0.26
37021	0.61	0.75	0.013	0.024	0.19
40307	0.73	0.73	0.014	0.034	0.18
43607	0.73	0.79	0.020	0.037	0.27
46568	0.73	0.75	0.014	0.025	0.22
87120	0.72	0.77	0.020	0.027	0.22
831021	0.72	0.70	0.014	0.038	0.23
921614	0.72	0.77	0.022	0.035	0.20
46L223	0.52	0.69	0.014	0.031	0.20
46L256	0.61	0.75	0.027	0.039	0.21
47L193	0.70	0.77	0.010	0.032	0.22
59R316	0.71	0.68	0.014	0.029	0.22
E6270	0.48	0.68	0.030	0.030	0.26

This page is intentionally blank.

Recent Publications of The Engineering Experiment Station

Books

History of the Development of Building Construction in Chicago, by Frank A. Randall. 1949. A publication of the University of Illinois Press; sponsored jointly by the Engineering Experiment Station and the Graduate College. 388 pages. Price: cloth, *five dollars;* paper, *four dollars.*

Bulletins

NO.

361. Residual Stresses in Welded Structures, by W. M. Wilson and Chao-Chien Hao. 1946. *Forty cents.*
362. The Bonding Action of Clays: Part II—Clays in Dry Molding Sands, by R. E. Grim and F. L. Cuthbert. 1946. *Free upon request.*
363. Studies of Slab and Beam Highway Bridges: Part I—Tests of Simple-Span Right I-Beam Bridges, by N. M. Newmark, C. P. Siess, and R. R. Penman. 1946. *Sixty-five cents.*
364. Steam Turbine Blade Deposits, by F. G. Straub. 1946. *Fifteen cents.*
365. Experience in Illinois with Joints in Concrete Pavements, by J. S. Crandell, V. L. Glover, W. C. Huntington, J. D. Lindsay, F. E. Richart, and C. C. Wiley. 1947. *Free upon request.*
366. Performance of an Indirect Storage Type of Hot-Water Heater, by A. P. Kratz and W. S. Harris. 1947. *Free upon request.*
367. Influence Charts for Computation of Vertical Displacements in Elastic Foundations, by N. M. Newmark. 1947. *Twenty cents.*
368. The Effect of Eccentric Loading, Protective Shells, Slenderness Ratios, and Other Variables in Reinforced Concrete Columns, by F. E. Richart, J. O. Draffin, T. A. Olson, and R. H. Heitman. 1947. *Sixty-five cents.*
369. Studies of Highway Skew Slab-Bridges with Curbs: Part I—Results of Analyses, by V. P. Jensen and J. W. Allen. 1947. *Free upon request.*
370. The Illinois Smokeless Furnace, by J. R. Fellows, A. P. Kratz, and S. Konzo. 1947. *Forty cents.*
371. Rate of Propagation of Fatigue Cracks in 12-inch by ¾-in. Steel Plates with Severe Geometrical Stress-Raisers, by W. M. Wilson and J. L. Burke. 1947. *Ten cents.*
372. The Effect of Non-Uniform Distribution of Stress on the Yield Strength of Steel, by D. Morkovin and O. Sidebottom. 1947. *Forty cents.*
373. History of Building Foundations in Chicago, by R. B. Peck. 1948. *Thirty cents.*
374. The Free Surface Around, and Interference Between, Gravity Wells, by H. E. Babbitt and D. H. Caldwell. 1948. *Thirty cents.*
375. Studies of Slab and Beam Highway Bridges: Part II—Tests of Simple-Span Skew I-Beam Bridges, by N. M. Newmark, C. P. Siess, and W. M. Peckham. 1948. *Free upon request.*
376. Highspeed Freight Train Resistance: Its Relation to Average Car Weight, by John K. Tuthill. 1948. *Free upon request.*
377. Flexural Fatigue Strength of Steel Beams, by W. M. Wilson. 1948. *Twenty cents.*
378. An Investigation of Creep, Fracture, and Bending of Lead and Lead Alloys for Cable Sheathing—Series 1946, by C. W. Dollins. 1948. *Free upon request.*
379. Non-Pressure Treatments of Round Northern White Cedar Timbers with Creosote, by E. E. King. 1948. *Free upon request.*
380. Fatigue Strength of Fillet-Weld, Plug-Weld, and Slot-Weld Joints Connecting Steel Structural Members, by W. M. Wilson, W. H. Munse, and W. H. Bruckner. 1949. *Sixty cents.*
381. An Investigation of the Backwater Profile for Steady Flow in Prismatic Channels, by W. M. Lansford and W. D. Mitchell. 1949. *Fifty cents.*

Bulletins (Continued)

NO.

382. The Fatigue Strength of Various Details Used for the Repair of Bridge Members, by W. M. Wilson and W. H. Munse. 1949. *Forty cents.*

383. Progress Report on Performance of a One-Pipe Heating System in the $I = B = R$ Research Home, by W. S. Harris. 1949. *Twenty-five cents.*

384. Fatigue Strength of Butt Welds, by W. M. Wilson, W. H. Munse, and I. S. Snyder. 1949. *Free upon request.*

385. Moments in Two-Way Concrete Floor Slabs, by C. P. Siess and N. M. Newmark. 1950. *Free upon request.*

386. Studies of Highway Skew Slab-Bridges with Curbs: Part II, by M. L. Gossard, C. P. Siess, N. M. Newmark, and L. E. Goodman. 1950. *Free upon request.*

387. The Effect of Brake Shoe Action on Thermal Cracking and on Failure of Wrought Steel Railway Car Wheels, by H. R. Wetenkamp, O. M. Sidebottom, and H. J. Schrader. 1950. *Free upon request.*

Circulars

NO.

49. The Drainage of Airports, by W. W. Horner. 1944. *Twenty-five cents.*

50. Bibliography of Electro-Organic Chemistry, by S. Swann, Jr. 1948. *Fifty cents.*

51. Rating Equations for Hand-Fired Warm-Air Furnaces, by A. P. Kratz, S. Konzo, and J. A. Henry. 1945. *None available.*

52. The Railroad Dynamometer Car of the University of Illinois and the Illinois Central Railroad, by J. K. Tuthill. 1947. *Free upon request.*

53. Papers Presented at the Seventh Short Course in Coal Utilization, held at the University of Illinois, September 17-19, 1946. 1948. *One dollar.*

54. Papers Presented at the First Short Course on Hot Water and Steam Heating Systems, held at the Undergraduate Division, University of Illinois, Navy Pier, Chicago, September 9-11, 1947. 1948. *Fifty cents.*

55. Contributions to Proceedings of the Second International Conference on Soil Mechanics and Foundation Engineering. 1949. *Thirty-five cents.*

56. Papers Presented at the First Annual Short Course on Industrial Packaging and Materials Handling, held in Chicago, October 4-7, 1948. 1949. *None available.*

57. A Survey of Electrical Insulation Practices, by M. A. Faucett, C. Houpis, and G. E. Leibinger. 1949. *Seventy cents.*

58. Papers Presented at the Eighth Conference on Coal Utilization. 1949. *Seventy-five cents.*

59. Input Impedance of a Slotted Cylinder Antenna, by C. A. Holt. 1950. *Free upon request.*

60. Lectures on Foundation Engineering, by A. E. Cummings. 1949. *Free upon request.*

Reprints

NO.

39. Progress Reports of Investigation of Railroad Rails and Joint Bars, by R. E. Cramer and R. S. Jensen. 1948. *Fifteen cents.*

40. Third Progress Report of the Investigation of Methods of Roadbed Stabilization, by R. Smith. 1948. *Fifteen cents.*

41. Phase-Sensitive Indicating Devices, by H. C. Roberts. 1948. *Fifteen cents.*

42. First Progress Report of a Laboratory Investigation of Roadbed Stabilization, by R. B. Peck. 1949. *Free upon request.*

43. Progress Reports of Investigation of Railroad Rails, Joint Bars, and Manganese Steel Castings, by R. E. Cramer and R. S. Jensen. 1949. *Free upon request.*

44. Present Status of the Development of Hand-Fired Smokeless Coal Heaters, by J. R. Fellows. 1949. *Fifteen cents.*

45. Highway Bridge Floors, by F. E. Richart, N. M. Newmark, and C. P. Siess. 1949. *None available.*

UNIVERSITY OF ILLINOIS

Divisions of Instruction

Institute of Aviation
College of Agriculture
College of Commerce and Business Administration
College of Dentistry
College of Education
College of Engineering
College of Fine and Applied Arts
Graduate College
School of Journalism
Institute of Labor and Industrial Relations
College of Law
College of Liberal Arts and Sciences
Library School
College of Medicine
Department of Military Science and Tactics
Department of Naval Science
College of Pharmacy
School of Physical Education
Division of Social Welfare Administration
Division of Special Services for War Veterans
Summer Session
University Extension Division
College of Veterinary Medicine

University Experiment Stations and Research and Service Organizations at Urbana

Agricultural Experiment Station
Bureau of Community Planning
Bureau of Economic and Business Research
Bureau of Institutional Research
Bureau of Research and Service
Engineering Experiment Station
Extension Service in Agriculture and Home Economics
General Placement Bureau
High School Testing Bureau
Institute of Communications Research
Institute of Government and Public Affairs
Radio Station (WILL)
Services for Crippled Children
Small Homes Council
Student Counseling Bureau
University of Illinois Press

State Scientific Surveys and Other Divisions at Urbana

State Geological Survey
State Natural History Survey
State Water Survey
State Diagnostic Laboratory (for Animal Pathology)
U. S. Regional Soybean Laboratory

For general catalog of the University, special circulars, and other information, address The Director of Admissions and Records, University of Illinois, Urbana, Illinois